





# Smart Shading Devices: Innovation in the Design of Semi-Open Spaces to Enhance Thermal Comfort in Hot and Arid Cities – Case Study: Mashhad

Danial. Goshayeshi<sup>1</sup>, Seyyed Majid. Mofidi Shemirani<sup>2\*</sup>, Shabnam. Teimourtash<sup>3</sup>, Mohsen. Tabass<sup>4</sup>

<sup>1</sup> Ph.D. Student, Department of Architecture, Mashhad Branch, Islamic Azad University, Mashhad, Iran

<sup>2</sup> Assistant Professor, Department of Architecture, Iran University of Science and Technology, Tehran, Iran

<sup>3</sup> Assistant Professor, Department of Architecture, Mashhad Branch, Islamic Azad University, Mashhad, Iran

<sup>4</sup> Associate Professor, Department of Architecture, Mashhad Branch, Islamic Azad University, Mashhad, Iran

\* Corresponding author email address: m.mofidi.s1400@gmail.com

## Article Info

### Article type:

Original Research

### How to cite this article:

Goshayeshi, D., Mofidi Shemirani, S. M., Teimourtash, S., & Tabass, M. (2024). Smart Shading Devices: Innovation in the Design of Semi-Open Spaces to Enhance Thermal Comfort in Hot and Arid Cities – Case Study: Mashhad. *Journal of Resource Management and Decision Engineering*, 3(3), 71-126.

<https://doi.org/10.61838/kman.jrmde.3.3.7>



© 2024 the authors. Published by KMAN Publication Inc. (KMANPUB). This is an open access article under the terms of the Creative Commons Attribution-NonCommercial 4.0 International (CC BY-NC 4.0) License.

## ABSTRACT

This study investigates the impact of smart shading device design on the thermal behavior of semi-open spaces in four-story buildings in the city of Mashhad. Using two simulation software programs (Honeybee and Envi-met), the results indicate that models with greater shading coverage (three enclosed sides) demonstrate superior thermal performance on the summer solstice compared to models with minimal shading (one enclosed side). Additionally, balconies located at the central façade of the building exhibit the best thermal behavior on the summer solstice, while centrally placed balconies with two enclosed sides yield the best results on the winter solstice. The study concludes that balcony design should ensure three shaded sides during summer and two shaded sides during winter. It is recommended that balconies be designed with two enclosed sides and a movable canopy in order to achieve both optimal summer thermal performance and desirable winter conditions. In response to the research questions, the study analyzes the factors affecting the thermal behavior of semi-open spaces and the variables influencing the design of shading devices across different seasons. Overall, this research contributes to the optimal design of smart shading devices in Mashhad and may serve as a practical guide for architects and designers aiming to enhance thermal comfort in semi-open spaces.

**Keywords:** smart shading devices, innovation, semi-open space, thermal comfort, Mashhad

## 1. Introduction

As climate change accelerates and urban populations grow, ensuring outdoor thermal comfort in dense, hot-arid urban environments has become both a scientific

and architectural imperative. Urban design and construction strategies must adapt to increasing heat stress, particularly in semi-open and transitional spaces such as balconies, courtyards, and shaded corridors, which are essential in providing microclimatic relief to inhabitants. These spatial

typologies, due to their hybrid nature—neither fully open nor entirely enclosed—require special attention in the design of shading systems, building geometry, and material selection to optimize thermal conditions throughout the year (Aghapour & Taban, 2020; Rodríguez-Algeciras et al., 2018; Roshan et al., 2019).

Semi-open spaces such as balconies and transitional thresholds between indoor and outdoor environments play a vital role in shaping thermal experience and energy performance in buildings, especially in hot-arid regions. These areas are particularly sensitive to fluctuations in solar radiation, wind exposure, and radiant heat exchange. The role of architectural elements like balconies in modulating thermal comfort has been emphasized across numerous studies. Ribeiro et al. (2020) argue that balconies significantly influence indoor environmental quality by acting as climatic buffers between outdoor extremes and indoor zones (Ribeiro et al., 2020). Similarly, Moghadam Ziabari and Mozaffari (2018) underline their role in improving natural ventilation and attenuating outdoor noise levels in residential contexts (Moghadam Ziabari & Mozaffari, 2018).

However, in hot-arid climates, which experience significant diurnal temperature swings and high solar exposure, the challenge lies in mitigating heat gain during peak hours while preserving outdoor usability and visual openness. Recent research on thermal comfort in urban environments indicates that the spatial orientation and degree of enclosure of balconies can dramatically affect comfort levels. For example, Akbari and Hosseini-najad (2019) explored the optimal orientation angles for maximizing solar radiation benefits in Tehran and concluded that even small angular variations can drastically alter heat gain dynamics in transitional spaces (Akbari & Hosseini-najad, 2019).

Technological advancements in building simulation tools, such as ENVI-met, Honeybee, and EnergyPlus, have allowed researchers to evaluate and refine design strategies for optimizing thermal performance in such spaces. Aleksandrowicz et al. (2023) evaluated the accuracy of ENVI-met in simulating mean radiant temperature in hot Mediterranean contexts and found that calibrated models provide valuable insights for passive design strategies in summer conditions (Aleksandrowicz et al., 2023). Likewise, Badino et al. (2021) conducted comparative assessments of various simulation tools to model outdoor radiant temperature, reinforcing the need for multi-dimensional

modeling to capture the complexity of outdoor comfort conditions (Badino et al., 2021).

In line with these methodological developments, this study utilizes Honeybee and Envi-met to evaluate smart shading systems and their influence on thermal comfort in semi-open balconies in hot-arid environments. As suggested by Sudarsanam and Kannamma (2023), thermal vulnerability varies across demographics and spatial configurations, highlighting the importance of tailored, simulation-driven design in achieving equitable comfort outcomes (Sudarsanam & Kannamma, 2023). This is particularly relevant in cities of the Middle East and Central Asia, where rapid urban expansion intersects with extreme summer temperatures and cultural preferences for outdoor living spaces.

Moreover, thermal comfort in semi-open spaces is not merely a function of temperature but is shaped by interactions between humidity, wind, solar exposure, and human factors. Qin et al. (2024) propose that a holistic approach to outdoor comfort should integrate acoustic, thermal, and humidity variables to accurately assess livability in urban environments (Qin et al., 2024). This perspective aligns with the concept of "bioclimatic architecture" and the application of climatology in design proposed by Pourdeihimi (2018), who argues for micro-scale environmental planning to achieve sustainable thermal conditions (Pourdeihimi, 2018).

From a morphological standpoint, the geometry of urban blocks and the openness of facades directly affect airflow, shading, and heat retention. Khoshbakht et al. (2020) demonstrated that during the cold season, compact geometries in cities like Hamadan can trap solar heat and improve thermal conditions in semi-open spaces, but in warmer months, the same configurations may exacerbate heat stress unless paired with adaptive shading (Khoshbakht et al., 2020). Furthermore, Parsaee et al. (2021) explored how different configurations of shading panels and window sizes affect daylighting and photobiological responses in Arctic climates, underscoring the critical balance between comfort and visual exposure (Parsaee et al., 2021).

Urban microclimates also interact with vegetation, water features, and built morphology in intricate ways that determine the efficacy of passive cooling strategies. Zhao et al. (2018) examined how the location and density of trees impact outdoor thermal comfort, revealing that targeted tree placement can significantly reduce mean radiant temperature in residential settings (Zhao et al., 2018). Aghapour and Taban (2020) similarly emphasized the

importance of vegetation in mitigating heat in open spaces in Ahvaz, where evapotranspiration and shading play a crucial role in comfort provision (Aghapour & Taban, 2020).

Thermal comfort evaluation metrics such as the Physiological Equivalent Temperature (PET) and the Universal Thermal Climate Index (UTCI) are essential tools in these assessments. As Sanagar Darbani et al. (2018) showed in their study on Mashhad, PET is a robust index for quantifying outdoor thermal stress and understanding seasonal comfort variations in Iranian cities (Sanagar Darbani et al., 2018). Similarly, Roshan et al. (2017) provided empirical comfort thresholds for heating and cooling demand estimation across diverse Iranian climates, which are vital for calibrating localized design interventions (Roshan et al., 2017).

The relationship between building design, occupant experience, and energy demand is further explored in the work of Jun and Fei (2024), who applied multi-objective optimization to balance thermal comfort with energy efficiency, highlighting trade-offs inherent in shading, insulation, and ventilation strategies (Jun & Fei, 2024). Fattahi and Sharbatdar (2023) introduced machine learning into thermal comfort prediction, advocating for personalized comfort models that integrate environmental parameters with occupant data to enhance energy recovery and comfort satisfaction (Fattahi & Sharbatdar, 2023).

Traditional architecture in hot-arid regions also offers valuable lessons. Jafarian and Mahmoudian (2024) examined the historical urban fabric of Sirvan and identified passive techniques, such as wind catchers and thermal mass, which naturally regulate temperature and enhance comfort without relying on mechanical systems (Jafarian & Mahmoudian, 2024). Similarly, Pakzad et al. (2018) argue that the theoretical foundations of Iranian urban design are inherently climate-responsive, structured around principles of shade, ventilation, and courtyard-based spatial organization (Pakzad et al., 2018).

In sum, this research integrates simulation-based evaluation and architectural insight to develop an evidence-based model for smart shading design in semi-open balconies.

## 2. Methods and Materials

This study was designed with the aim of identifying the factors influencing the thermal behavior of semi-open spaces in the city of Mashhad, from a developmental and explanatory perspective, using quantitative data (numerical

simulations with Envi-met and Honeybee software). The primary research method is descriptive-analytical and applied, focusing on analyzing climatic conditions and the design of semi-open spaces based on thermal requirements.

### Research Methodology Steps:

- **Initial Questioning:** The research begins by formulating main and sub-questions regarding the factors that affect the thermal behavior of semi-open spaces.
- **Exploratory Studies:** A review of existing theories in climatology, Mashhad's climatic conditions, and thermal comfort standards leads to the development of ideas and hypotheses.
- **Theoretical Framework:** At this stage, the relevant variables are identified, and the network of relationships among them is established to formulate hypotheses.
- **Conceptual Model Development:** The conceptual model explores the relationship between factors influencing thermal comfort and generates testable hypotheses.
- **Data Collection Tools:** Instruments such as documentation, observation, interviews, and questionnaires are used to gather data from the statistical population (common balconies in Mashhad).
- **Data Analysis:** Collected data are analyzed using Envi-met and Honeybee simulation software to model thermal comfort conditions in the studied spaces.
- **Conclusion:** Finally, the results and analyses identify optimal design strategies for shading devices in Mashhad's semi-open spaces, presenting appropriate design patterns.
- **Library Studies:** With the help of literature review and reference to existing documentation, concepts and theories relevant to the research topic are extracted.
- **Field Observation and Data Collection:** To assess the current condition of the study area and gather necessary data—especially quantitative data and statistics related to thermal comfort—field evaluation and temperature variation measurements were conducted.

In this research, different architectural forms of balconies in five-story residential buildings commonly found in Mashhad were examined in terms of their shading patterns

(one-sided, two-sided, and three-sided shading). To determine the required sample size, field studies were conducted to identify common architectural balcony types in the city. Based on these, dominant dimensions and proportions were extracted and standardized as fixed variables to be input into the simulation software. Subsequently, based on statistical sampling methods, the number of necessary samples for simulation and analysis using digital tools was determined.

### 3. Findings and Results

Three balcony series on the southern façade of a four-story apartment building in Mashhad, with identical vertical height across floors but differing in terms of enclosure and

recess/protrusion configurations, were modeled using Envi-met software. The simulations were conducted for two critical solar dates—summer solstice (June 21) and winter solstice (December 22)—from 06:00 to 19:00, reflecting maximum and minimum annual solar radiation, respectively. The simulations were set under climatic and thermal comfort conditions calibrated through the meteorological data integrated into the software. The building was assumed to be insulated, with asphalt ground cover, and balcony dimensions were defined as 4 meters in height, 1 meter in width, and 3 meters in depth. Additional climatic parameters (wind speed, air temperature, humidity) were input based on multi-decade average data from the Mashhad synoptic meteorological station.

**Figure 1**

*Modeling of Balcony Series No. 1 on the Eastern Side Facing South*

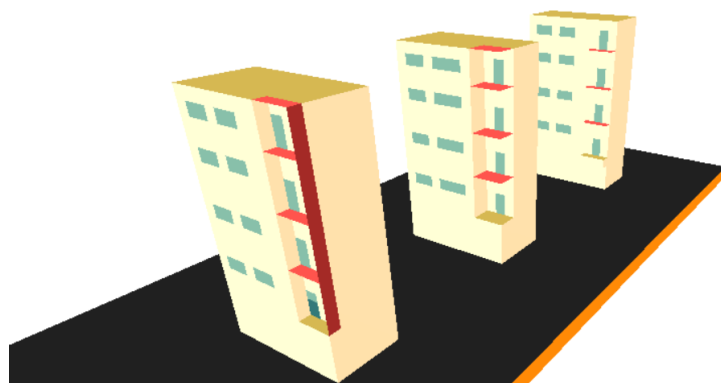


**Figure 2**

*Modeling of Balcony Series No. 2 in the Central Position Facing South*

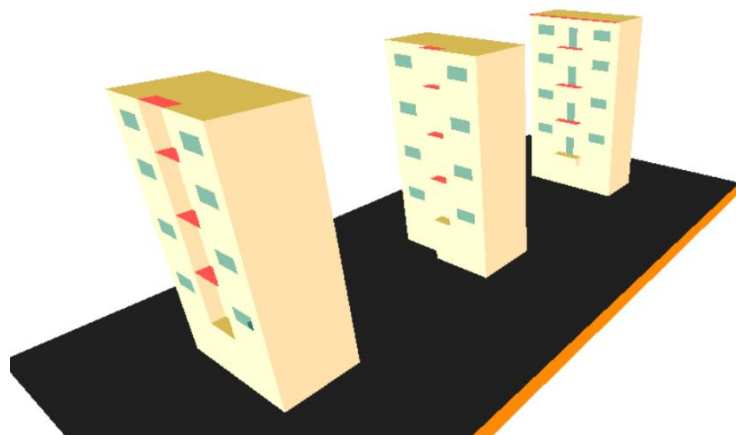


**Figure 3**

*Modeling of Balcony Series No. 3 on the Western Side Facing South*

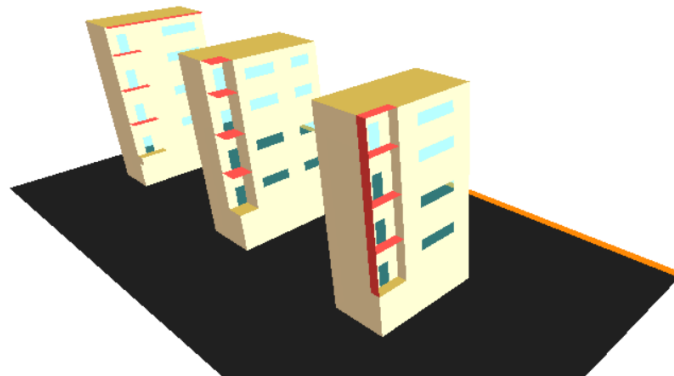


**Figure 4**

*Software Settings for Summer in the Studied Models*

Initial meteorological conditions			
<b>Wind uvw</b>			
Wind speed measured in 10 m height (m/s):	3.23		
Wind direction (deg):	140.00		(0= from North...180= from South...)
Roughness length at measurement site:	0.010		
<b>Temperature T</b>			
Min. and max. temperature of atmosphere (°C):	25.00	(min.)	41.00 (max.)
<b>Humidity q</b>			
Min. and max. relative humidity in 2m (%):	9.00	(min.)	39.00 (max.)

**Figure 5**

*Software Settings for Winter in the Studied Models*

Initial meteorological conditions			
<b>Wind uvw</b>			
Wind speed measured in 10 m height (m/s):	2.60		
Wind direction (deg):	168.00		(0= from North...180= from South...)
Roughness length at measurement site:	0.010		
<b>Temperature T</b>			
Min. and max. temperature of atmosphere (°C):	-7.00	(min.)	0.00 (max.)
<b>Humidity q</b>			
Min. and max. relative humidity in 2m (%):	55.00	(min.)	100.00 (max.)

### Graph Analysis for Balcony Series No. 1

The modeled balconies in Series 1 are located on the southeastern side, on the first floor, and at a height of 4.5 meters above ground level. This series consists of three configurations: Model No. 1 – double-side enclosed recessed balcony; Model No. 2 – single-side enclosed protruding balcony; Model No. 3 – fully open (two-side open) balcony. As seen in Figures 4 and 5, the meteorological data entered into the software are derived from historical records at the Mashhad synoptic station (located at Hashemi Nejad Airport) for June 21 and December 22. The time interval from 06:00 to 19:00 was selected for analysis, corresponding to sunrise and sunset in Mashhad on the specified dates.

The Envi-met output graphs for these balconies illustrate thermal behavior at 12:00 PM during the summer and winter solstices, along with surface temperature profiles of the building in these two scenarios, as shown in Figures 6 to 9.

As indicated in Figure 6, in Series 1 models (eastern façade), the greatest surface temperature range at 12:00 PM on the summer solstice is observed respectively in the double-side enclosed, single-side enclosed, and fully open balcony configurations. Although the surface temperature adjacent to the building is higher in the fully open model compared to the single-side enclosed version, the extent of thermal diffusion is greater in the single-side enclosed model than in the fully open one. Therefore, it can be inferred that while the fully open model on the eastern side generates higher surface temperatures near the building on the summer solstice, its thermal diffusion range is limited. Conversely, on the winter solstice at 12:00 PM, the highest surface heat emission from the eastern balconies is observed in the fully open, single-side enclosed, and double-side enclosed models, respectively.

**Figure 6**

*Building Thermal Behavior at 12:00 PM during the Summer Solstice*

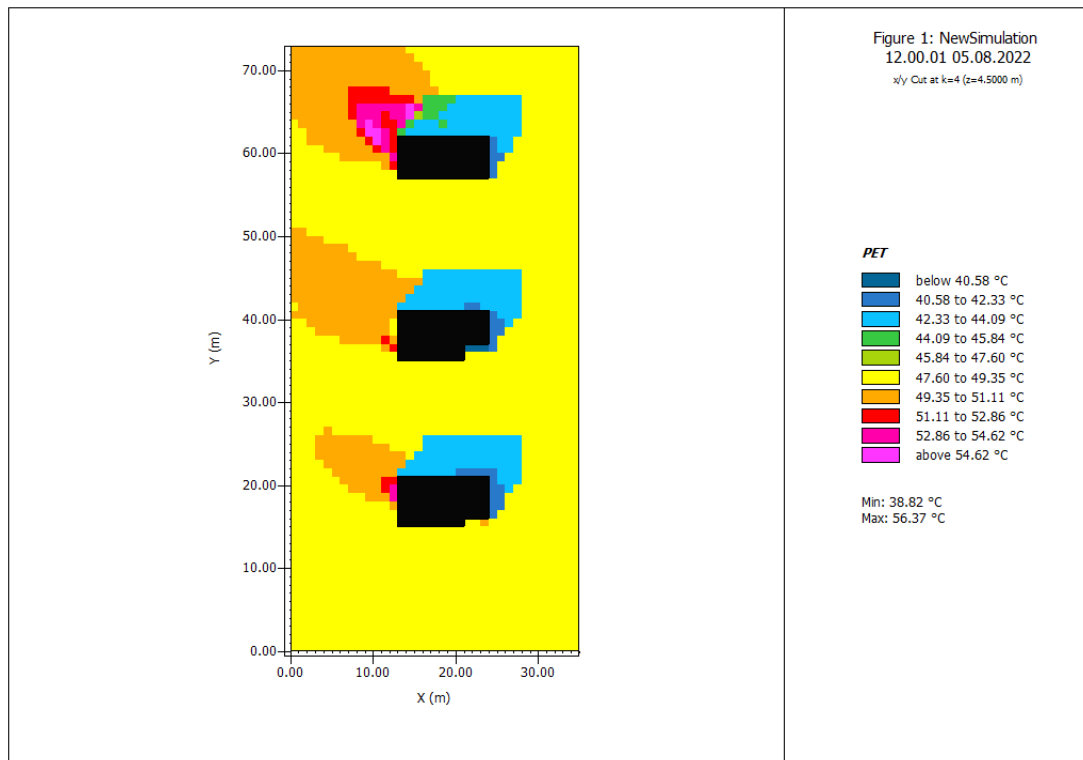


**Figure 7**

*Building Thermal Behavior at 12:00 PM during the Winter Solstice*

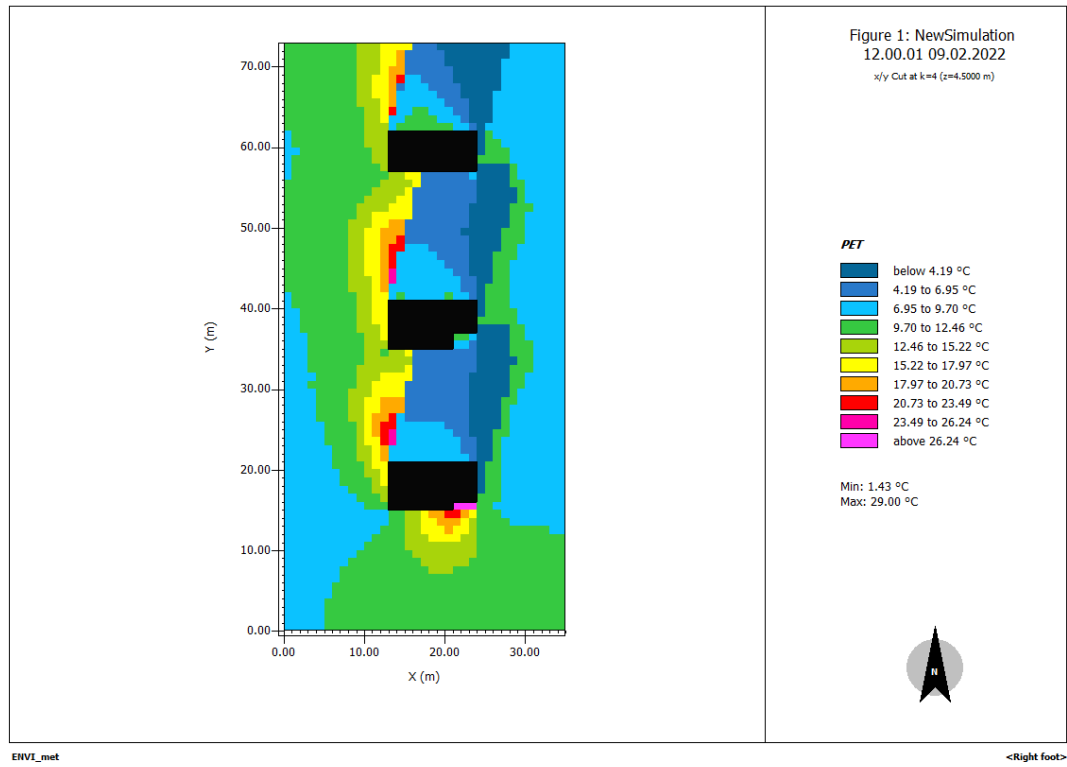


**Figure 8**

*Surface Temperature of the Building at 12:00 PM during the Summer Solstice*

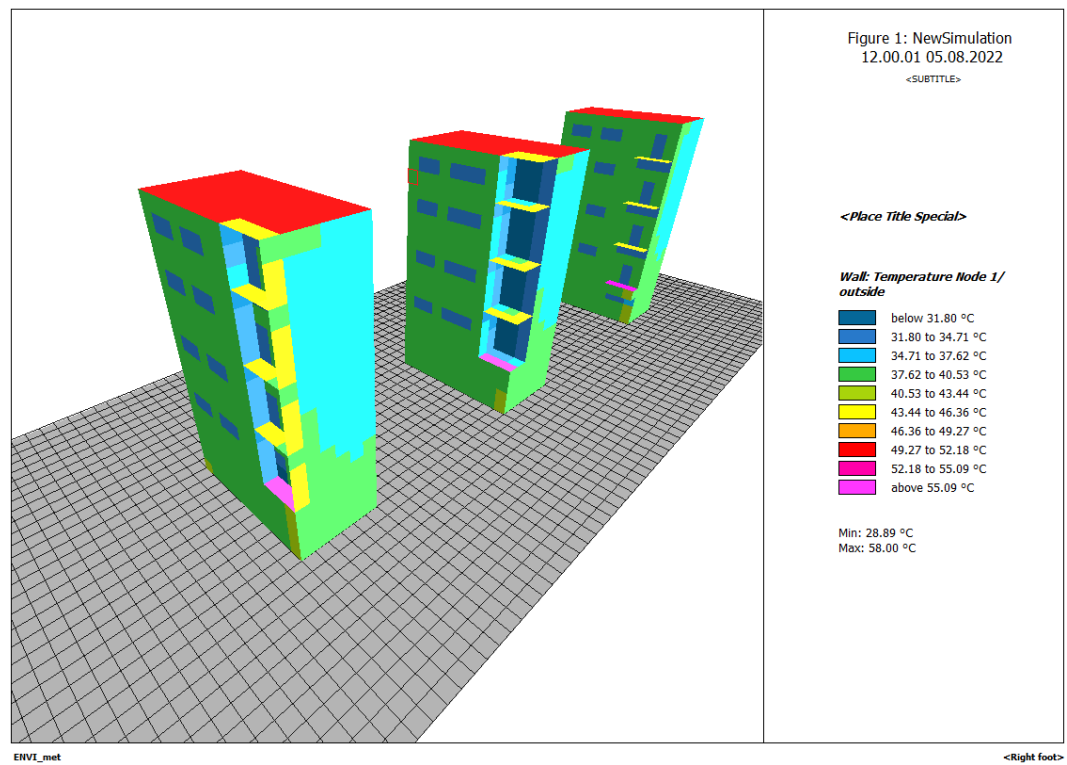
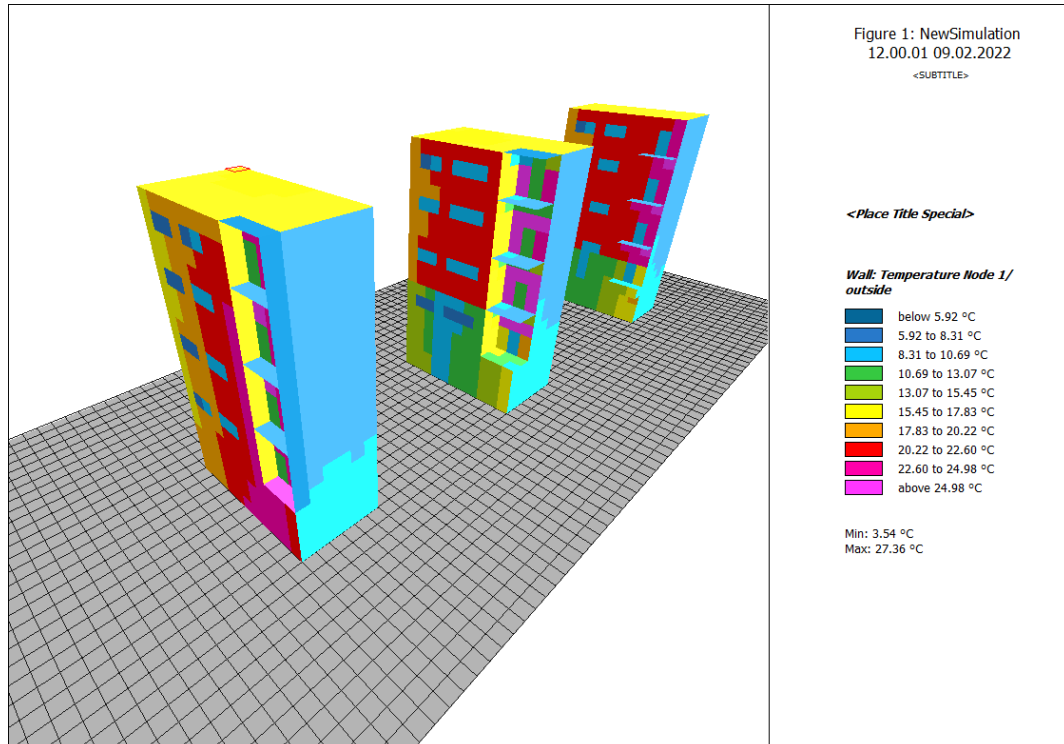




**Figure 9**

*Surface Temperature of the Building at 12:00 PM during the Winter Solstice*



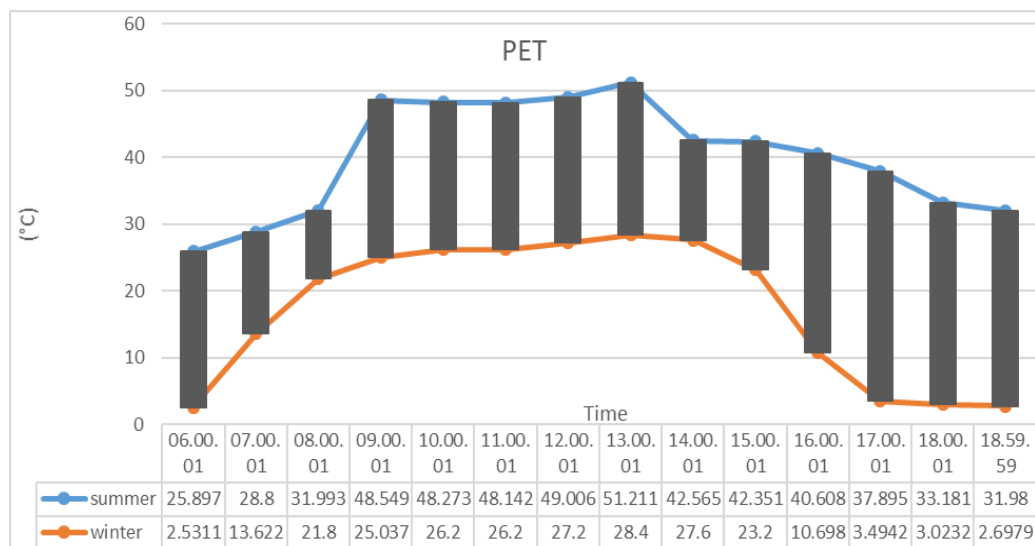
#### Analysis of Balcony Series 1 – Model 1 (Double-Side Enclosed)

In Model No. 1 of Series 1, the balconies are recessed within the structure and enclosed on two sides, while open on the remaining two. On the summer solstice, the lowest PET (Physiological Equivalent Temperature) is recorded at 25.89°C at 06:00 AM, while the highest PET reaches

51.21°C at 01:00 PM. On the winter solstice, the lowest PET is 2.53°C at 06:00 AM, while the peak PET reaches 28.4°C at 01:00 PM. Compared to the other two models on the eastern façade, this balcony exhibits the highest heat emission to the surrounding outdoor environment on the summer solstice and the lowest on the winter solstice.

**Chart 1**

*Comparison of PET for Balcony Series 1 – Model 1 (Double-Side Enclosed) during Summer and Winter Solstices*





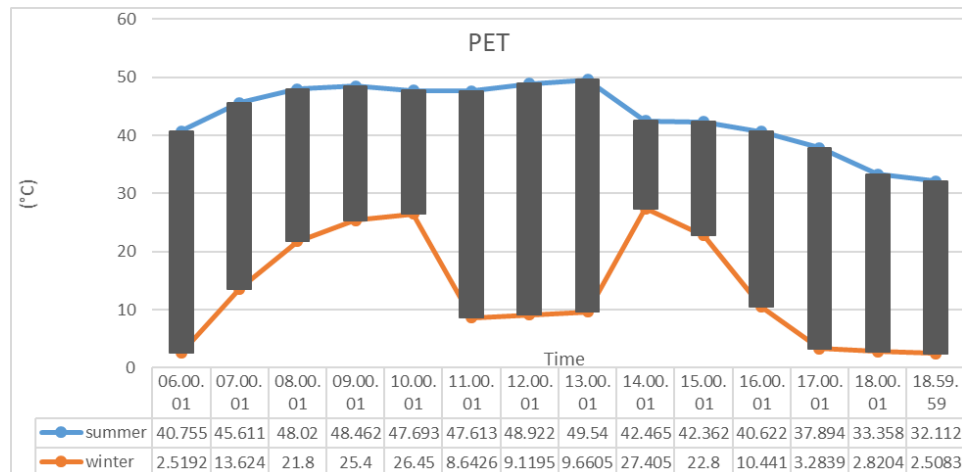
### Analysis of Balcony Series 1 – Model 2 (Single-Side Enclosed)

In Model No. 2 of Series 1, the balconies are implemented as protruding structures, enclosed on one side and open on the remaining three. On the summer solstice, the minimum

PET is recorded at 32.11°C at 07:00 PM, while the maximum PET reaches 49.54°C at 01:00 PM. During the winter solstice, the lowest PET is recorded at 2.5°C at 07:00 PM, and the highest PET is 27.4°C at 02:00 PM.

#### Chart 2

Comparison of PET for Balcony Series 1 – Model 2 (Single-Side Enclosed) during Summer and Winter Solstices



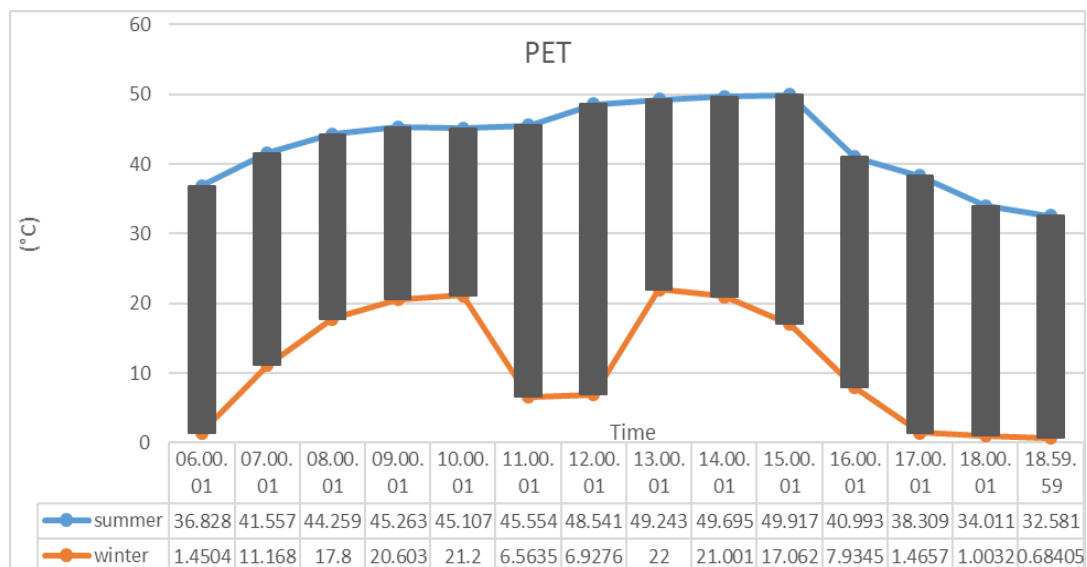
### Analysis of Balcony Series 1: Model Three (Three-Sided Enclosed)

In Model No. 3 of Series 1, where the balconies are enclosed on three sides and open on one side, recessed into the building (with the distinction that on the eastern side, the structure is not built with construction materials but rather acts as a barrier against solar radiation and wind), the lowest PET (Physiological Equivalent Temperature) on the summer

solstice was recorded at 32.5°C at 7:00 PM, while the highest PET reached 49.91°C at 3:00 PM. In winter, the lowest PET was recorded at 0.68°C at 7:00 PM and the highest at 22°C at 1:00 PM. Compared to the other two balcony models on the eastern side, this model produced the least heat diffusion in the exterior surrounding space on the summer solstice and the most on the winter solstice.

#### Chart 3

Comparison of PET Temperatures for Balcony Series 1: Model Three (Three-Sided Enclosed) during Summer and Winter Solstices



## Comparative Analysis of Different Balcony Models in Series 1

To achieve a proper understanding of the comparison among the balconies in Series 1, the three configurations were evaluated on the summer and winter solstices under identical climatic conditions. Therefore, dedicated charts

were constructed for summer and winter solstice scenarios to facilitate a more precise comparative analysis of these three models. Charts 4 and 5 illustrate the comparative PET performance of the three balcony models in Series 1 under both solstice conditions.

### Chart 4

Comparison of the Three Balcony Models in Series 1 on the Summer Solstice

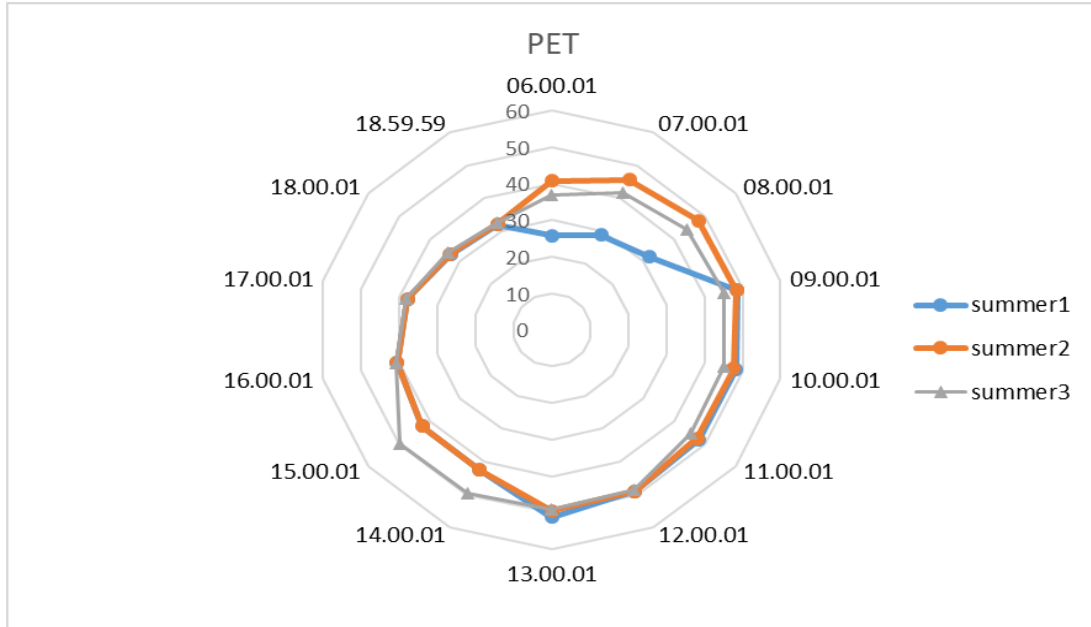
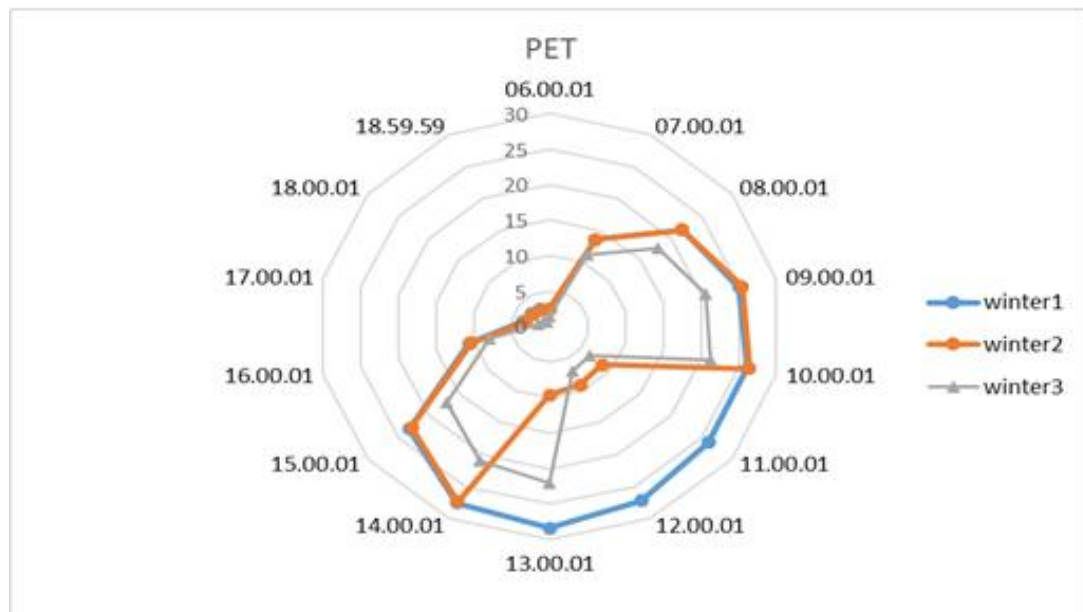


### Chart 5

Comparison of the Three Balcony Models in Series 1 on the Winter Solstice



### Conclusion of the Comparison of the Three Models in Series 1 (Eastern Façade)

According to the comparative assessments among the three balcony models in Series 1, none of the eastern-facing balconies achieved thermal comfort on the summer solstice. On the winter solstice, the double-sided enclosed model reached the comfort zone at 8:00 AM; the single-sided enclosed model did so at 8:00 AM and 3:00 PM (total of two hours); and the three-sided enclosed model achieved comfort between 8:30–10:00 AM and 1:00–2:00 PM. However, due to the fluctuating thermal patterns observed in the double-sided and single-sided enclosed models on the winter solstice, the overall thermal behavior of the double-sided enclosed balcony in both solstice scenarios is more stable and favorable than the other models on the eastern façade.

### Graph Analysis for Balcony Series No. 2

The balconies in Series 2, all located on the southern side and at a height of 4.5 meters above ground level, were modeled in three different configurations: Model No. 1 – three-sided enclosed recessed within the building; Model No. 2 – single-sided enclosed as a protruding volume; Model No. 3 – double-sided open with building setback allowing

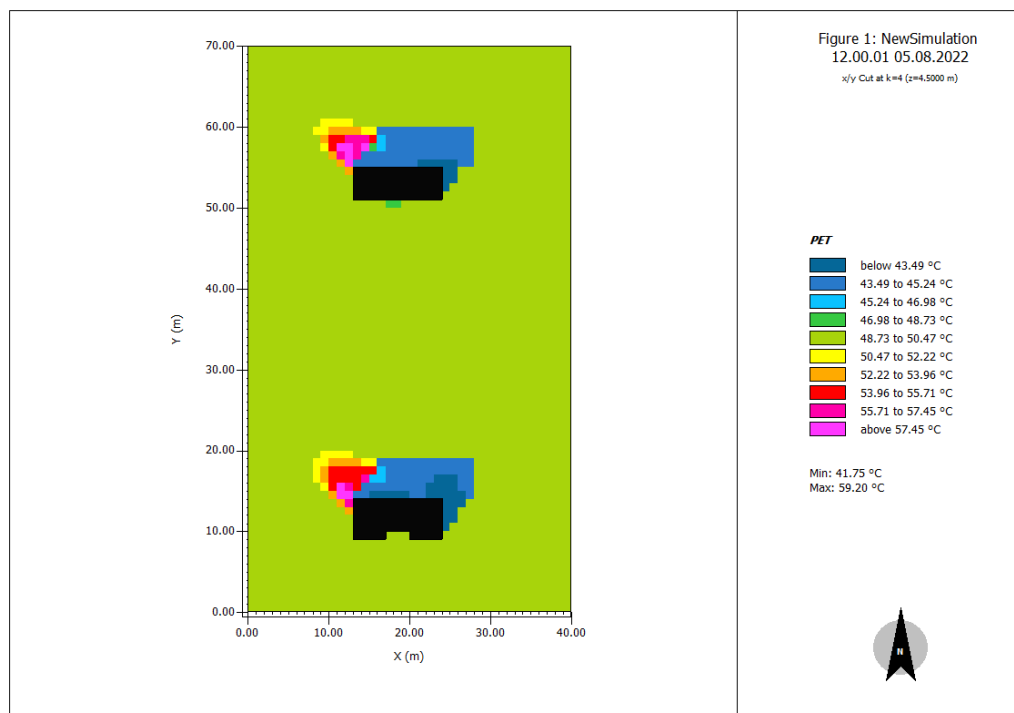
light access from the west. The thermal behavior outputs of the Envi-met software for these models at 12:00 PM during the summer and winter solstices are presented in the following figures.

As illustrated in Figures 10 and 11, in the models of Series 2 (central façade), the highest exterior surface temperatures at 12:00 PM on the summer solstice are found in the double-sided enclosed, single-sided enclosed, and three-sided enclosed configurations, respectively. The heat diffusion range in the double-sided enclosed model is slightly broader than in the other two configurations, although the difference is minimal. Thus, the thermal behavior of these three models at 12:00 PM on the summer solstice does not show substantial variation in terms of external heat dispersion.

However, at 12:00 PM on the winter solstice, the double-sided enclosed, single-sided enclosed, and three-sided enclosed models sequentially exhibit the greatest thermal radiation to the building's outer surface and its surrounding environment. Unlike the summer solstice, the differences in thermal behavior among the three models are quite pronounced during the winter solstice.

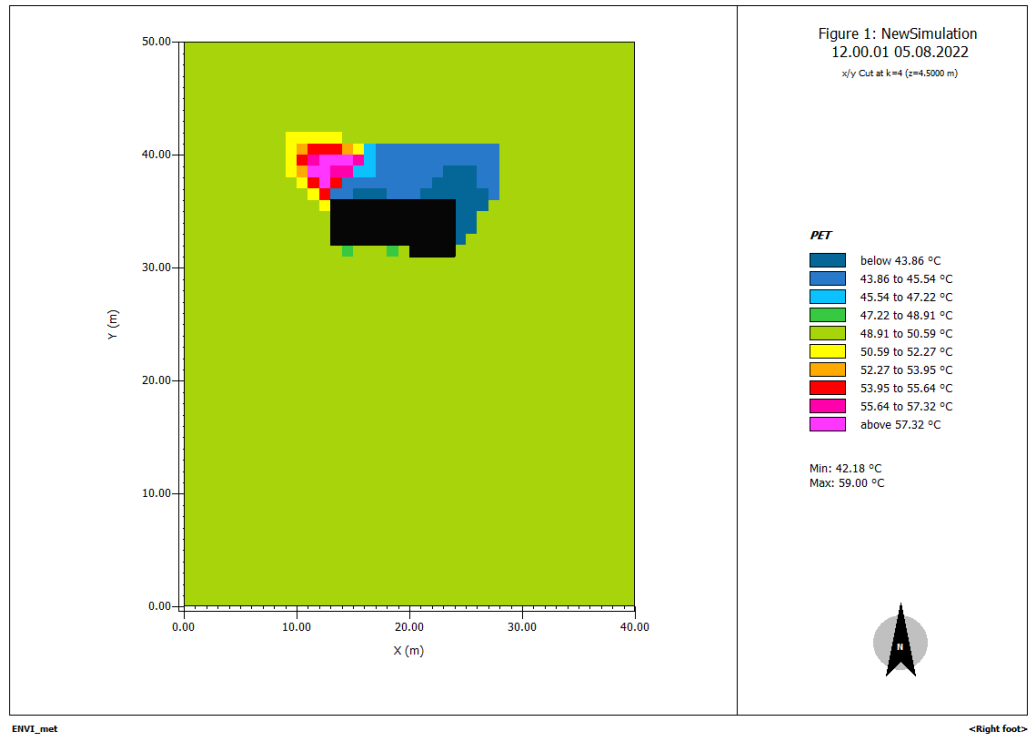
**Figure 10**

*Thermal Behavior of the First Two Models in Series 2 at 12:00 PM on the Summer Solstice*



**Figure 11**

*Thermal Behavior of the Third Model in Series 2 at 12:00 PM on the Summer Solstice*


**Figure 12**

*Thermal Behavior of the First Two Models in Series 2 at 12:00 PM on the Winter Solstice*

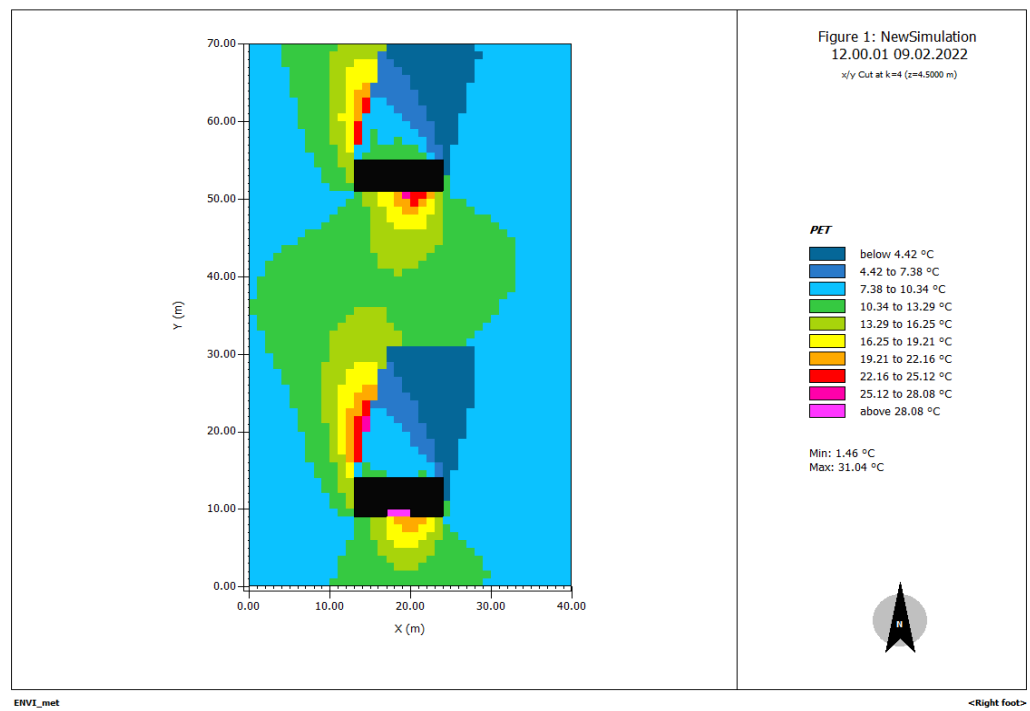


**Figure 13**

*Thermal Behavior of the Third Model in Series 2 at 12:00 PM on the Winter Solstice*

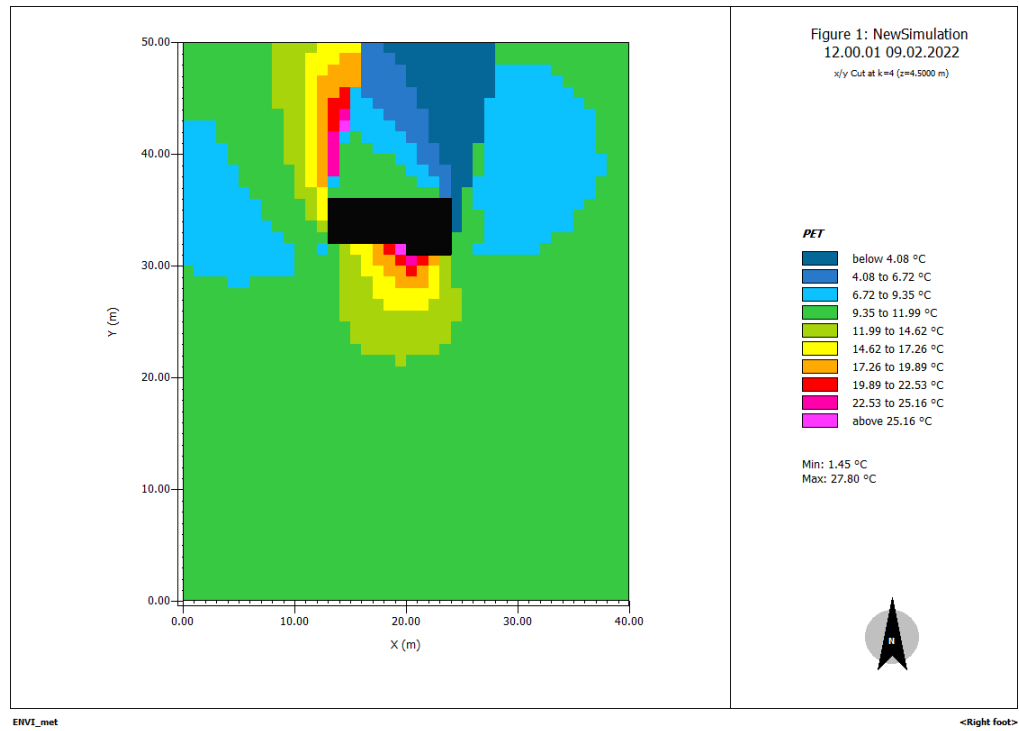


**Figure 14**

*Exterior Surface Temperatures of the First Two Models in Series 2 at 12:00 PM on the Summer Solstice*

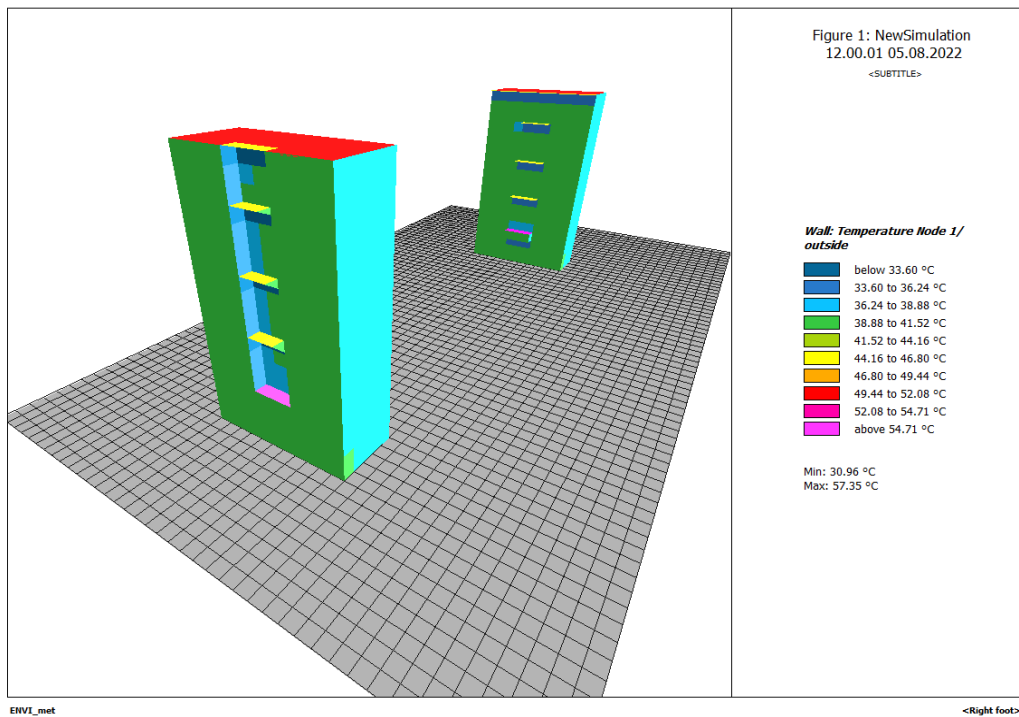


**Figure 15**

*Exterior Surface Temperature of the Third Model in Series 2 at 12:00 PM on the Summer Solstice*

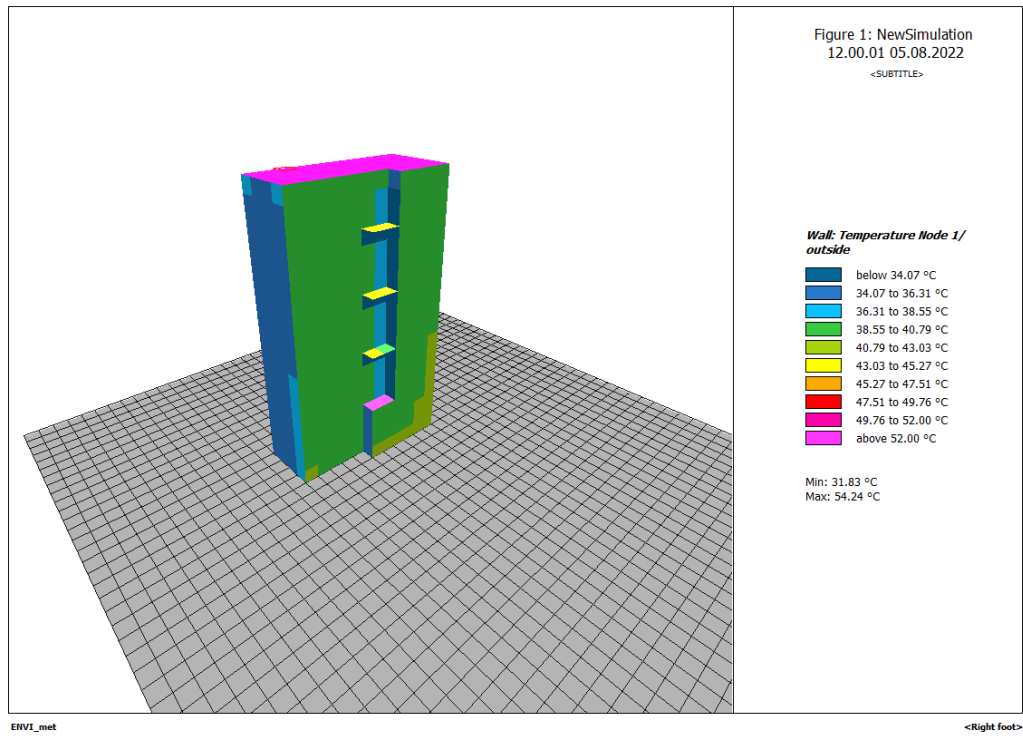


**Figure 16**

*Exterior Surface Temperatures of the First Two Models in Series 2 at 12:00 PM on the Winter Solstice*

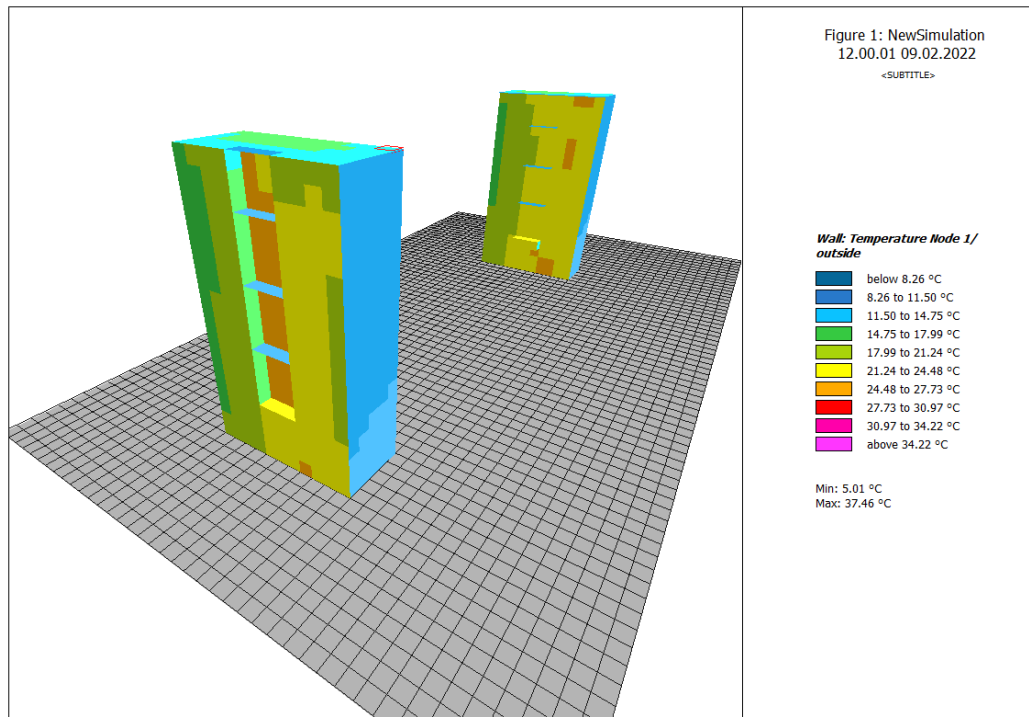
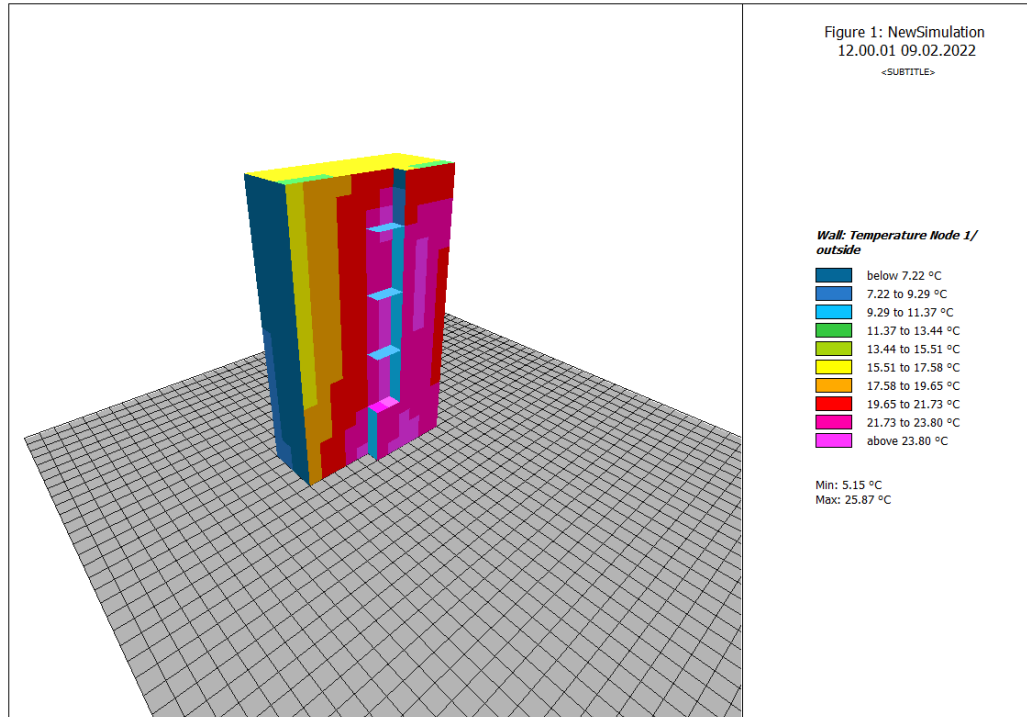


**Figure 17**

*Exterior Surface Temperature of the Third Model in Series 2 at 12:00 PM on the Winter Solstice*



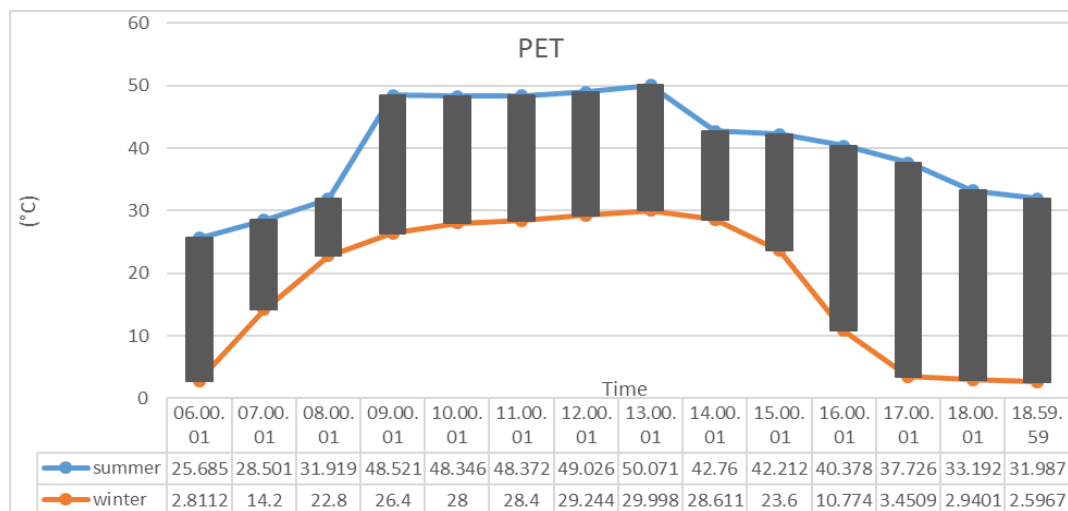
### Analysis of Balcony Series Two: Model 1 (Three-Sided Enclosure)

In Model 1 of Series Two, where balconies are enclosed on three sides and open on one side, recessed into the central section of the building, the lowest PET (Physiological Equivalent Temperature) on the summer solstice was

recorded at 25.68°C at 6:00 AM, and the highest temperature reached 50°C at 1:00 PM. On the winter solstice, the lowest PET was 2.59°C at 7:00 PM, and the highest was 29.9°C at 1:00 PM. Figure 6 provides further details, showing the hourly variation trends for both solstices.

**Chart 6**

*Comparison of PET Temperatures – Series Two Balconies: Model 1 (Three-Sided Enclosure) during Summer and Winter Solstices*





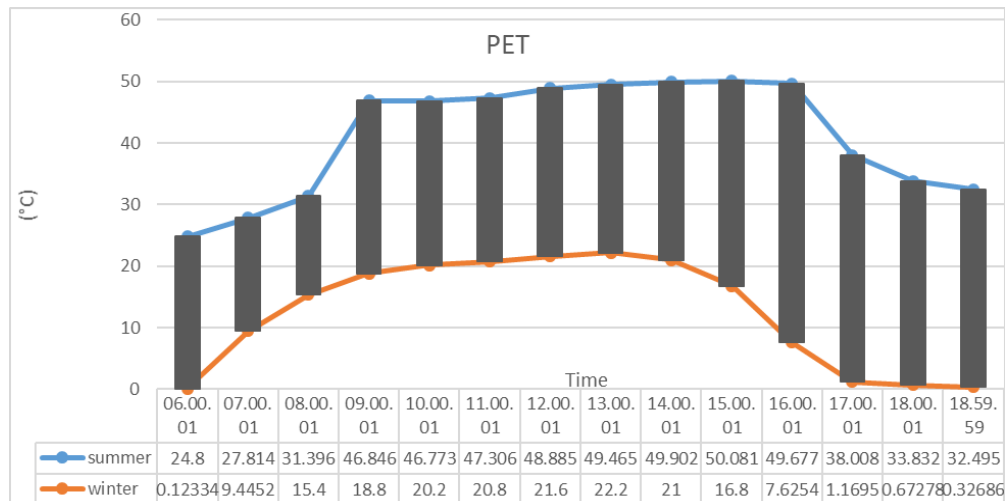
### Analysis of Balcony Series Two: Model 2 (One-Sided Enclosure)

In Model 2 of Series Two, where balconies are open on three sides and enclosed on one side, protruding from the

central part of the building, the lowest PET on the summer solstice was 24.8°C at 6:00 AM, and the highest was 50°C at 3:00 PM. In winter, the lowest PET was 0.12°C at 6:00 AM, and the highest was 22.2°C at 1:00 PM.

Chart 7

Comparison of PET Temperatures – Series Two Balconies: Model 2 (One-Sided Enclosure) during Summer and Winter Solstices



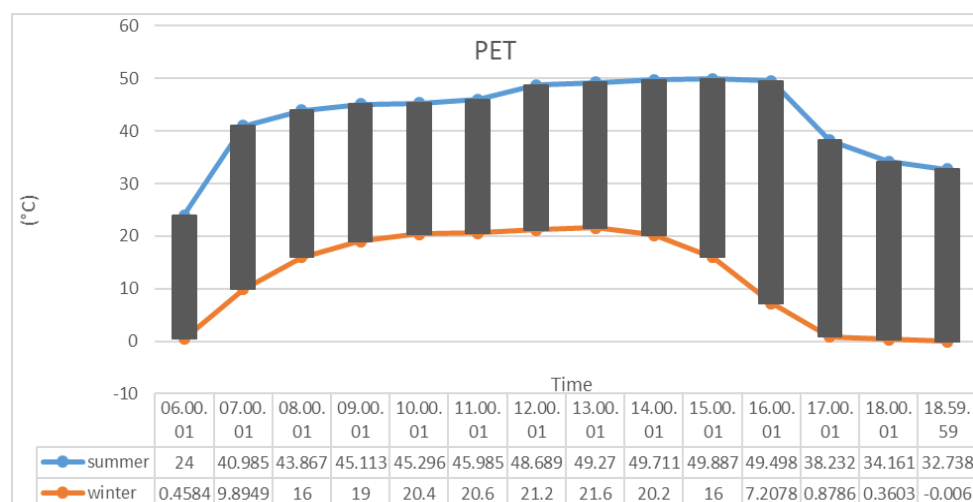
### Analysis of Balcony Series Two: Model 3 (Two-Sided Enclosure)

Model 3 in Series Two includes balconies open on two sides and enclosed on two sides. The balcony is located centrally, and due to building setbacks, it receives daylight

from the west. On the summer solstice, the lowest PET was 24°C at 7:00 PM, and the highest was 49.88°C at 3:00 PM. In winter, the PET ranged from 0°C at 7:00 PM to 21.6°C at 1:00 PM.

Chart 8

Comparison of PET Temperatures – Series Two Balconies: Model 3 (Two-Sided Enclosure) during Summer and Winter Solstices



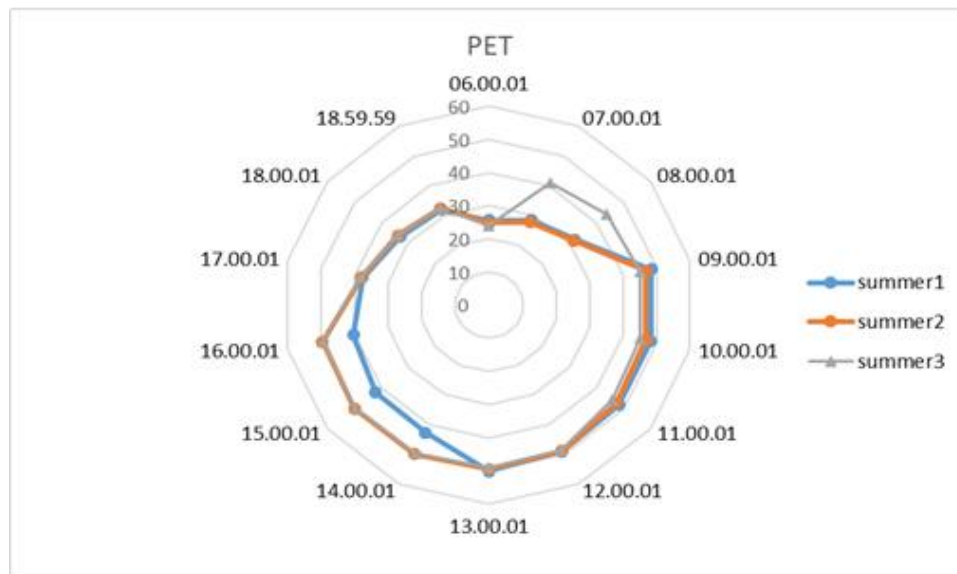
### Comparative Analysis of Balcony Series Two Models

To accurately compare the three models of Series Two, it is necessary to analyze them under identical climatic

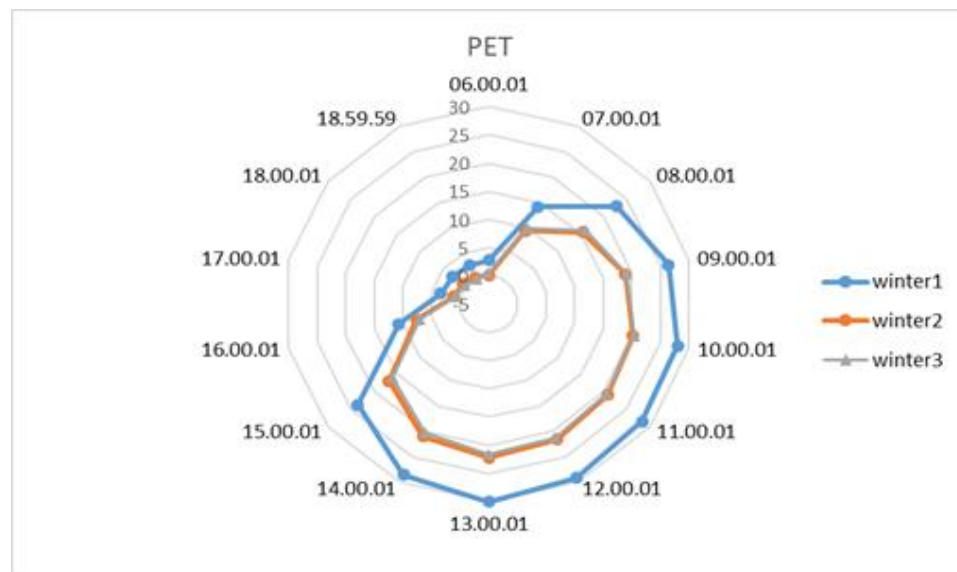
conditions in both summer and winter. Therefore, individual graphs for summer and winter solstices are presented.

**Chart 9**

*Comparison of Three Balcony Models – Series Two (Summer Solstice)*


**Chart 10**

*Comparison of Three Balcony Models – Series Two (Winter Solstice)*



### Evaluation of the Comparison – Series Two (Central Façade)

In both summer and winter, the two-sided enclosed balconies (Model 3) showed better thermal conditions compared to the other models, with temperatures in the first floor closer to the thermal comfort range. On the summer solstice, none of the central façade balconies met thermal comfort criteria. However, on the winter solstice, the two-sided model reached thermal comfort from 8:30 AM to 2:30

PM, the one-sided model from 9:00 AM to 2:00 PM, and the three-sided model only at 8:00 AM.

### Graph Analysis – Balcony Series Three

Series Three balconies are located on the southwest side of the building, first floor, 4.5 meters above ground. The three variations include:

Model 1: Two-sided enclosure recessed into the building with a western barrier preventing sun penetration.

Model 2: One-sided enclosure, protruding from the western-southern side.

Model 3: Two open sides, not recessed.

Envi-met output graphs show thermal behavior at 12:00 PM on both solstices and the surface temperature of the building.

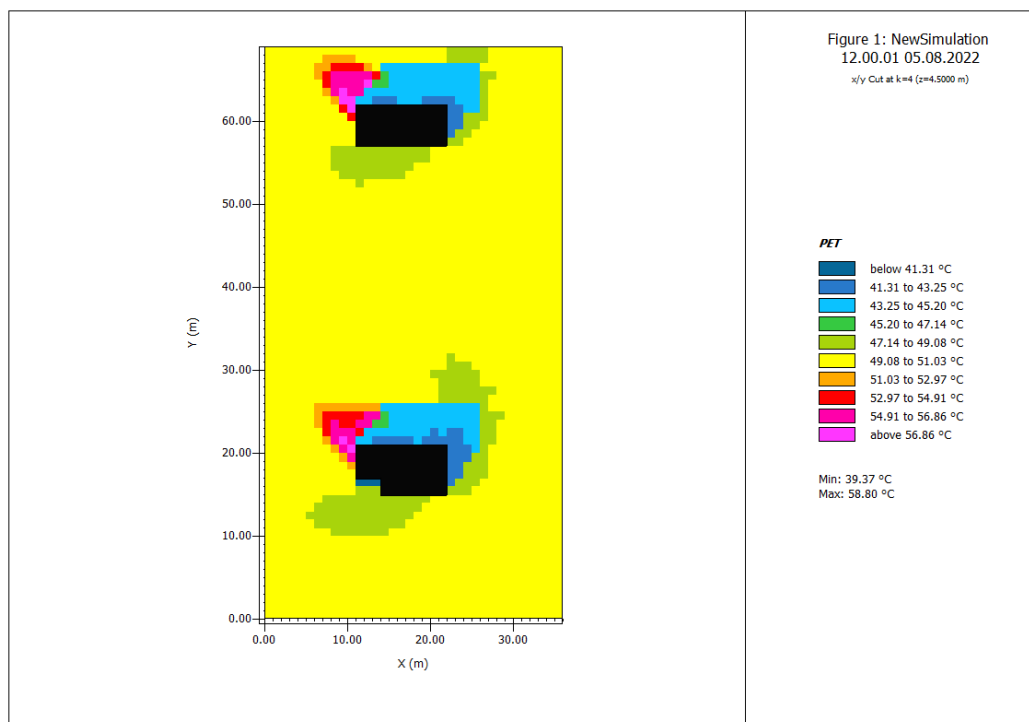
As illustrated in Figures 18 and 19, in the western façade models (Series Three), the highest surface temperatures at 12:00 PM on the summer solstice occurred in the following order: one-sided, two-sided, then three-sided. However, no notable difference was observed in the lowest surrounding

temperatures. The spread of heat in the two-sided model was smaller than in the other two models.

According to Figure 20, on the winter solstice at noon, the highest surrounding temperatures were recorded for the three-sided, one-sided, and two-sided models, respectively. Similarly, the widest heat dispersion was found in the three-sided model, followed by the two-sided and one-sided models. Thus, the three-sided balcony on the western side exhibited the highest surrounding temperature and the broadest heat dispersion at noon during the winter solstice.

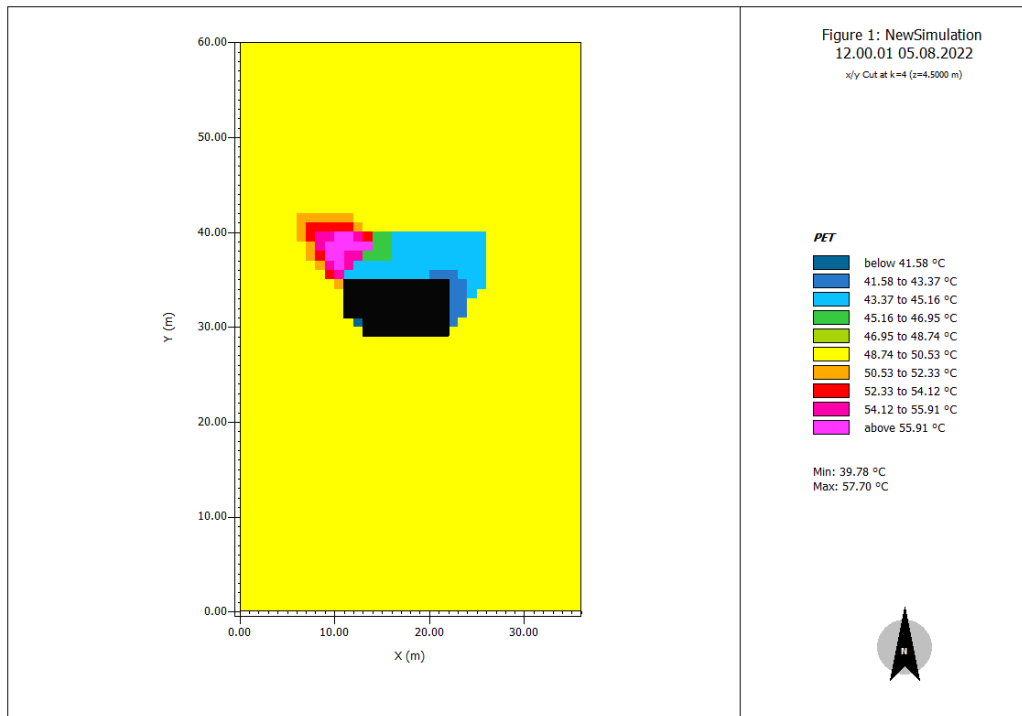
**Figure 18**

*Thermal Behavior of Two Initial Models – Series Three (Summer Solstice, 12:00 PM)*

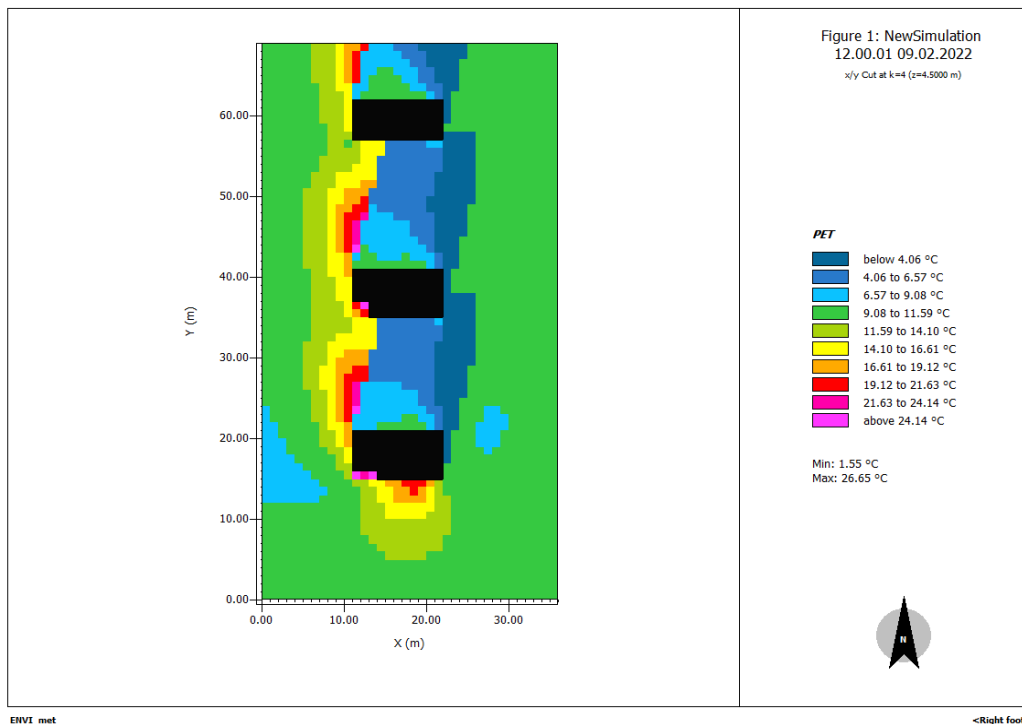


**Figure 19**

*Thermal Behavior of Model Three – Series Three (Summer Solstice, 12:00 PM)*


**Figure 20**

*Thermal Behavior of All Models – Series Three (Winter Solstice, 12:00 PM)*

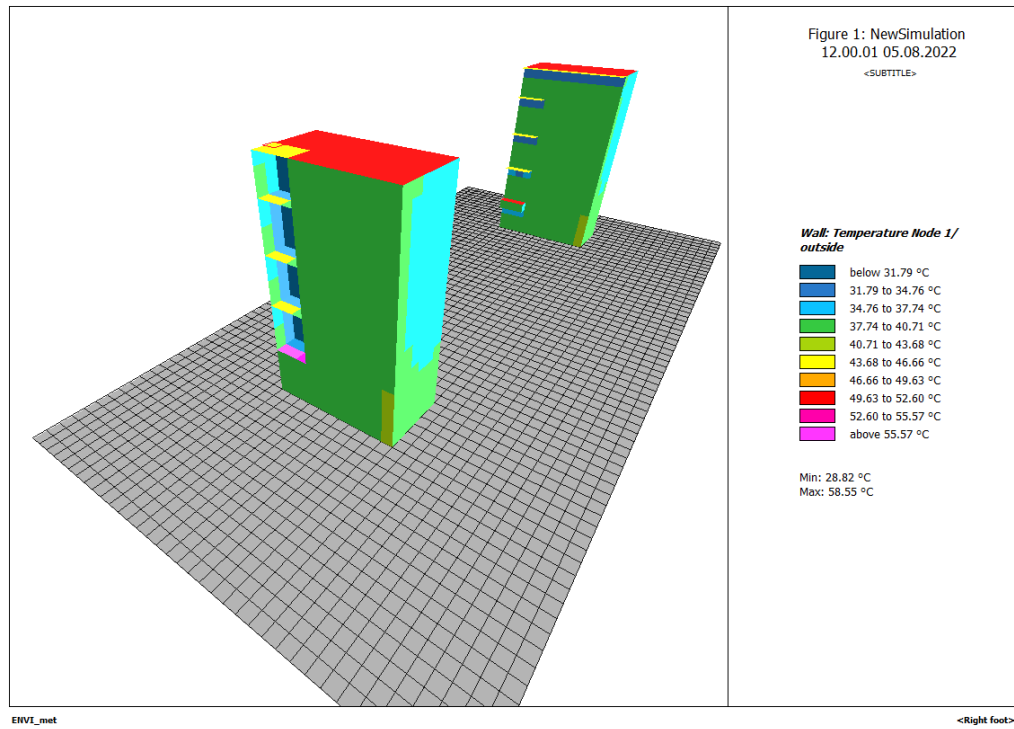


ENVI\_met

&lt;Right foot&gt;

**Figure 21**

*Surface Temperatures – Two Initial Models – Series Three (Summer Solstice, 12:00 PM)*


**Figure 22**

*Surface Temperature – Model Three – Series Three (Summer Solstice, 12:00 PM)*

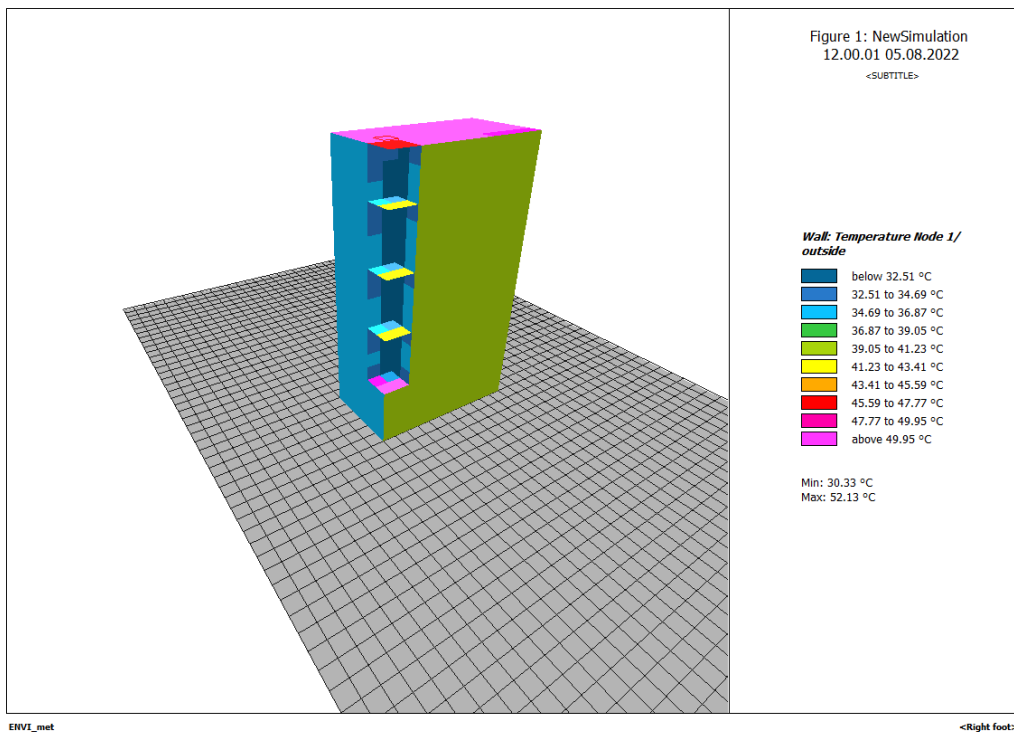
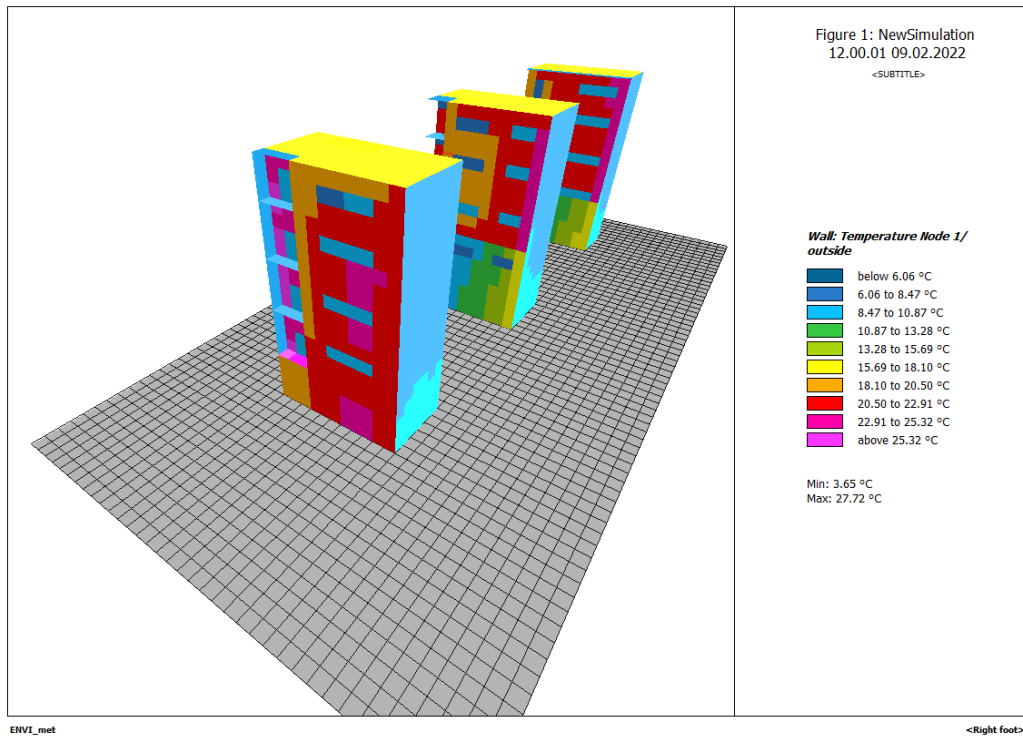


**Figure 23**

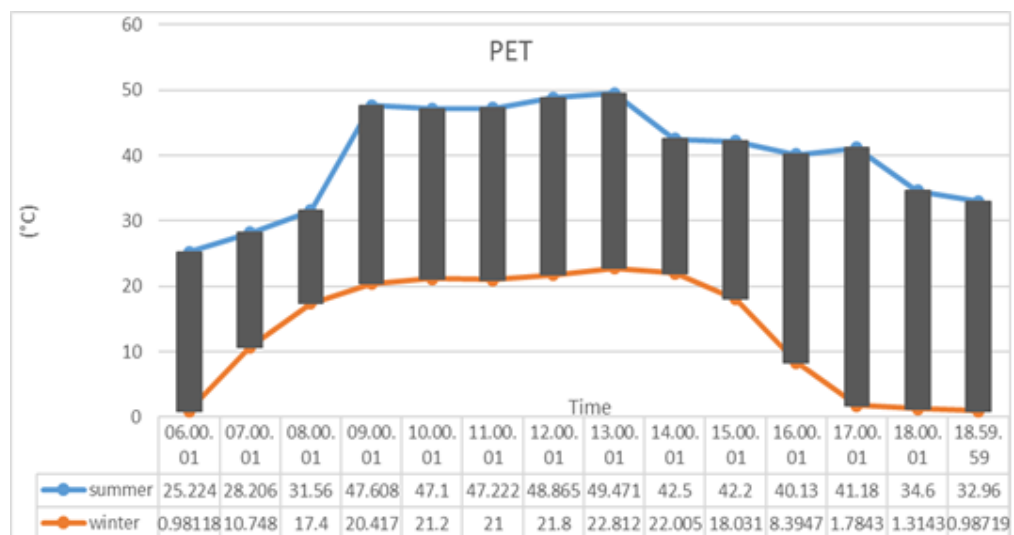
Surface Temperatures – All Models – Series Three (Winter Solstice, 12:00 PM)



### Analysis of Balcony Series Three: Model 1 (Three-Sided Enclosure)

**Chart 11**

Comparison of PET Temperatures – Series Three: Model 1 (Three-Sided Enclosure) during Summer and Winter Solstices



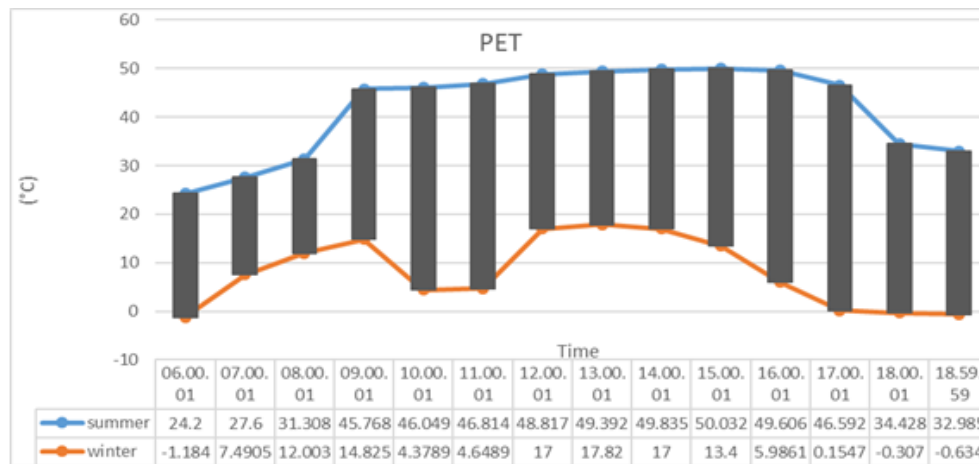
Model 1 in Series Three is recessed, enclosed on three sides, and shielded from western sunlight. The lowest PET during the summer solstice was 25.22°C at 6:00 AM, and the

highest was 49.47°C at 1:00 PM. In winter, the PET ranged from 0.98°C at 6:00 AM to 22.8°C at 1:00 PM.

### Analysis of Balcony Series Three: Model 2 (One-Sided Enclosure)

**Chart 12**

Comparison of PET Temperatures – Series Three: Model 2 (One-Sided Enclosure) during Summer and Winter Solstices



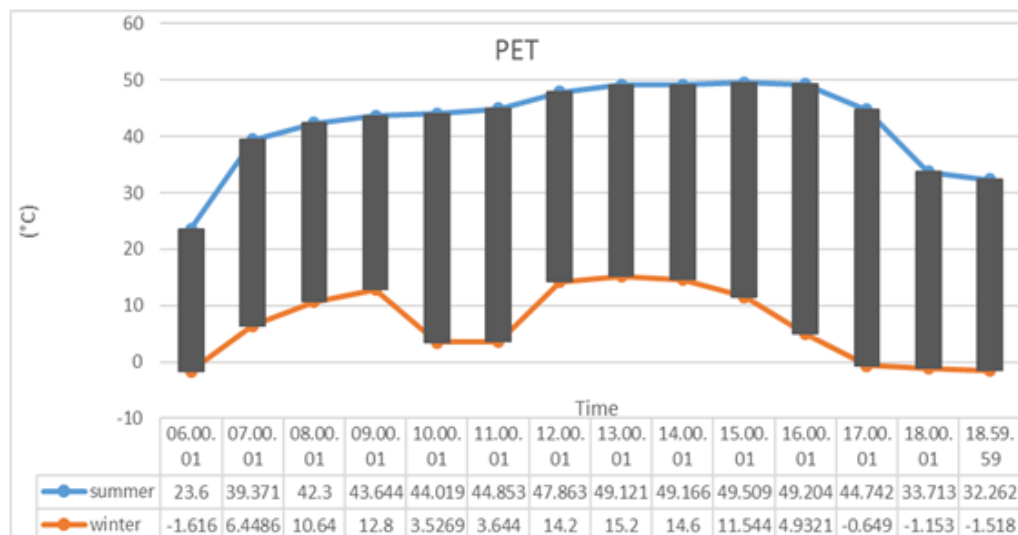
Model 2 in Series Three is a one-sided enclosed balcony protruding from the southwestern section of the building. The summer solstice PET ranged from 24.2°C at 6:00 AM to 50°C at 3:00 PM. In winter, PET ranged from -1.18°C at 6:00 AM to 17.8°C at 1:00 PM.

#### Analysis of Balcony Series Three: Model 3 (Two-Sided Enclosure)

In Model 3 of Series Three, the balcony is open on two sides and enclosed on two sides, located on the southwestern façade. The summer PET ranged from 23.6°C at 6:00 AM to 49.5°C at 3:00 PM. In winter, PET ranged from -1.6°C at 6:00 AM to 15.2°C at 1:00 PM.

**Chart 13**

Comparison of PET Temperatures – Series Three: Model 3 (Two-Sided Enclosure) during Summer and Winter Solstices



#### Comparative Analysis of Series Three Balcony Models

To better understand the conditions and derive a precise comparative analysis of Series Three balconies, the three configurations must be compared for both summer and

winter under identical climatic conditions. Therefore, the aggregate graphs below can be generated separately for the summer and winter solstices. Charts 14 and 15 present a comparison of the three Series Three balcony models on the summer and winter solstice days, respectively.



Chart 14

Comparison of the Three Balcony Models – Series Three (Summer Solstice)

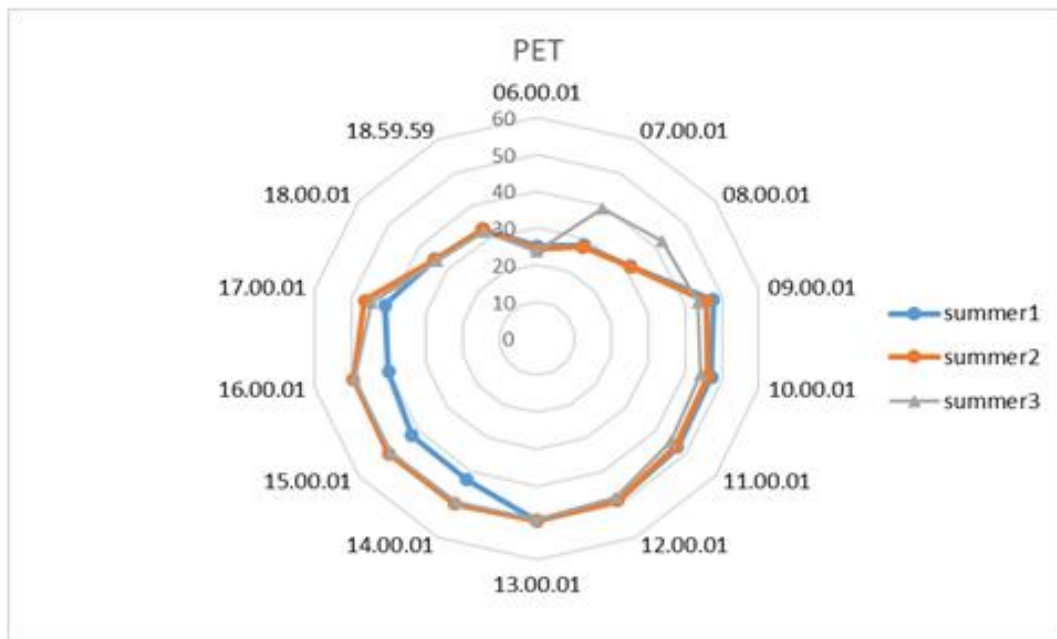
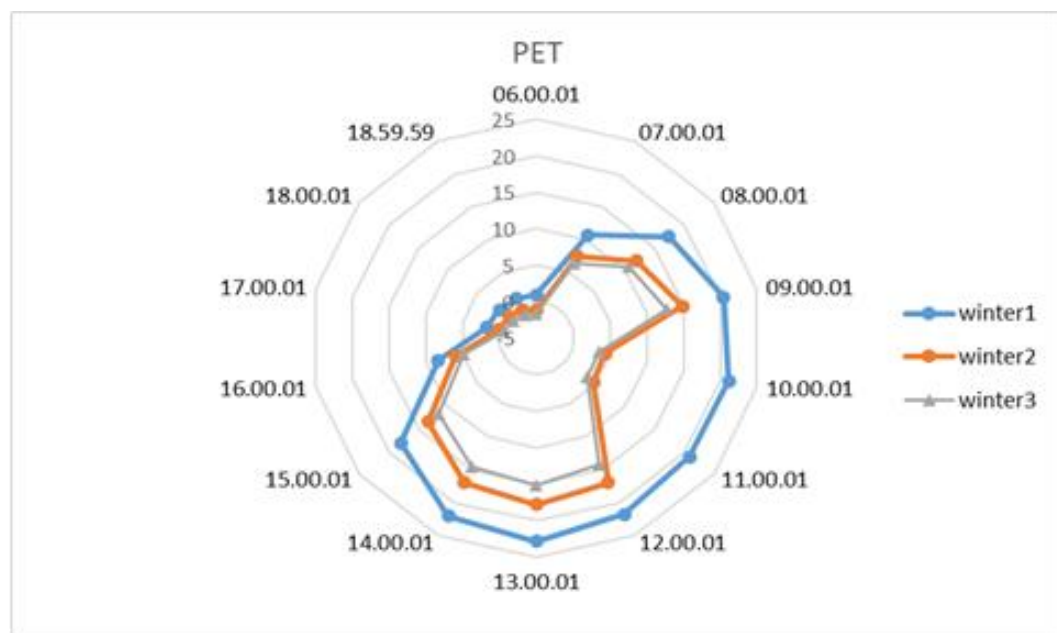


Chart 15

Comparison of the Three Balcony Models – Series Three (Winter Solstice)



### Conclusion of the Comparison – Series Three Models (Western Façade)

Based on the analysis conducted for both solstice days, the three-sided enclosed balcony model (Model 3) performs better than the other two models in this series. More specifically, on the summer solstice, none of the three western façade balcony models meet thermal comfort

conditions. However, on the winter solstice, the three-sided enclosed model on the western side maintains thermal comfort between 9:00 AM and 2:00 PM, while the other two Series Three models do not achieve thermal comfort at any point during the day.

### Evaluation of Thermal Behavior in Models Created with Envi-met Software

**Table 1**

*Summary of Output Results from Envi-met Software*

Balcony Series	Balcony Model	Comfort Hours (Summer Solstice)	Comfort Hours (Winter Solstice)	Avg. PET (Summer)	Avg. PET (Winter)	Max/Min PET (Summer)	Max/Min PET (Winter)
Series One (East)	Model 1: Two-Sided Enclosure	0	1.00	40.02	17.26	51.21 / 25.89	28.4 / 2.53
	Model 2: One-Sided Enclosure	0	2.00	43.24	13.32	49.54 / 32.11	27.4 / 2.5
	Model 3: Three-Sided Enclosure	0	2.50	42.98	11.21	49.91 / 32.5	22.0 / 0.68
Series Two (Center)	Model 1: Three-Sided Enclosure	0	1.00	39.90	18.13	50.0 / 25.68	29.9 / 2.59
	Model 2: One-Sided Enclosure	0	5.00	41.23	17.32	50.0 / 24.8	22.2 / 0.12
	Model 3: Two-Sided Enclosure	0	6.00	42.67	12.41	49.88 / 24.0	21.6 / 0.0
Series Three (West)	Model 1: Three-Sided Enclosure	0	5.00	39.91	13.5	49.47 / 25.22	22.8 / 0.98
	Model 2: One-Sided Enclosure	0	0	44.96	8.04	50.0 / 24.2	17.8 / -1.18
	Model 3: Two-Sided Enclosure	0	0	42.38	6.61	49.5 / 23.6	15.2 / -1.6

By comparing the different models simulated with Envi-met, it can be concluded that none of the models achieve thermal comfort on the summer solstice. However, on the winter solstice, the two-sided enclosed model located at the center of the building provides the highest duration of thermal comfort (6 hours). Following this, the centrally located one-sided model and the three-sided enclosed model on the western façade offer the next longest durations. The weakest performing models in terms of thermal comfort duration are the one-sided and two-sided enclosed balconies on the western façade, which do not meet comfort conditions on either solstice.

### Simulation Process Using the HoneyBee Plugin within EnergyPlus

The HoneyBee plugin, part of the Ladybug Tools suite, was first released in 2014. HoneyBee functions as a user interface for EnergyPlus, transferring energy simulation data from Rhino and Grasshopper environments to EnergyPlus and OpenStudio. After simulation, it returns the results back to Rhino and Grasshopper. As a result, architects and designers can conduct energy simulations through Rhino modeling without dealing with the complexities of EnergyPlus.

**Figure 24**

*HoneyBee Plugin Capabilities (Source: <https://www.ladybug.tools>, 2022)*

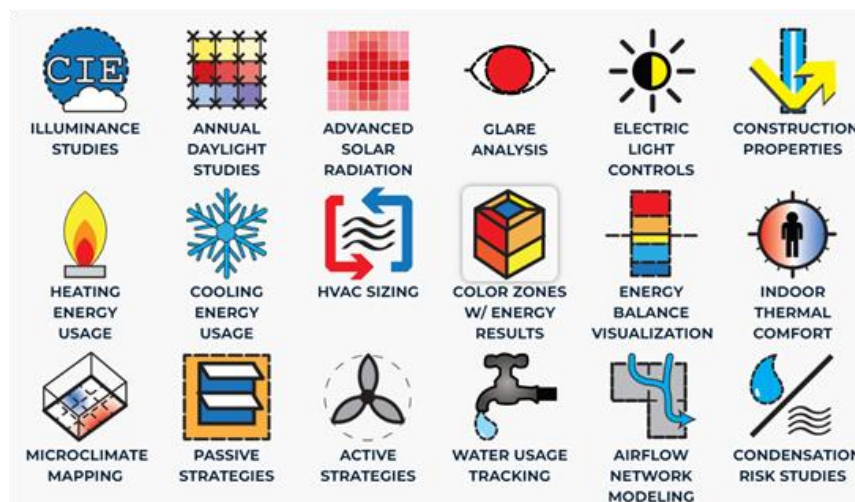


**Figure 25**

Interface Structure and Relationship Between Software and Plugin (Source: <https://www.ladybug.tools>, 2022)

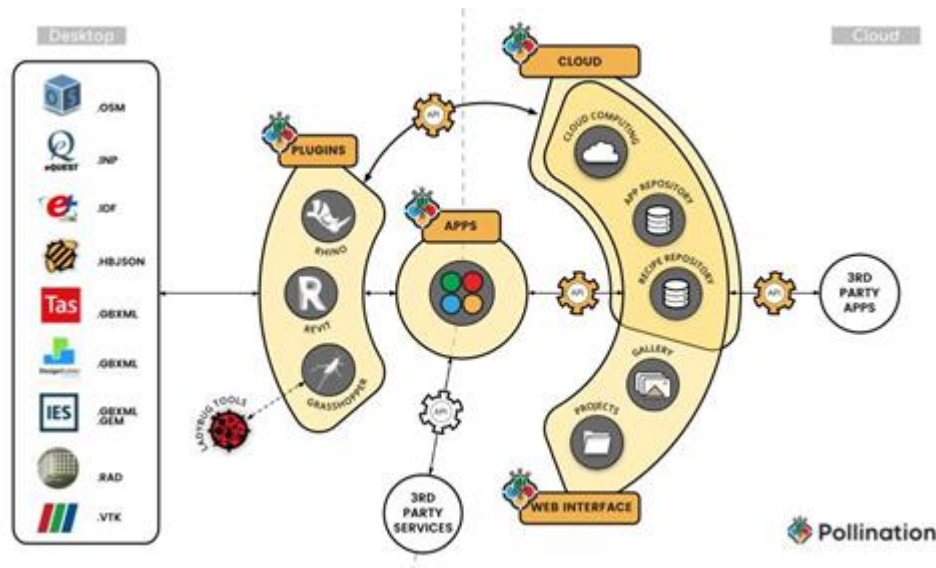
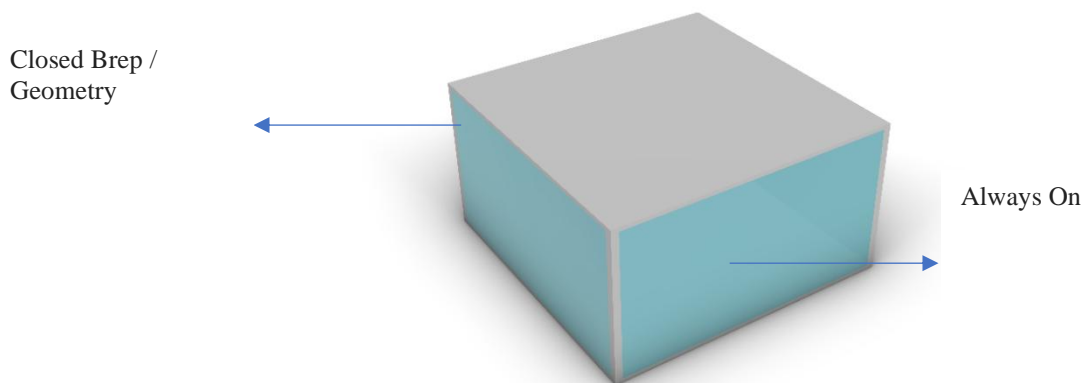


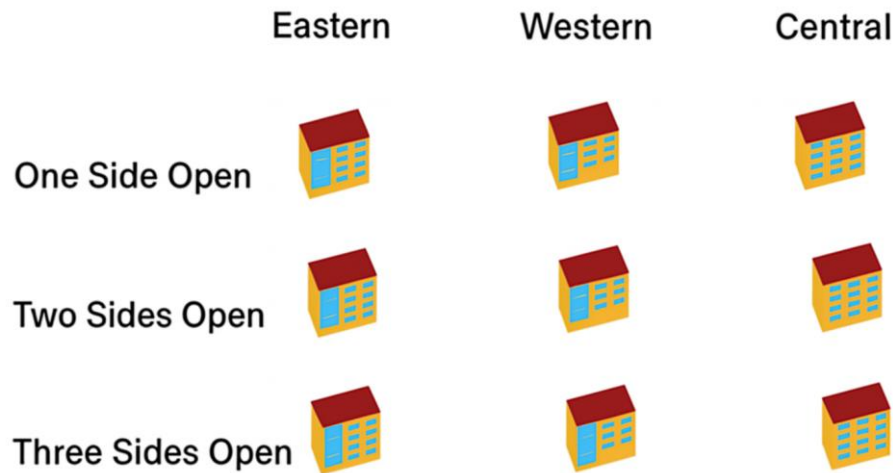
**Figure 26**

Modeling Semi-Open Spaces in the HoneyBee Energy Simulation Software



In building energy simulation software, it is not possible to model open or semi-open spaces directly. These tools only simulate enclosed geometries. Therefore, to simulate spaces like balconies, a closed geometry must first be created, and then windows are added. These windows must be set to always open to simulate airflow, thus emulating the thermal behavior of semi-open terraces.

To simulate semi-open spaces in HoneyBee (EnergyPlus), a closed geometry is first drawn. Then, windows are placed on the walls and set to always open in the schedule to replicate a semi-open thermal environment. The modeling scenarios in this study are shown in the following figures:

**Figure 27**
*Balcony Study Models Designed in HoneyBee Plugin*


### Simulation Assumptions

#### Zoning

Only the zone affecting balcony thermal performance was modeled. The interior space was considered as a non-transmitting wall to exclude internal heat transfer effects.

Additionally, the interior was modeled as a space capable of both heating and cooling. The terrace and parking area, which significantly affect both internal and external thermal conditions and ground heat transfer, were modeled as unconditioned spaces to reflect realistic conditions.

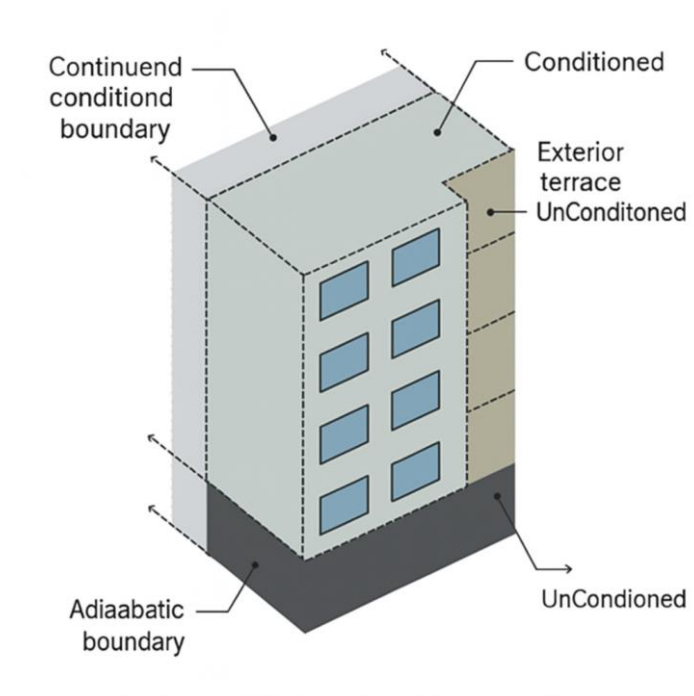
**Figure 28**
*Space Zoning Diagram in HoneyBee Software*


Table below details the assumptions for the different building zones used in the simulation.

**Table 2**

*Assignment of Heating and Cooling Loads to Different Zoning Categories in the Building*

Space Name (Usage)	Simulation Assumption
Residential Space Affecting Terrace Performance	With heating and cooling capability
Terraces	Without heating and cooling
Parking Area	Without heating and cooling
Partition Between Effective and Non-Effective Space	Non-transmitting wall

### Program

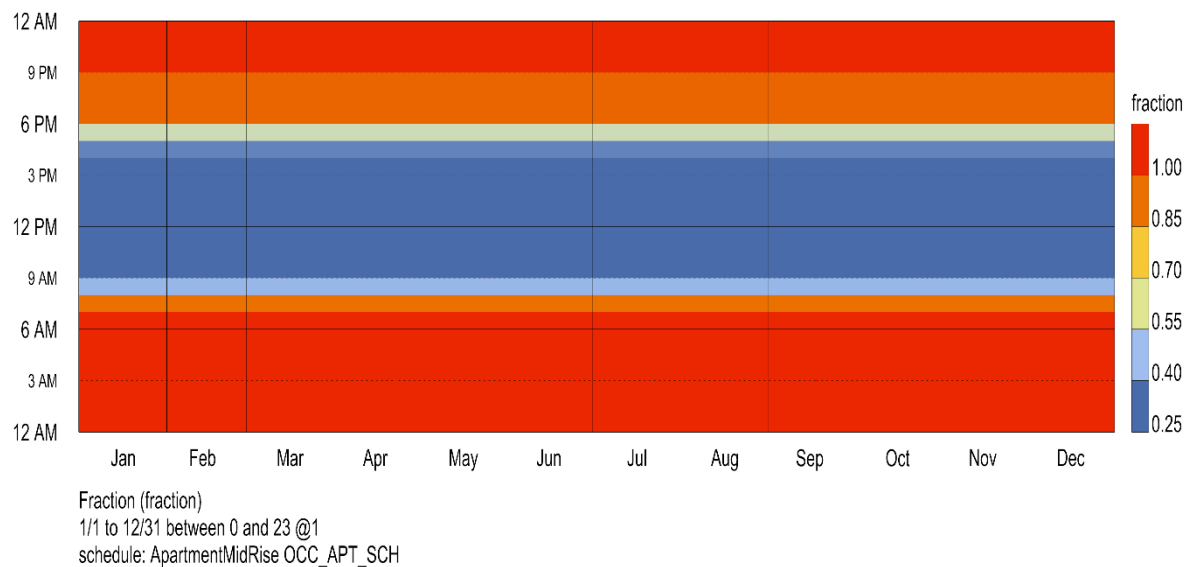
The usage schedule for the space is set as a mid-rise residential building. It is important to note that all simulation assumptions comply with ASHRAE 90.1 (2019 Edition). The scheduling program is detailed in multiple sections.

### Occupants

According to the standard, the occupant density is considered to be 0.028309 persons per square meter. The occupancy schedule is defined according to the following chart:

**Chart 16**

*Occupancy Schedule Across Different Months of the Year*

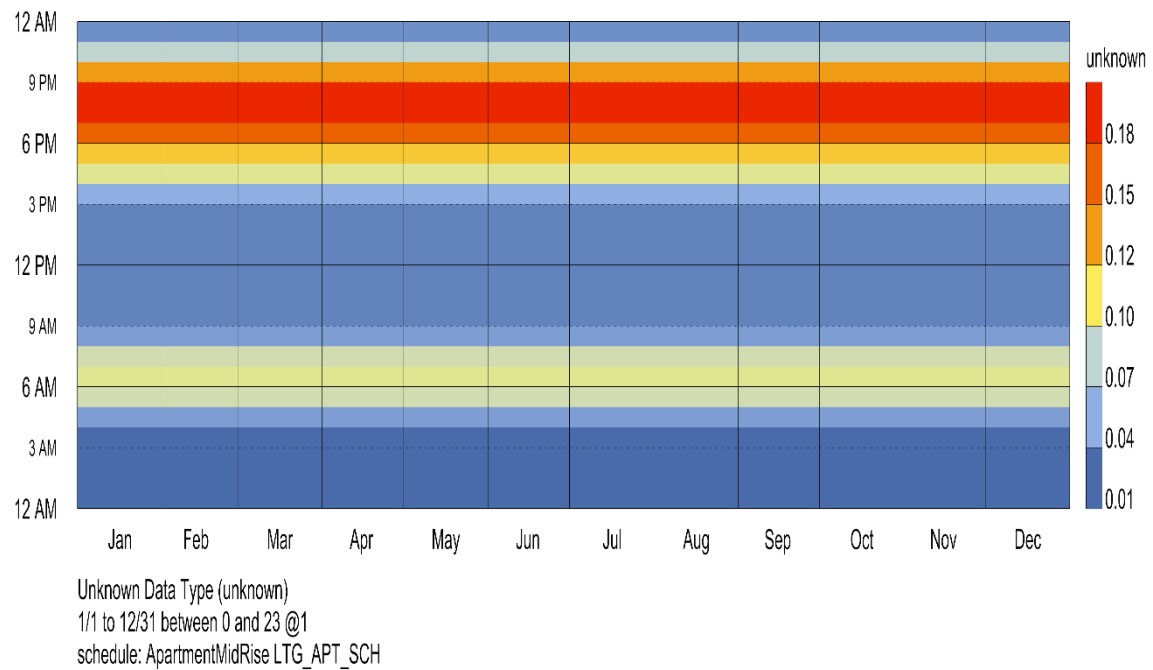


### Artificial Lighting Loads

The artificial lighting power density is assumed to be 6.45834 watts per square meter. The lighting usage schedule is shown in the chart below:

## Chart 17

### Artificial Lighting Usage Schedule by Month



The characteristics of the lighting system are also defined in the following table:

**Table 3**

*Lighting System Coefficients for Heating and Cooling Load Calculations*

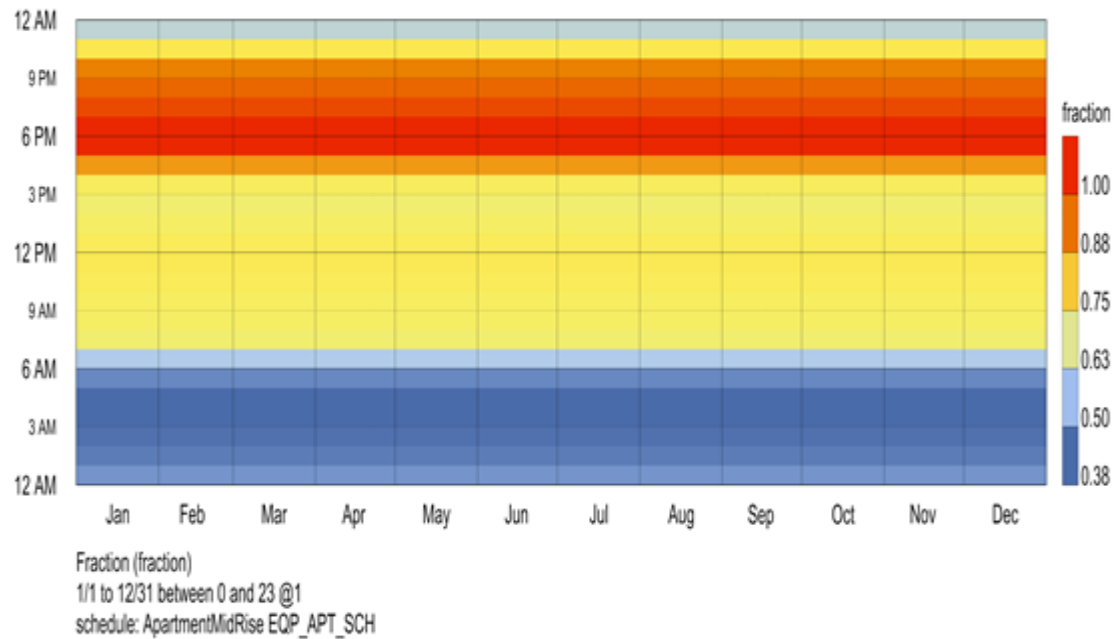
Coefficient Type	Value
Radiative Fraction	0.6
Visible Fraction	0.2
Return Fraction	0.0

## Equipment Loads

The assumed equipment energy usage in the residential space is 6.669994 watts per square meter. The equipment usage schedule is illustrated below:

## Chart 18

### Equipment Usage Schedule by Month



The characteristics of the equipment are outlined in the following table:

**Table 4**

### Equipment Characteristics for Heating and Cooling Load Calculations

Component Type	Value
Radiative Fraction	0.5
Latent Fraction	0.2
Loss Fraction	0.0

### Domestic Hot Water (DHW)

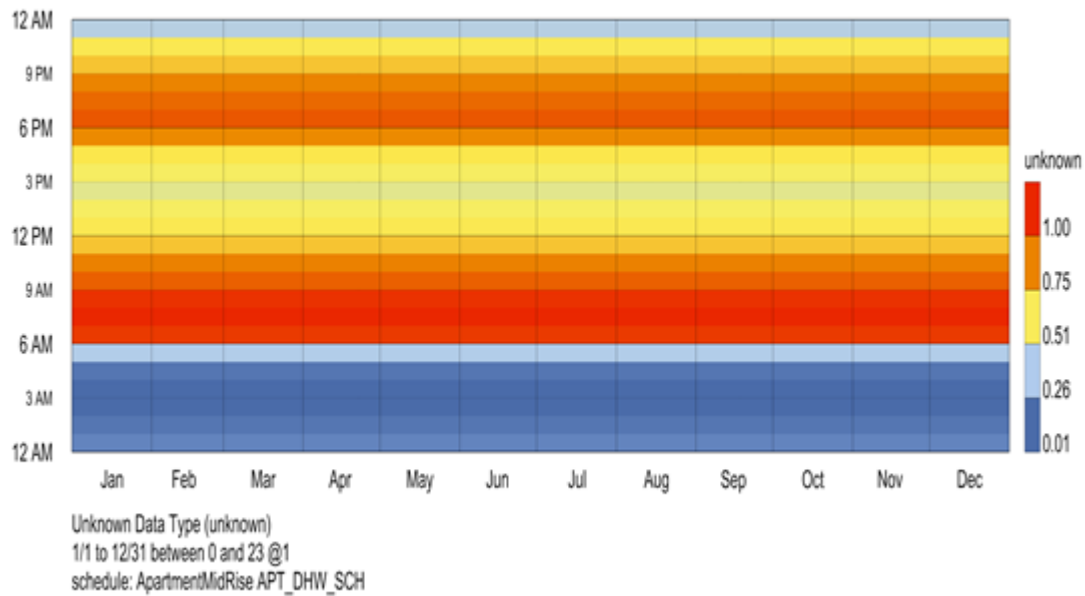
The domestic hot water consumption rate is assumed to be 0.149258 liters per hour per square meter in residential

spaces. The target temperature for hot water is 60°C. The DHW usage schedule is provided below:



**Chart 19**

*Domestic Hot Water Usage Schedule by Month*



The DHW equipment characteristics are detailed in the following table:

**Table 5**

*DHW Equipment Characteristics for Heating and Cooling Load Calculations*

Component Type	Value
Sensible Fraction	0.2
Latent Fraction	0.05

### Air Infiltration Rate

Unintended air infiltration for a standard building at 4 pascals of pressure is considered 0.0003 cubic meters per second per square meter of building envelope surface. This rate is assumed to be constant throughout the day.

### Natural Ventilation

The minimum natural ventilation rate for providing fresh air is set at 0.35 air changes per hour (ACH) per zone volume.

### HVAC System Settings

The heating system activation temperature is considered 21.7°C, and the cooling system activation temperature is set at 24.4°C.

### Construction Materials and Method

**Table 6**

*Summary of Wall Assemblies*

Assembly Type	U-value (W/m <sup>2</sup> ·K)	R-value (m <sup>2</sup> ·K/W)	SHGC
Exterior Wall	0.599647	1.503895	—
Roof	0.208244	4.638297	—
Floor	0.394078	2.373814	—
Window	2.404504	0.247408	0.25
Interior Wall	2.116724	0.308675	—
Interior Floor/Ceiling	1.155239	0.701869	—

According to ASHRAE standards, construction methods and materials are proposed based on ASHRAE climate zone classification and the building structure type. The climate of Mashhad is classified as BSk based on the Köppen system

and as 3B under ASHRAE. Therefore, the relevant details used in this study are based on this classification and for reinforced concrete structures.

**Figure 29**

*Input of Mashhad Climate Zone Classification in Honeybee Software*

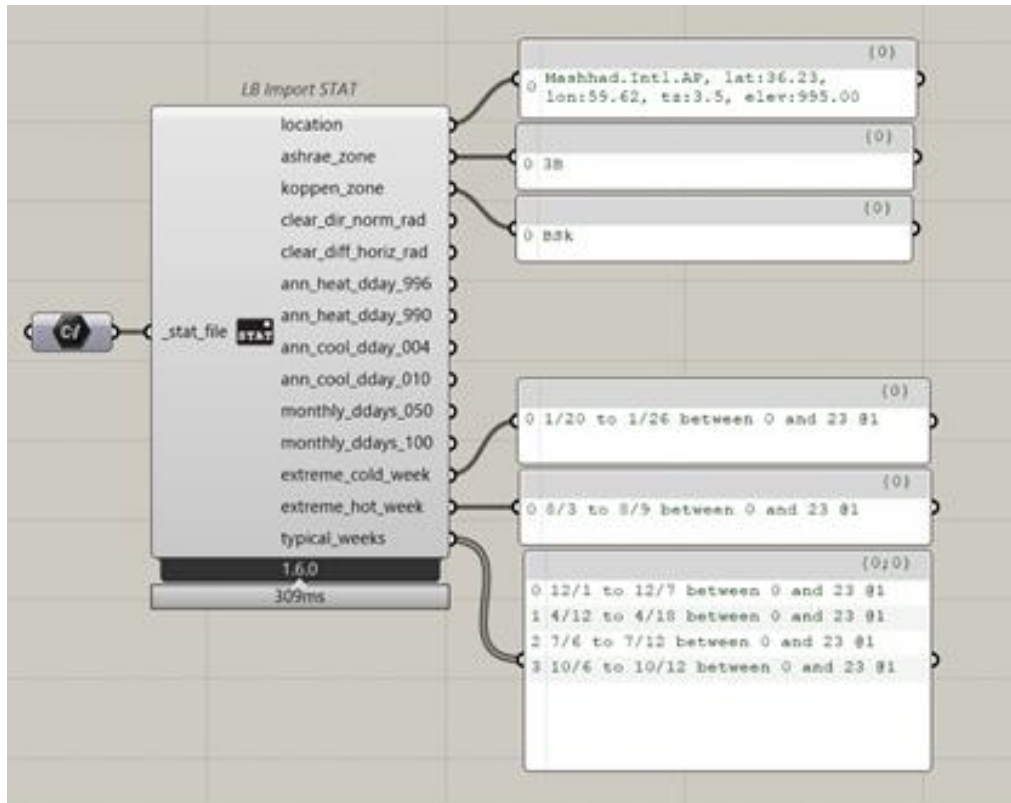


**Table 7**

*Thermal Properties of Wall Assemblies*

Element Type	Material Name	Thickness (m)	Conductivity (W/m·K)	Density (kg/m³)	Specific Heat (J/kg·K)	Thermal Absorptance	Solar Absorptance	Visible Absorptance
Exterior Wall	1IN Stucco	0.0253	0.6913	1858.00	836.46	0.9	0.7	0.92
	8IN Concrete HW RefBldg	0.2032	1.3101	2240.01	836.26	0.9	0.7	0.7
	Typical Insulation-R7 (massless)	R=1.2328	—	—	—	0.9	0.7	0.7
Roof	1/2IN Gypsum	0.0127	0.1599	784.90	829.46	0.9	0.4	0.4
	Roof Membrane – Reflective	0.0095	0.1599	1121.29	1459.06	0.75	0.45	0.7
	Typical Insulation-R26 (massless)	R=4.5789	—	—	—	0.9	0.7	0.7
Floor	Metal Roof Surface	0.0008	45.2497	7824.02	499.68	0.9	0.7	0.7
	Typical Insulation-R12 (massless)	R=2.1133	—	—	—	0.9	0.7	0.7
	Normalweight Concrete Floor	0.1016	2.3085	2322.01	831.46	0.9	0.7	0.7
	Typical Carpet Pad (massless)	R=0.2165	—	—	—	0.9	0.7	0.8

Window	Simple Glazing (U=0.42, SHGC=0.25, VT=0.6)	—	—	—	—	—	—	—
Interior Wall	Generic Gypsum Board	0.0127	0.16	800.0	1090.0	0.9	0.5	0.5
	Generic Wall Air Gap	0.1	0.667	1.28	1000.0	0.9	0.7	0.7
	Generic Gypsum Board	0.0127	0.16	800.0	1090.0	0.9	0.5	0.5
Interior Floor/Ceiling	Generic LW Concrete	0.1	0.53	1280.0	840.0	0.9	0.8	0.8
	Generic Ceiling Air Gap	0.1	0.556	1.28	1000.0	0.9	0.7	0.7
	Generic Acoustic Tile	0.02	0.06	368.0	590.0	0.9	0.2	

### Balcony Modeling and Analysis Using Honeybee Software

This section addresses the detailed modeling of balconies in the Honeybee software and their thermal performance analysis.

#### Model No. 1: East-Facing Balcony (Open on One Side)

**Figure 30**

*Modeling of Balcony Model 1 in Honeybee Software*

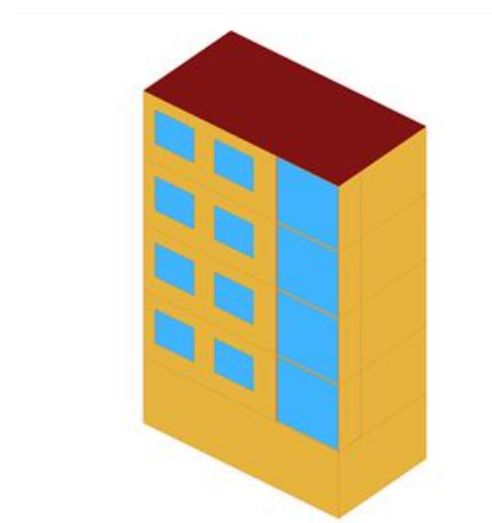
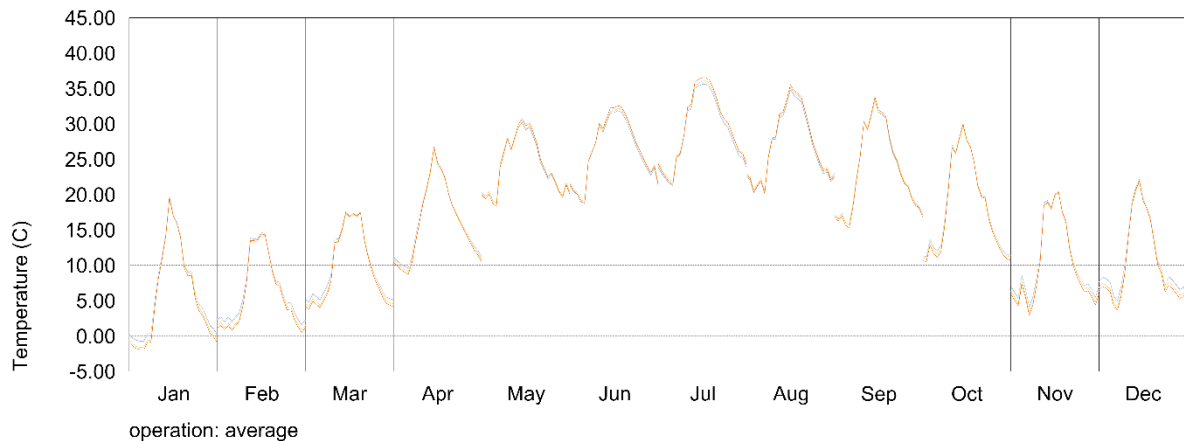


**Figure 31**

*Average Surface Temperatures on Summer Solstice (Right) and Winter Solstice (Left) for Model 1 Between 6:00 and 19:00*


**Chart 20**

*Annual Balcony Temperature (PET) for Model 1*



To assess the thermal behavior of Model 1, simulations were conducted throughout the year, with special attention to the summer and winter solstice days between 6:00 and 19:00. Over the span of a year, the PET (Physiological Equivalent Temperature) in Model 1 ranges from  $-2.5^{\circ}\text{C}$  to  $36.7^{\circ}\text{C}$ . On the summer solstice (June 21), this model achieves thermal comfort for only 0.05 hours. In contrast, on the winter solstice (December 22), thermal comfort is

achieved for 1.75 hours. The average PET on the summer and winter solstice days is  $28.5^{\circ}\text{C}$  and  $20.06^{\circ}\text{C}$ , respectively. During the study hours on the summer solstice, the maximum and minimum PET were  $34.02^{\circ}\text{C}$  and  $24.6^{\circ}\text{C}$ , respectively. For the winter solstice, these values were  $30.7^{\circ}\text{C}$  and  $7.3^{\circ}\text{C}$ . The highest PET for this model occurred at 7:00 AM on the summer solstice and at 12:00 PM on the winter solstice.

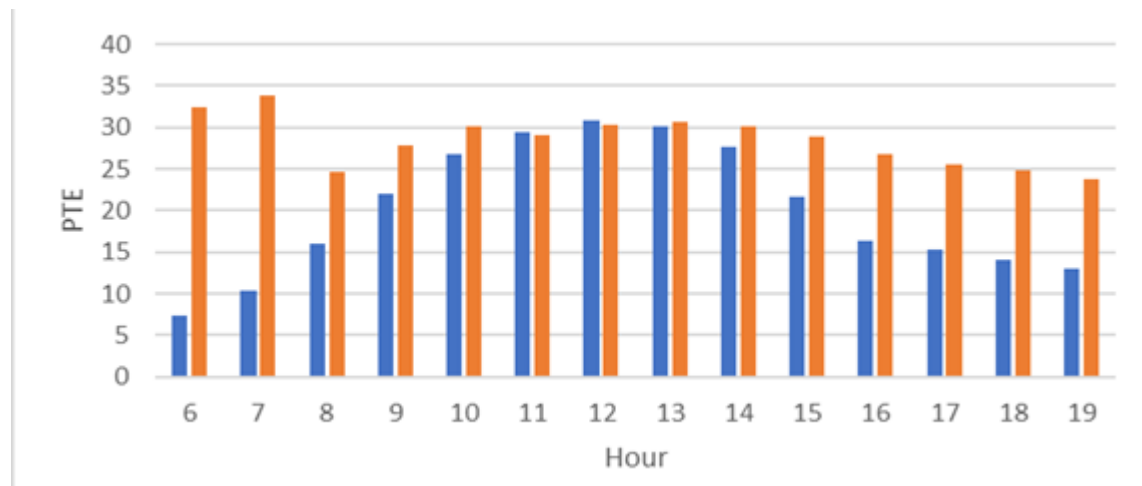
**Table 8**

*Quantitative Output Data for Model 1*

Balcony Type	Comfort Hours (Summer Solstice)	Comfort Hours (Winter Solstice)	Avg. PET (Summer Solstice)	Avg. PET (Winter Solstice)
East, One Side Open	0.05	1.75	28.50°C	20.06°C

**Chart 21**

*Balcony Temperature Within Study Hours on Summer and Winter Solstice for Sample 1*



**Model 2: East-Facing Balcony (Open on Two Sides)**

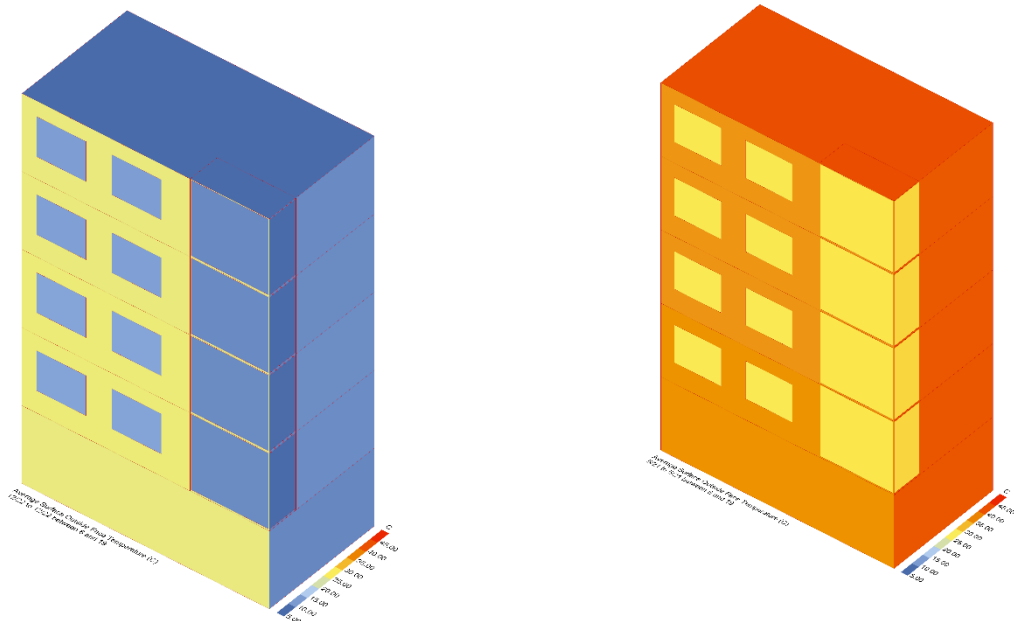
**Figure 32**

*Modeling of Balcony Model 2 in Honeybee Software*

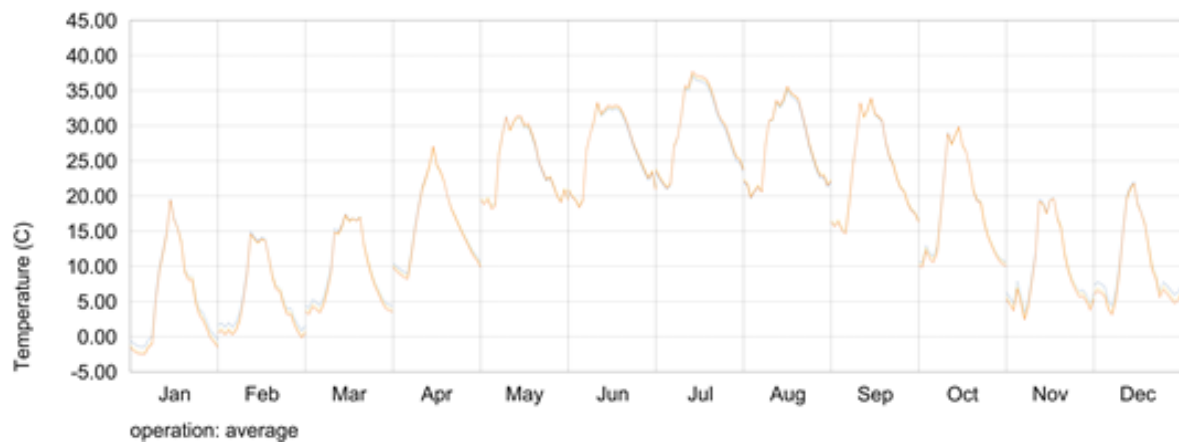


**Figure 33**

*Average Surface Temperatures on Summer Solstice (Right) and Winter Solstice (Left) for Model 2 Between 6:00 and 19:00*


**Chart 22**

*Annual Balcony Temperature (PET) for Model 2*



For evaluating the thermal behavior of Model 2, simulations were also conducted year-round and specifically on solstice days from 6:00 to 19:00. Model 2 experiences PET fluctuations ranging from  $-2.7^{\circ}\text{C}$  to  $37.3^{\circ}\text{C}$  throughout the year. On the summer solstice (June 21), it reaches thermal comfort for only 0.05 hours, while on the winter solstice (December 22), it achieves comfort for 1.5 hours.

The average PET values for summer and winter solstice days are  $29.78^{\circ}\text{C}$  and  $20.07^{\circ}\text{C}$ , respectively. During the summer solstice, maximum and minimum PET were recorded as  $38.2^{\circ}\text{C}$  and  $23.9^{\circ}\text{C}$ . For the winter solstice, the maximum and minimum values were  $30.9^{\circ}\text{C}$  and  $6.8^{\circ}\text{C}$ . The peak PET was observed at 7:00 AM in summer and at 12:00 PM in winter.

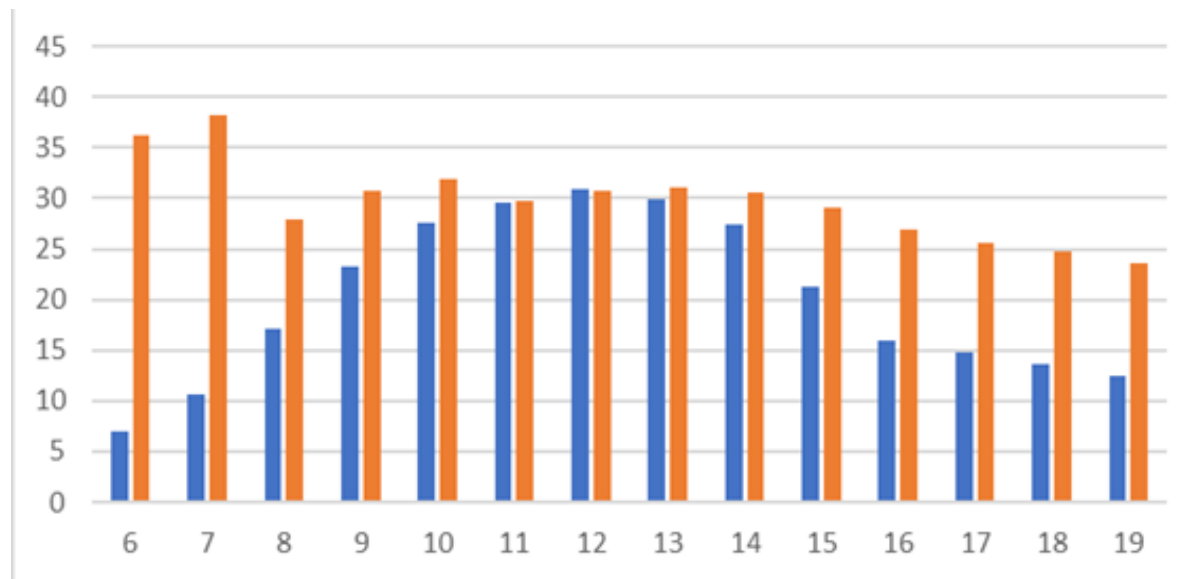
**Table 9**

*Quantitative Output Data for Model 2*

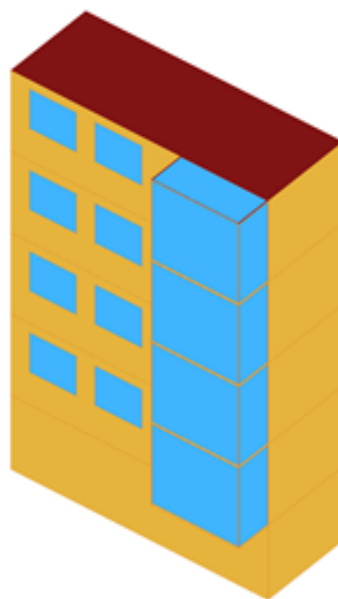
Balcony Type	Comfort Hours (Summer Solstice)	Comfort Hours (Winter Solstice)	Avg. PET (Summer Solstice)	Avg. PET (Winter Solstice)
East, Two Sides Open	0.05	1.50	29.78°C	20.07°C

**Chart 23**

*Balcony Temperature Within Study Hours on Summer and Winter Solstice for Sample 2*


**Model 3: East-Facing Balcony (Open on Three Sides)**
**Figure 34**

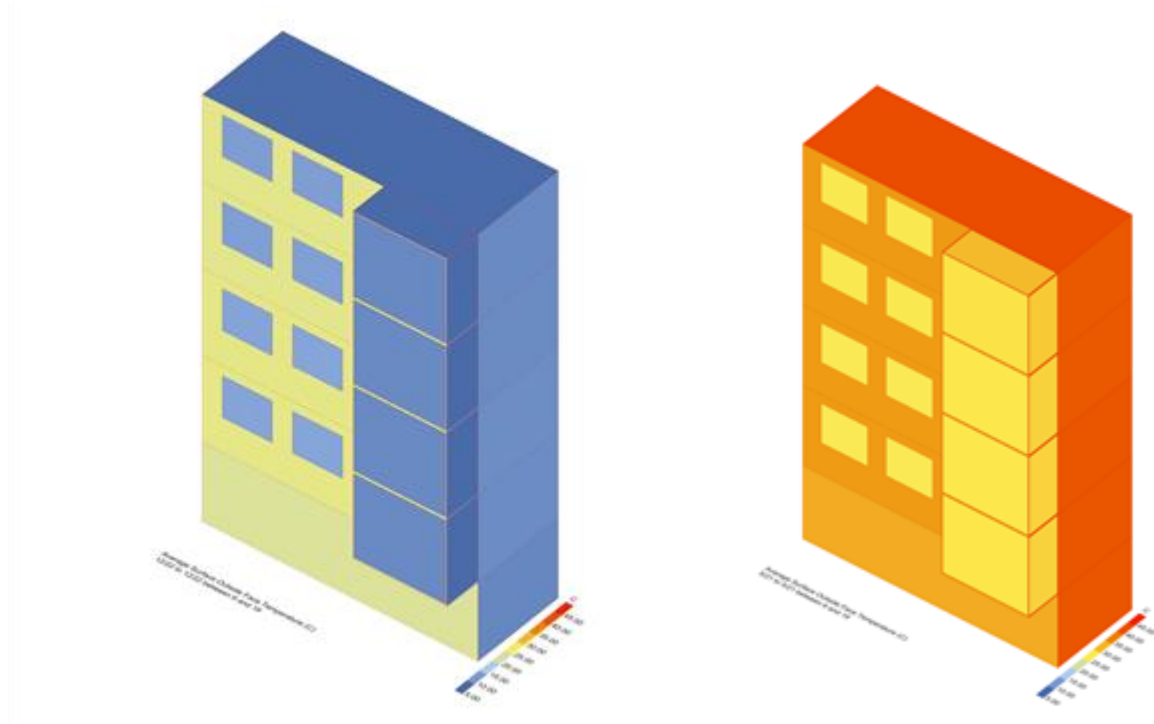
*Modeling of Balcony Model 3 in Honeybee Software*



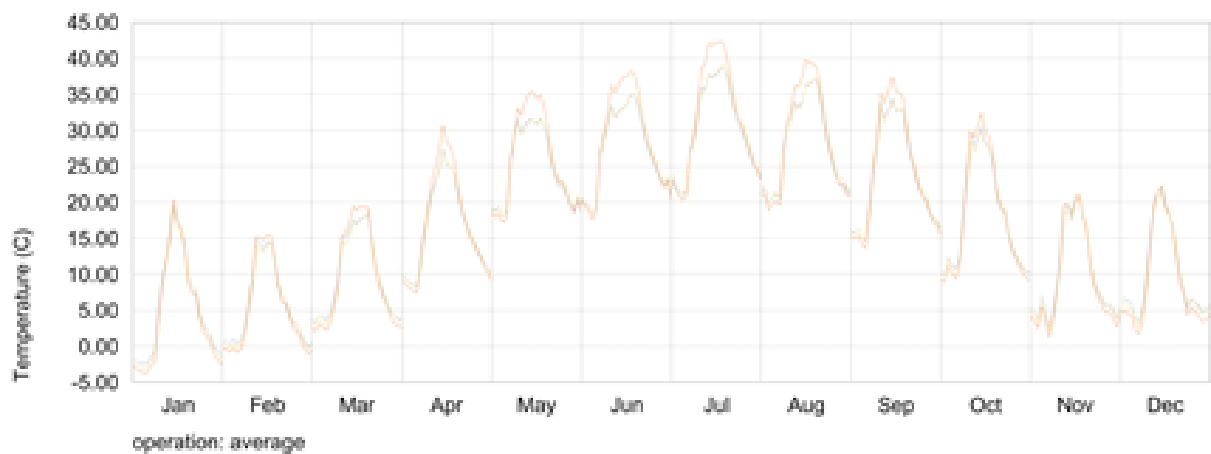


**Figure 35**

*Average Surface Temperatures on Summer Solstice (Right) and Winter Solstice (Left) for Model 3 Between 6:00 and 19:00*


**Chart 24**

*Annual Balcony Temperature (PET) for Model 3*



To evaluate the thermal performance of Model 3, simulations were similarly carried out over the entire year and particularly on the solstice days, from 6:00 to 19:00. Model 3 experiences PET variation from -4.2°C to 42.8°C. On the summer solstice, it achieves thermal comfort for 0.05 hours, and on the winter solstice, for 1.25 hours. The average

PET values for summer and winter solstice days are 31.09°C and 19.73°C, respectively. During the summer solstice, maximum and minimum PET were 38.4°C and 24.4°C, respectively. For the winter solstice, they were 31.6°C and 6.5°C. As in the previous models, the peak PET values occurred at 7:00 AM in summer and at 12:00 PM in winter.

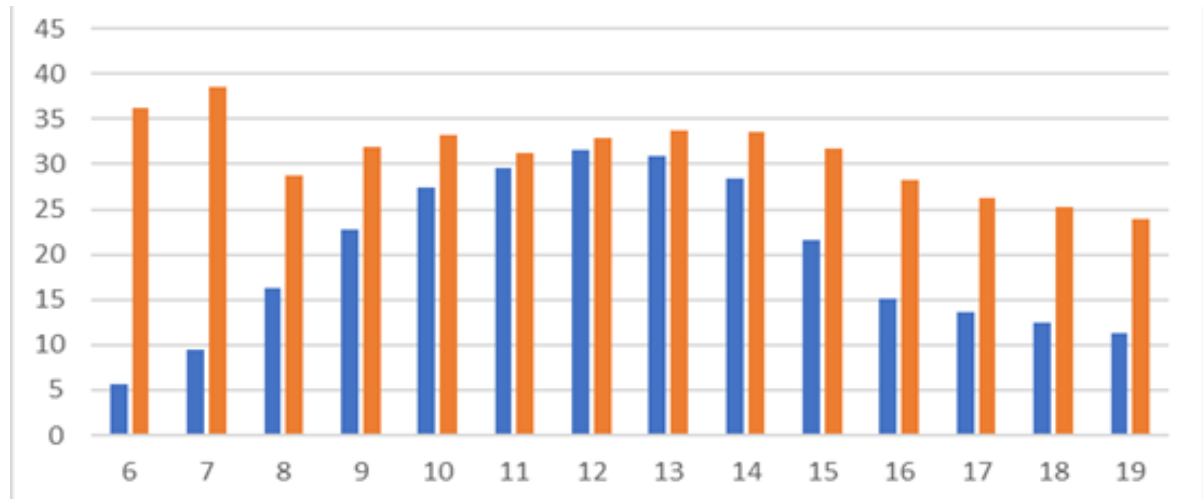
**Table 10**

*Quantitative Output Data for Model 3*

Balcony Type	Comfort Hours (Summer Solstice)	Comfort Hours (Winter Solstice)	Avg. PET (Summer Solstice)	Avg. PET (Winter Solstice)
East, Three Sides Open	0.05	1.25	31.09°C	19.73°C

**Chart 25**

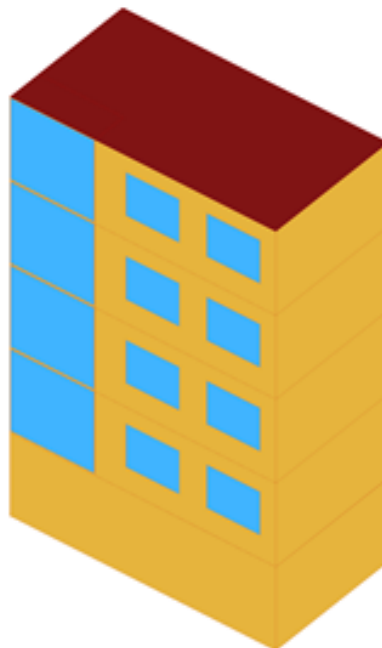
*Balcony Temperature Within Study Hours on Summer and Winter Solstice for Sample 3*



**Model No. 4: West-Facing Balcony (Open on One Side)**

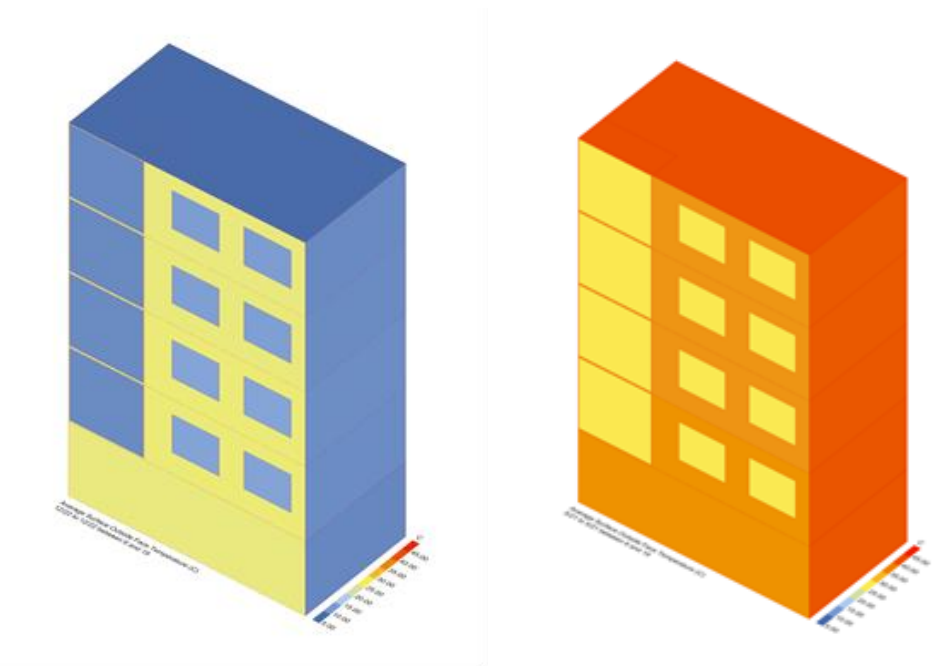
**Figure 36**

*Modeling of Balcony Model No. 4 in Honeybee Software*

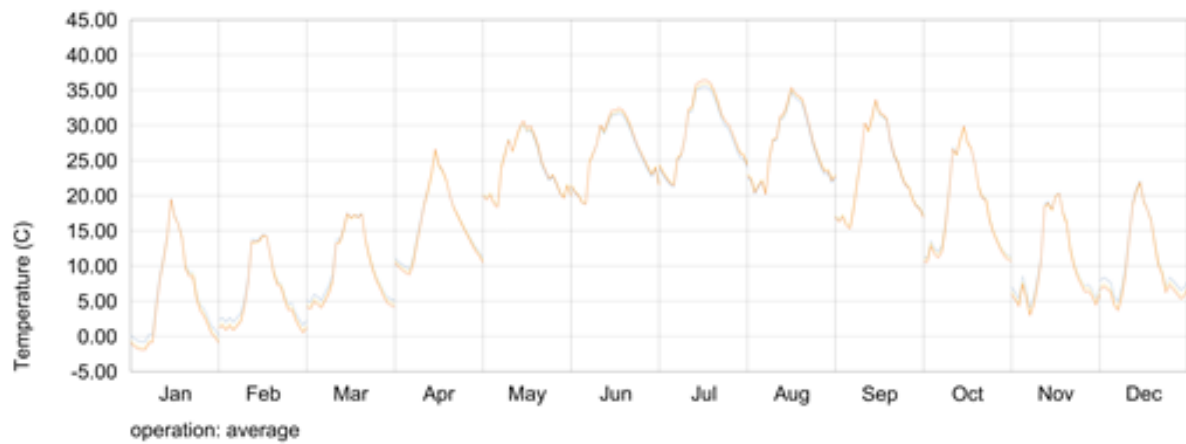


**Figure 37**

*Average Surface Temperatures on the Summer Solstice (Right) and Winter Solstice (Left) for Model 4 Between 6:00 and 19:00*


**Chart 26**

*Annual Balcony Temperature (PET) for Model No. 4*


**Table 11**

*Quantitative Output Data from Honeybee for Model No. 4*

Balcony Type	Comfort Hours (Summer Solstice)	Comfort Hours (Winter Solstice)	Avg. PET (Summer Solstice)	Avg. PET (Winter Solstice)
West, One Side Open	0.05	1.75	28.38°C	20.07°C

To evaluate the thermal performance of Model No. 4, this configuration was simulated across the entire year and specifically on the summer and winter solstice days between

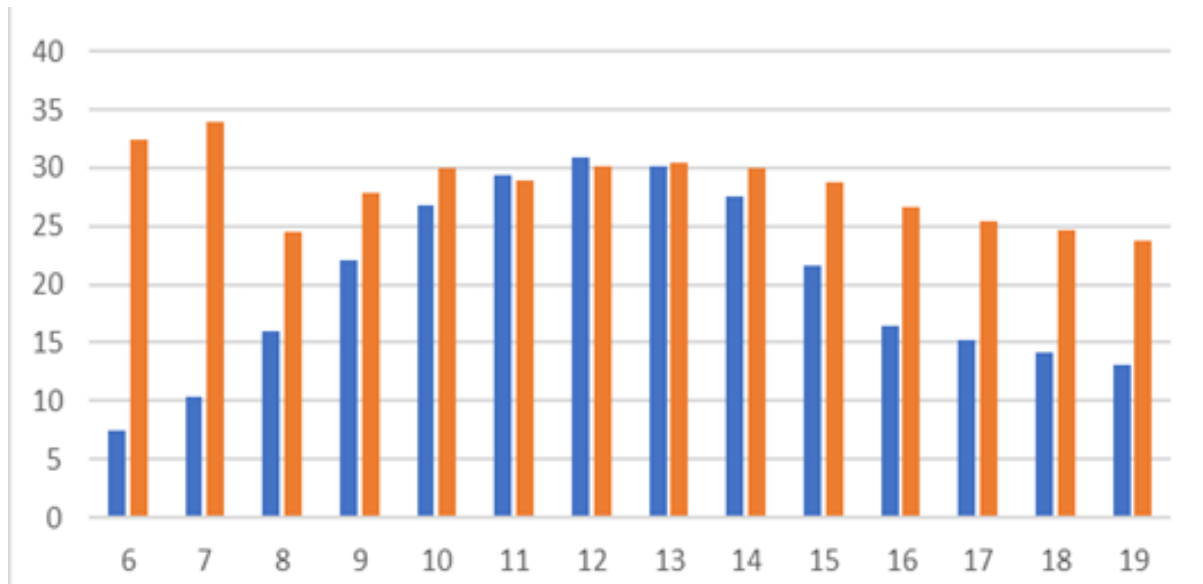
6:00 and 19:00. The PET (Physiological Equivalent Temperature) in this model ranged annually from -2.2°C to 36.2°C. On the summer solstice (June 21), it achieved

thermal comfort for only 0.05 hours, while on the winter solstice (December 22), it maintained comfort for 1.75 hours. The average PET values on the solstice days were 28.38°C and 20.07°C, respectively. During the summer solstice study hours, the maximum and minimum PET were

34.07°C and 23.7°C. For the winter solstice, those values were 31.3°C and 7.8°C. The highest PET occurred at 7:00 AM on the summer solstice and at 12:00 PM on the winter solstice.

### Chart 27

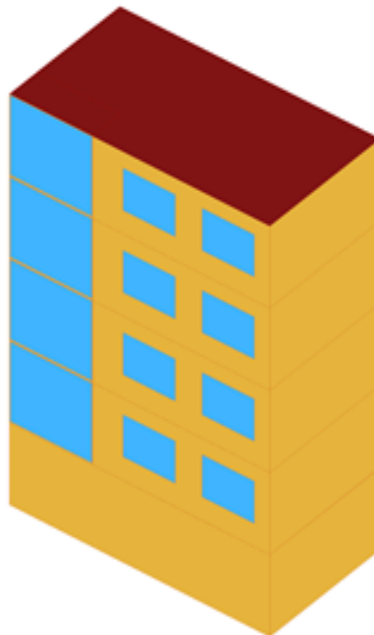
*Balcony Temperature Within Study Hours on the Summer and Winter Solstices for Sample No. 4*



**Model No. 5: West-Facing Balcony (Open on Two Sides)**

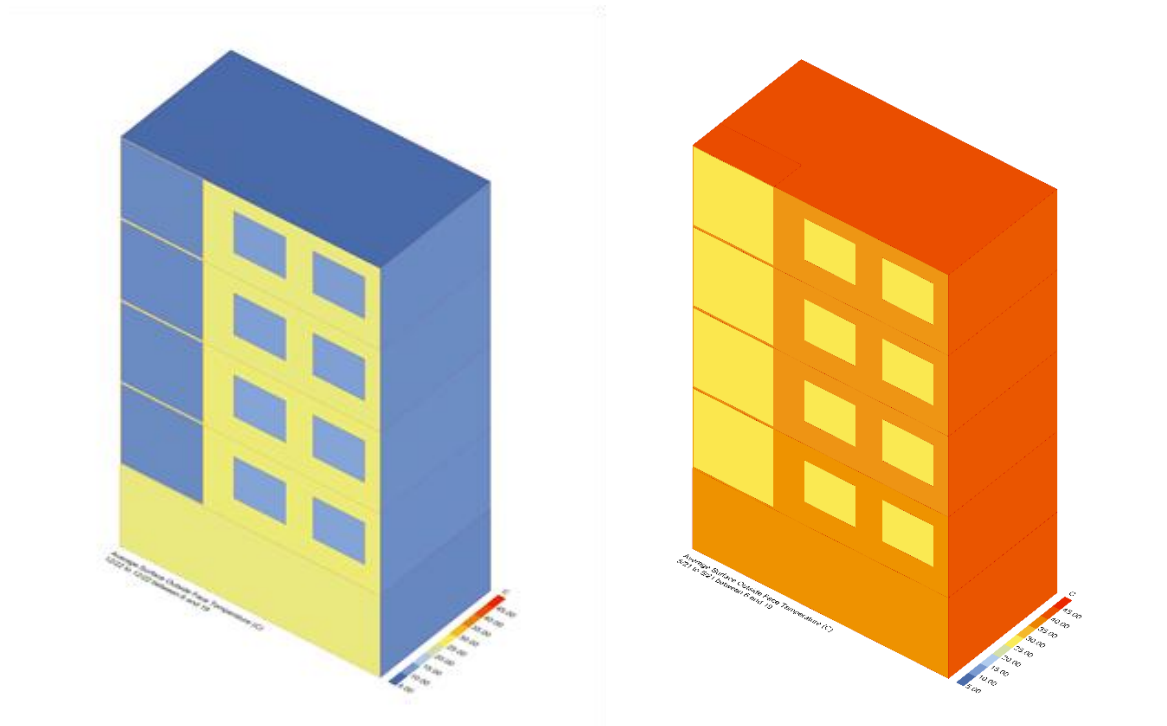
### Figure 38

*Modeling of Balcony Model No. 5 in Honeybee Software*

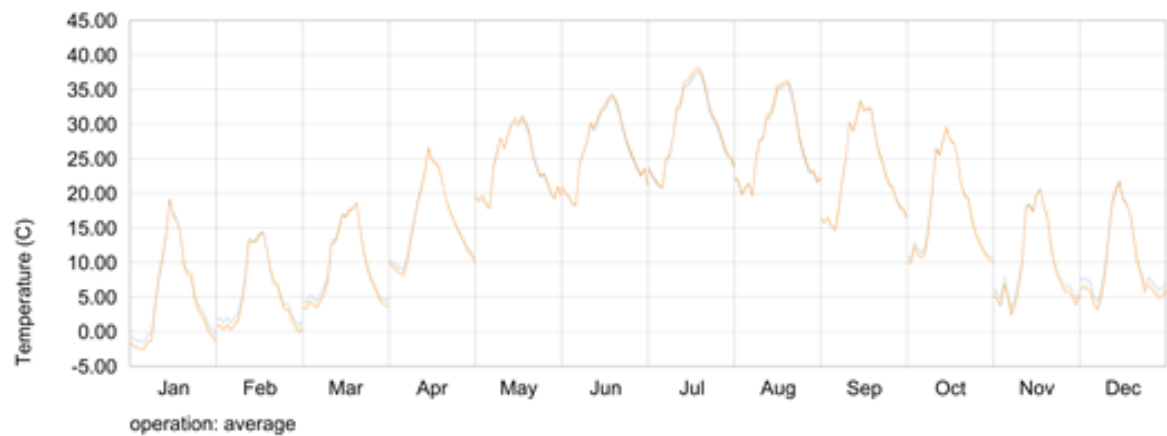


**Figure 39**

Average Surface Temperatures on the Summer Solstice (Right) and Winter Solstice (Left) for Model 5 Between 6:00 and 19:00


**Chart 28**

Annual Balcony Temperature (PET) for Model No. 5


**Table 12**

Quantitative Output Data from Honeybee for Model No. 5

Balcony Type	Comfort Hours (Summer Solstice)	Comfort Hours (Winter Solstice)	Avg. PET (Summer Solstice)	Avg. PET (Winter Solstice)
West, Two Sides Open	0.05	1.50	29.07°C	20.18°C

To assess the thermal performance of Model No. 5, year-round simulations and detailed solstice-day simulations

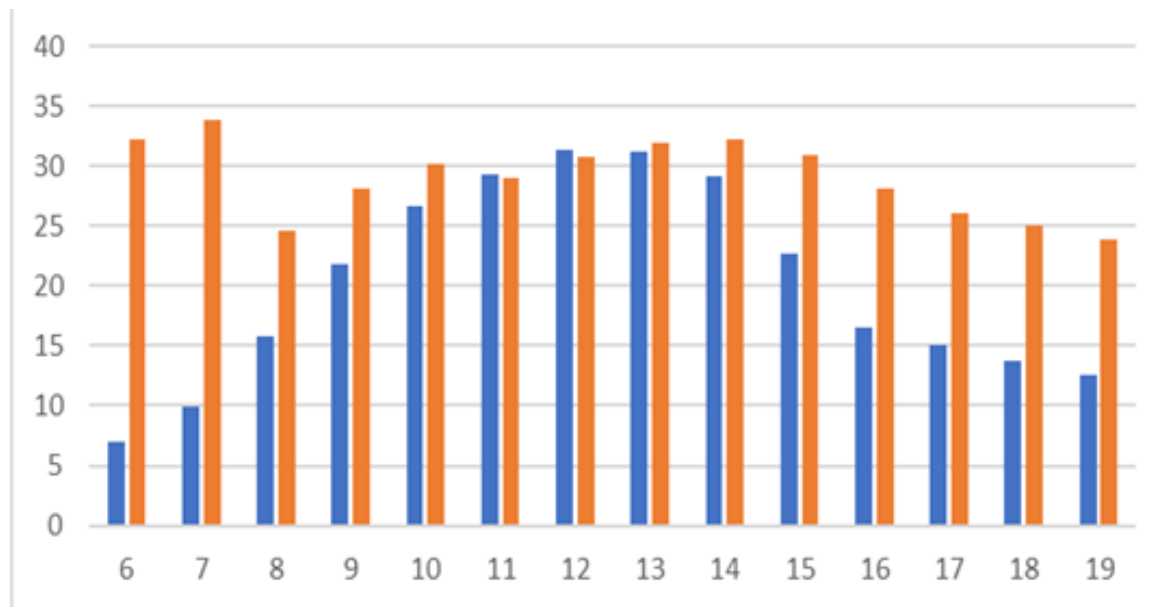
were conducted from 6:00 to 19:00. Over the year, PET varied from -2.6°C to 37.4°C. On June 21, thermal comfort

was reached for 0.05 hours, and on December 22, for 1.5 hours. Average PET values were 29.07°C and 20.18°C for summer and winter solstice days, respectively. During the summer solstice, the highest PET was 34.3°C and the lowest was 23.9°C. On the winter solstice, these values were 31.1°C

and 7.7°C. The peak PET occurred at 7:00 AM in summer and 12:00 PM in winter, while the lowest PET was observed at 19:00 on the summer solstice and 6:00 AM on the winter solstice.

### Chart 29

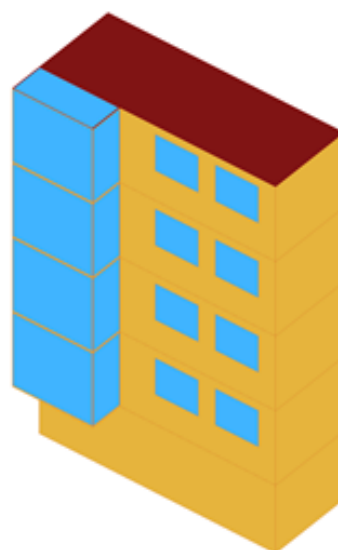
*Balcony Temperature Within Study Hours on the Summer and Winter Solstices for Sample No. 5*



### Model No. 6: West-Facing Balcony (Open on Three Sides)

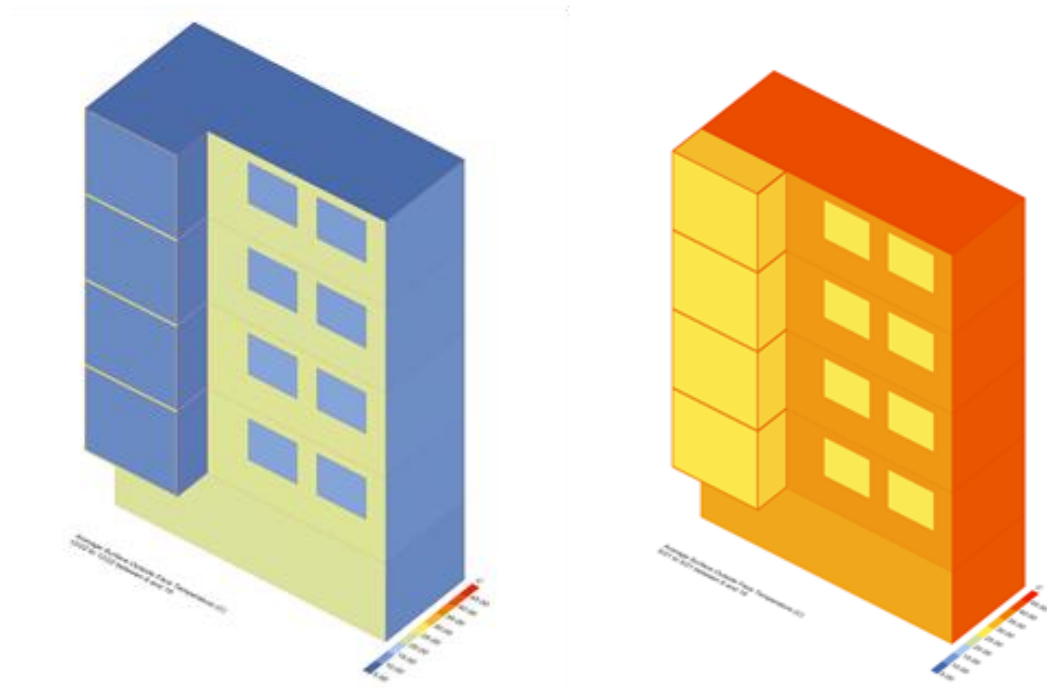
### Figure 40

*Modeling of Balcony Model No. 6 in Honeybee Software*

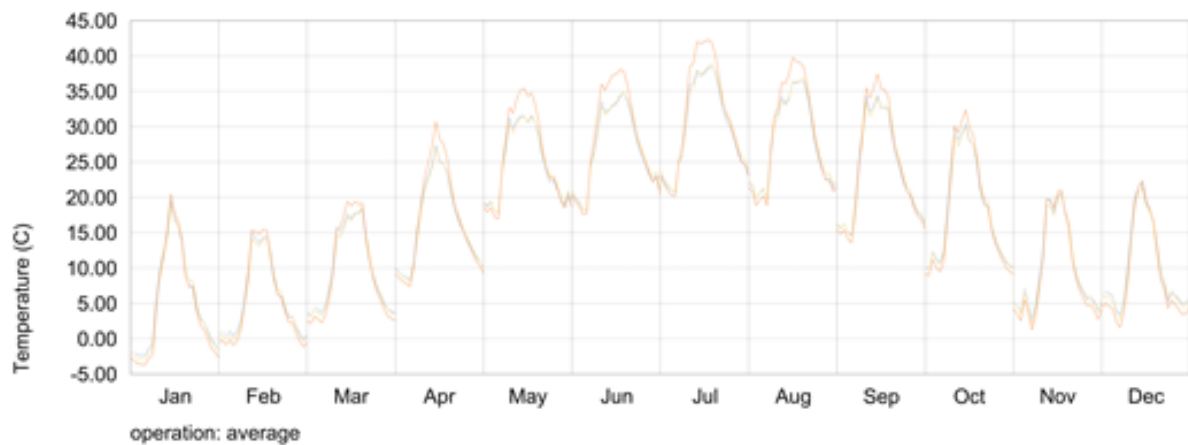


**Figure 41**

*Average Surface Temperatures on the Summer Solstice (Right) and Winter Solstice (Left) for Model 6 Between 6:00 and 19:00*


**Chart 30**

*Annual Balcony Temperature (PET) for Model No. 6*


**Table 13**

*Quantitative Output Data from Honeybee for Model No. 6*

Balcony Type	Comfort Hours (Summer Solstice)	Comfort Hours (Winter Solstice)	Avg. PET (Summer Solstice)	Avg. PET (Winter Solstice)
West, Three Sides Open	0.05	1.25	30.86°C	19.71°C

Model No. 6 was simulated throughout the year and on solstice days from 6:00 to 19:00. Annual PET ranged from -3.8°C to 42.9°C. It achieved thermal comfort for only 0.05

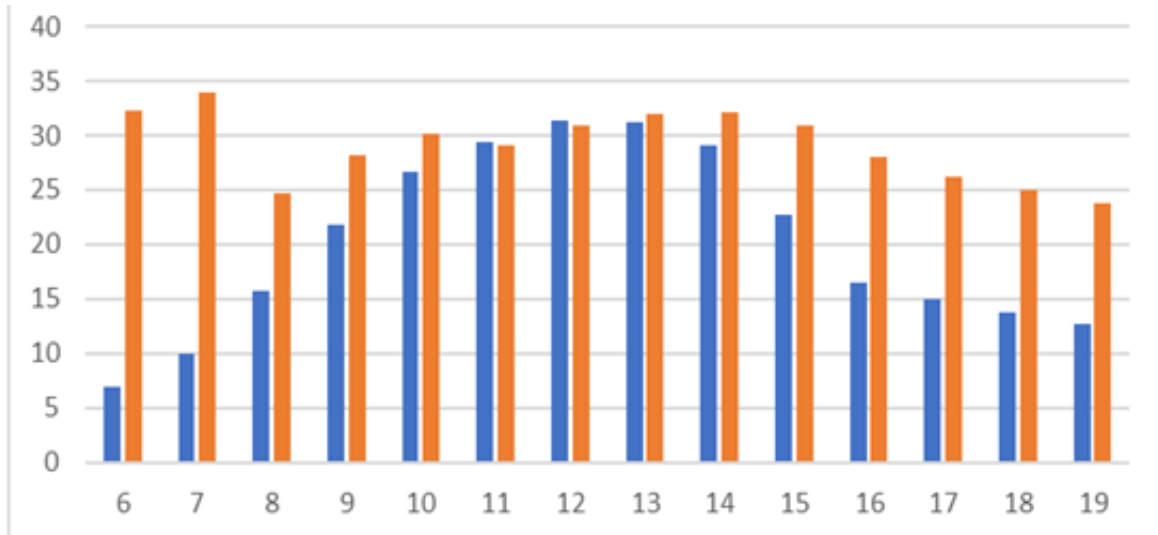
hours on the summer solstice and for 1.25 hours on the winter solstice. The average PET values were 30.86°C and 19.71°C, respectively. On the summer solstice, the PET

peaked at 34.1°C and dropped to 23.8°C. On the winter solstice, maximum and minimum PET values were 31.9°C and 7.3°C. The highest PET occurred at 7:00 AM on June 21

and at 12:00 PM on December 22. The lowest PETs on the solstice days were observed at 19:00 in summer and 6:00 in winter.

**Chart 31**

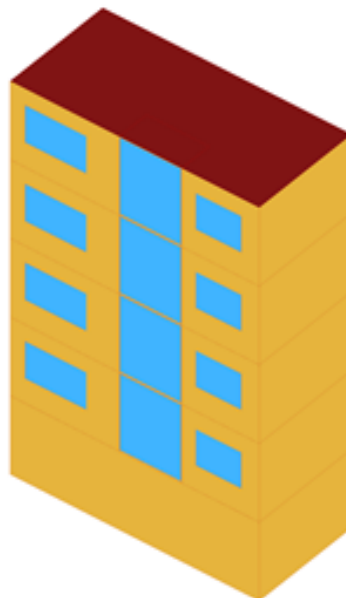
*Balcony Temperature Within Study Hours on the Summer and Winter Solstices for Sample No. 6*



**Model No. 7: Central Balcony (Open on One Side)**

**Figure 42**

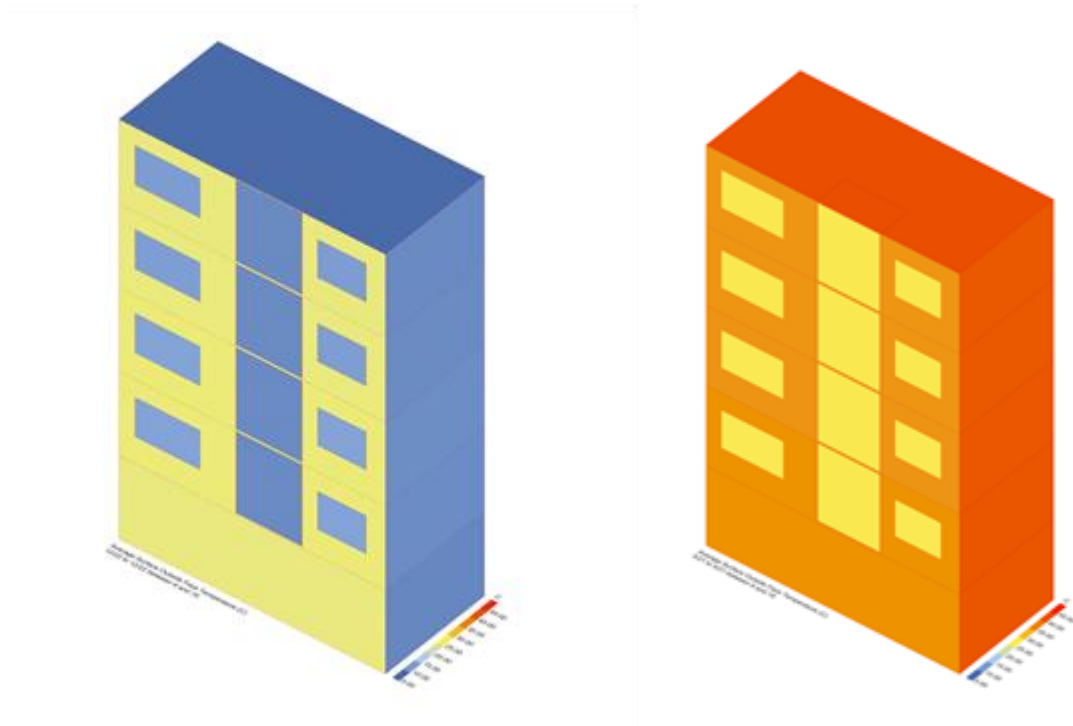
*Modeling of Balcony Model No. 7 in Honeybee Software*



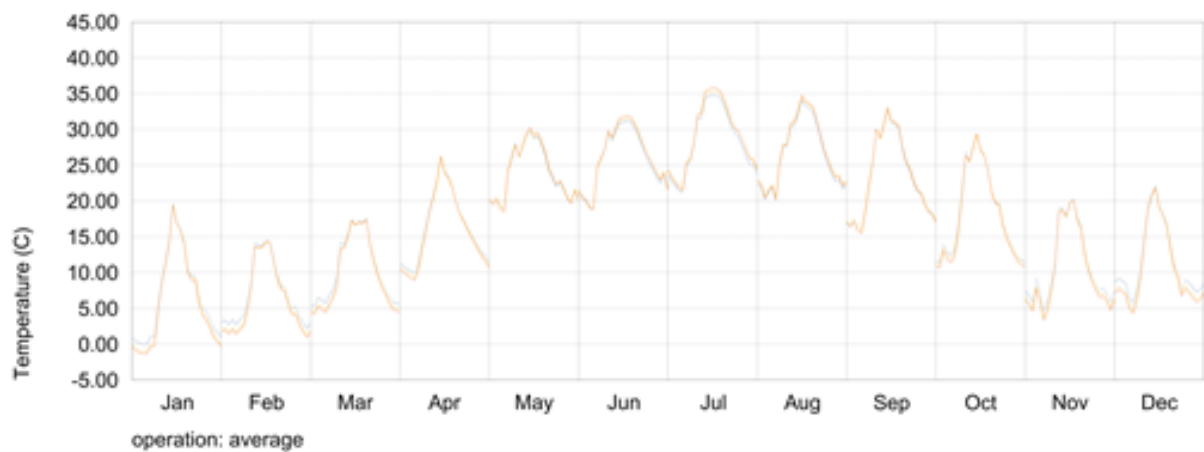


**Figure 43**

*Average Surface Temperatures on the Summer Solstice (Right) and Winter Solstice (Left) for Model 7 Between 6:00 and 19:00*


**Chart 32**

*Annual Balcony Temperature (PET) for Model No. 7*


**Table 14**

*Quantitative Output Data from Honeybee for Model No. 7*

Balcony Type	Comfort Hours (Summer Solstice)	Comfort Hours (Winter Solstice)	Avg. PET (Summer Solstice)	Avg. PET (Winter Solstice)
Central, One Side Open	0.05	1.75	28.13°C	20.43°C

To evaluate the thermal performance of Model No. 7, this configuration was simulated for the entire year and

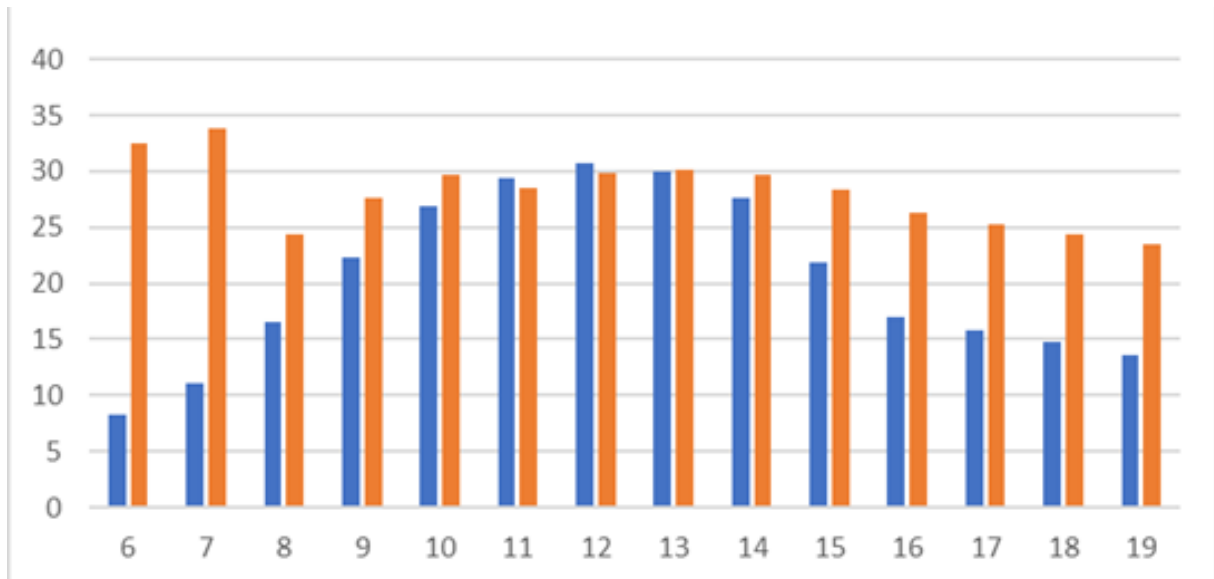
specifically on the summer and winter solstice days from 6:00 to 19:00. Over the course of the year, the PET

(Physiological Equivalent Temperature) ranged from  $-1.1^{\circ}\text{C}$  to  $35.4^{\circ}\text{C}$ . On the summer solstice (June 21), thermal comfort was achieved for 0.05 hours, while on the winter solstice (December 22), comfort was maintained for 1.75 hours. The average PET values on the solstice days were  $28.13^{\circ}\text{C}$  in summer and  $20.43^{\circ}\text{C}$  in winter. During the

summer solstice, the PET peaked at  $33.8^{\circ}\text{C}$  and dropped to  $23.5^{\circ}\text{C}$ , whereas on the winter solstice, these values were  $30.8^{\circ}\text{C}$  and  $7.7^{\circ}\text{C}$ . The highest PET was observed at 7:00 AM in summer and at 12:00 PM in winter. The lowest PET was recorded at 19:00 in summer and 6:00 AM in winter.

### Chart 33

*Balcony Temperature Within Study Hours on the Summer and Winter Solstices for Sample No. 7*



**Model No. 8: Central Balcony (Open on Two Sides – Western Orientation)**

### Figure 44

*Modeling of Balcony Model No. 8 in Honeybee Software*

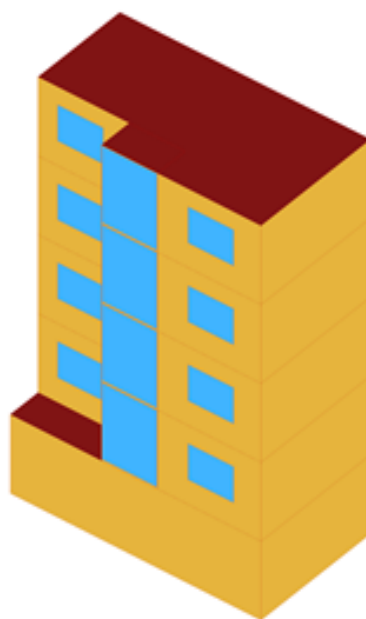


**Figure 45**

*Average Surface Temperatures on the Summer Solstice (Right) and Winter Solstice (Left) for Model 8 Between 6:00 and 19:00*

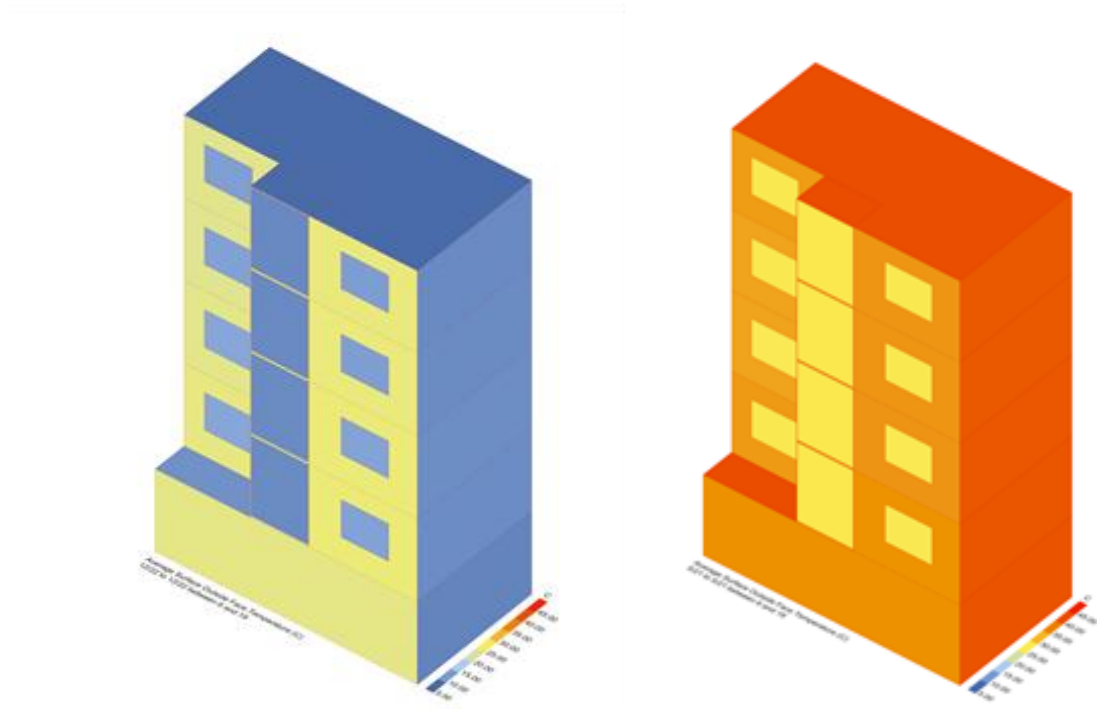


**Chart 34**

*Annual Balcony Temperature (PET) for Model No. 8*

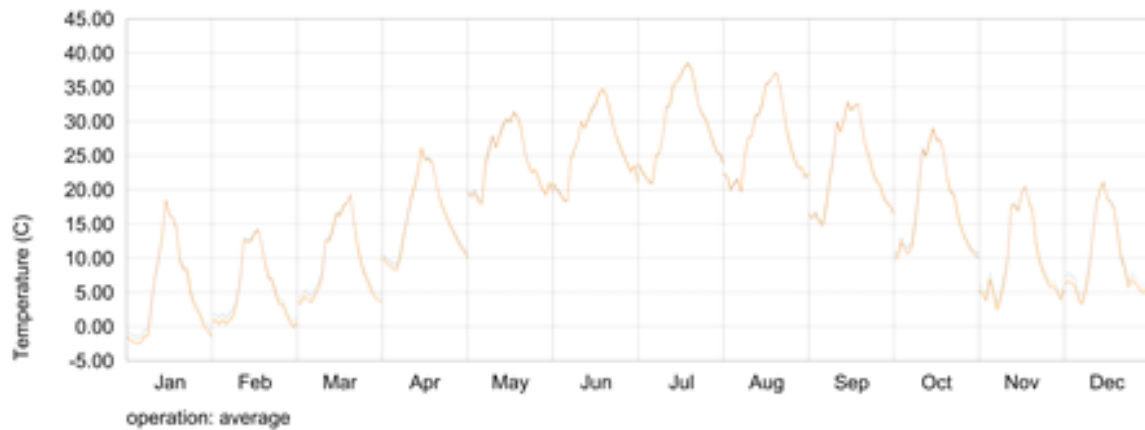


**Table 15**

*Quantitative Output Data from Honeybee for Model No. 8*

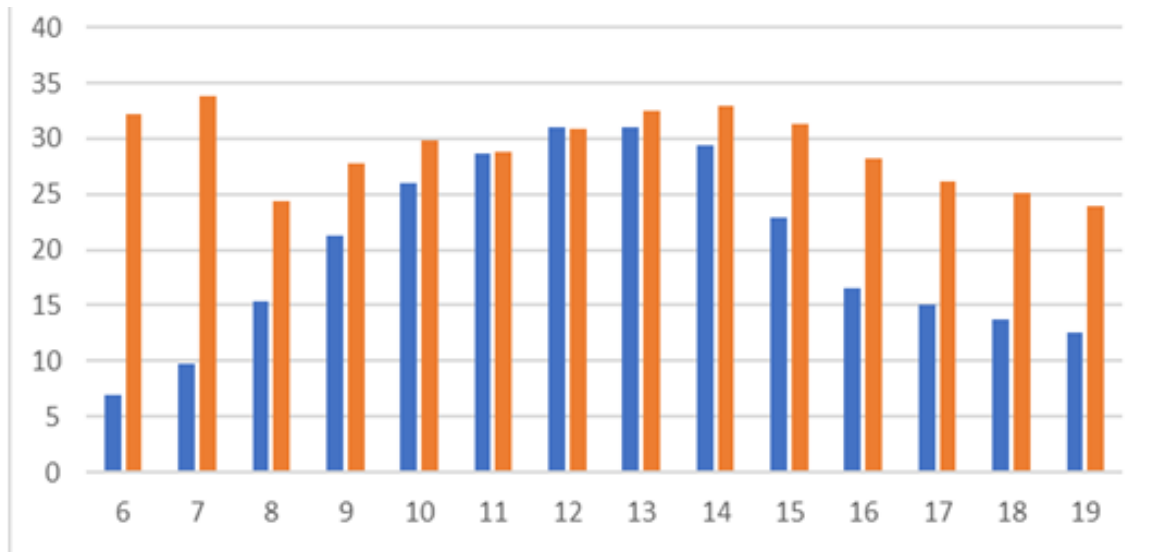
Balcony Type	Comfort Hours (Summer Solstice)	Comfort Hours (Winter Solstice)	Avg. PET (Summer Solstice)	Avg. PET (Winter Solstice)
Central, Two Sides Open – West	0.05	2.00	29.11°C	20.02°C

To evaluate the thermal behavior of Model No. 8, simulations were carried out throughout the year, with a focus on the summer and winter solstice days between 6:00 and 19:00. The PET fluctuated annually between  $-2.7^{\circ}\text{C}$  and  $38.8^{\circ}\text{C}$ . On the summer solstice, the model reached thermal comfort for 0.05 hours; on the winter solstice, it reached 2.00 hours. Average PET values for the solstice days were

$29.11^{\circ}\text{C}$  and  $20.02^{\circ}\text{C}$ , respectively. During the summer solstice, the maximum and minimum PET values were  $33.9^{\circ}\text{C}$  and  $24.1^{\circ}\text{C}$ , respectively. For the winter solstice, they were  $31.2^{\circ}\text{C}$  and  $7.2^{\circ}\text{C}$ . The highest PET was recorded at 7:00 AM in summer and between 12:00–13:00 PM in winter. The lowest PET occurred at 19:00 in summer and 6:00 AM in winter.

### Chart 35

*Balcony Temperature Within Study Hours on the Summer and Winter Solstices for Sample No. 8*



**Model No. 9: Central Balcony (Open on Two Sides – Eastern Orientation)**

### Figure 46

*Modeling of Balcony Model No. 9 in Honeybee Software*

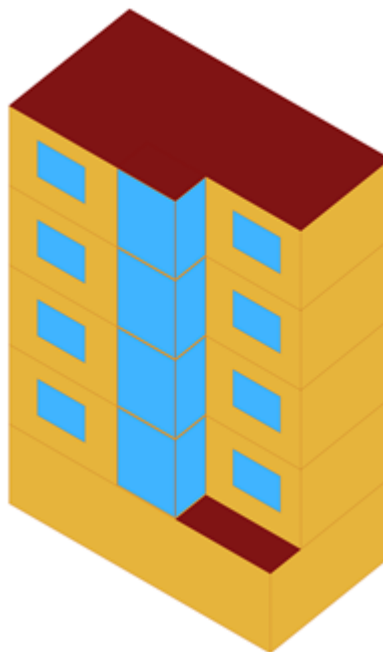


**Figure 47**

*Average Surface Temperatures on the Summer Solstice (Right) and Winter Solstice (Left) for Model 9 Between 6:00 and 19:00*

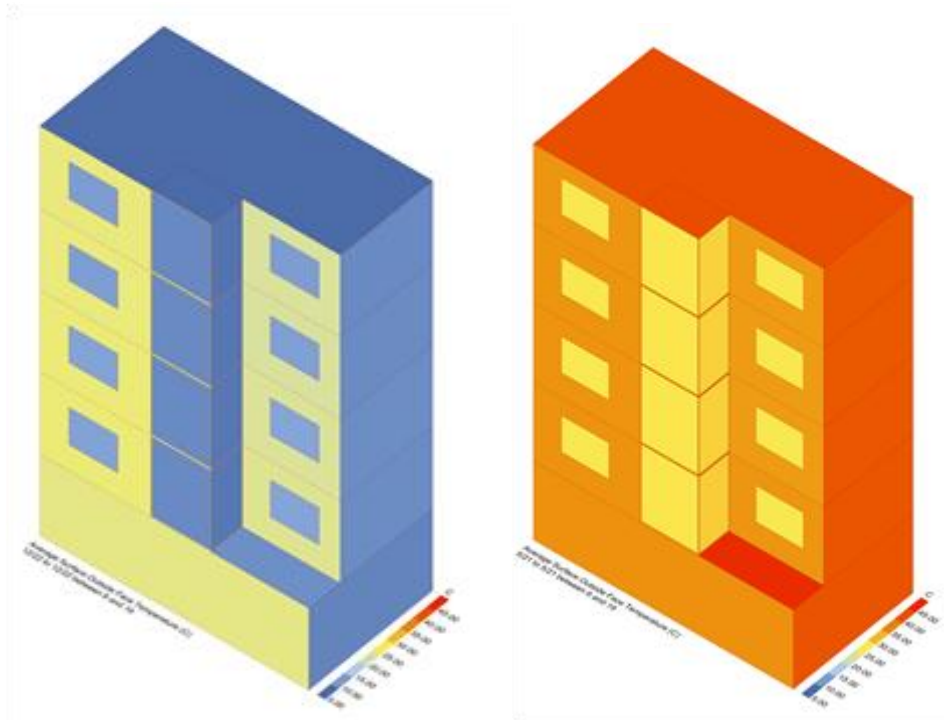


**Chart 36**

*Annual Balcony Temperature (PET) for Model No. 9*

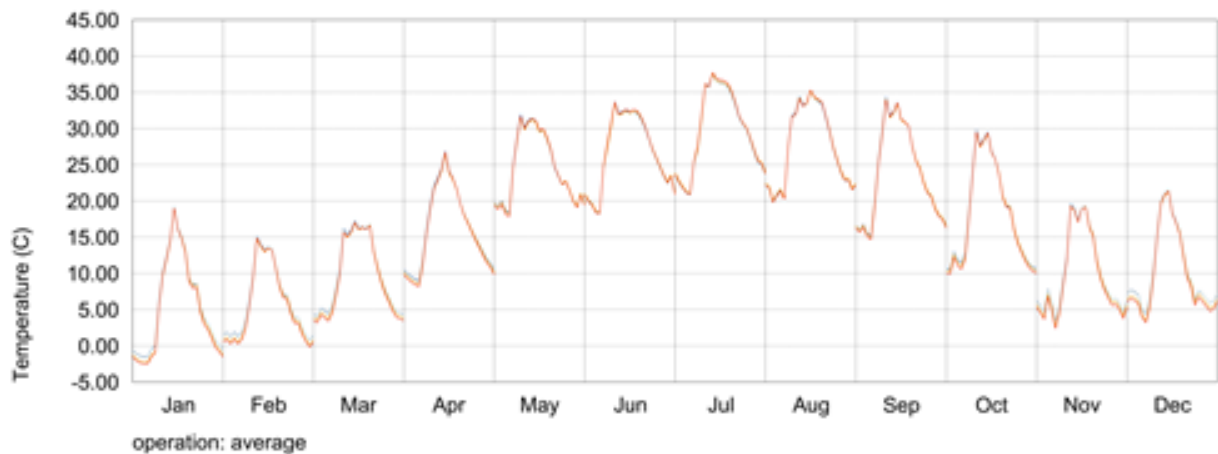


**Table 16**

*Quantitative Output Data from Honeybee for Model No. 9*

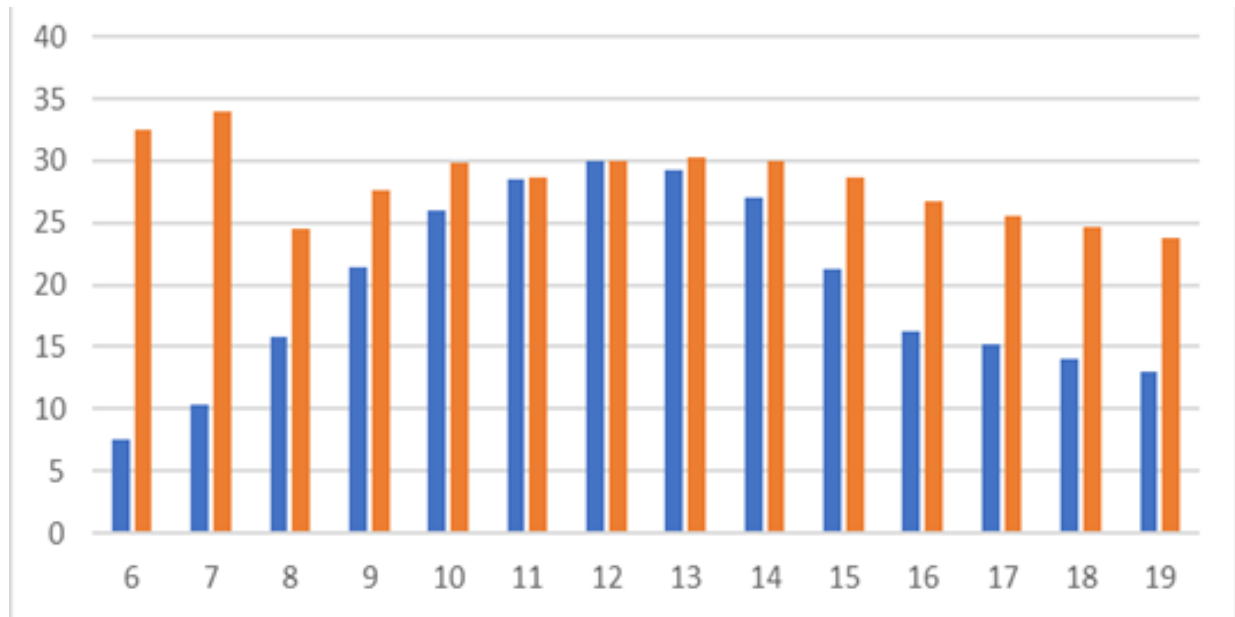
Balcony Type	Comfort Hours (Summer Solstice)	Comfort Hours (Winter Solstice)	Avg. PET (Summer Solstice)	Avg. PET (Winter Solstice)
Central, Two Sides Open – East	0.05	2.00	30.91°C	19.85°C

Model No. 9 was simulated over the full year and specifically on the solstice days between 6:00 and 19:00. Its PET range extended from  $-3.1^{\circ}\text{C}$  to  $37.5^{\circ}\text{C}$ . It achieved thermal comfort for 0.05 hours on the summer solstice and for 2.00 hours on the winter solstice. The average PET values for the solstice days were  $30.91^{\circ}\text{C}$  and  $19.85^{\circ}\text{C}$ . On

the summer solstice, PET peaked at  $34.3^{\circ}\text{C}$  and fell to  $23.7^{\circ}\text{C}$ . On the winter solstice, these values were  $30.0^{\circ}\text{C}$  and  $7.6^{\circ}\text{C}$ . The highest PET occurred at 7:00 AM in summer and at 12:00 PM in winter. The lowest PET was observed at 19:00 in summer and at 6:00 AM in winter.

### Chart 37

*Balcony Temperature Within Study Hours on the Summer and Winter Solstices for Sample No. 9*



### Model No. 10: Central Balcony (Open on Three Sides)

### Figure 48

*Modeling of Balcony Model No. 10 in Honeybee Software*

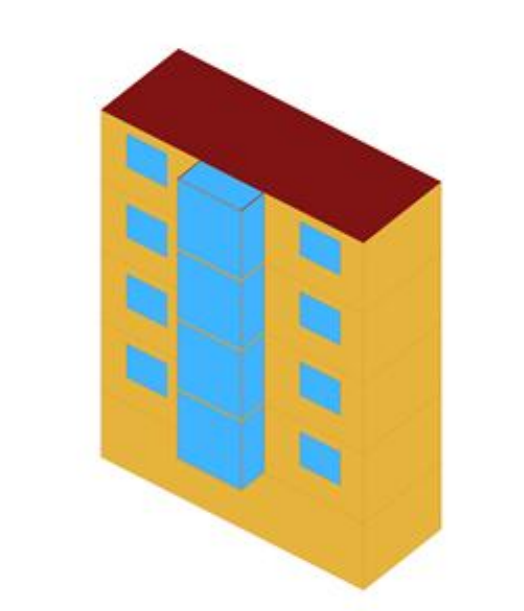


**Figure 49**

*Average Surface Temperature on the Summer Solstice (Right) and Winter Solstice (Left) for Model 10 Between 6:00 and 19:00*

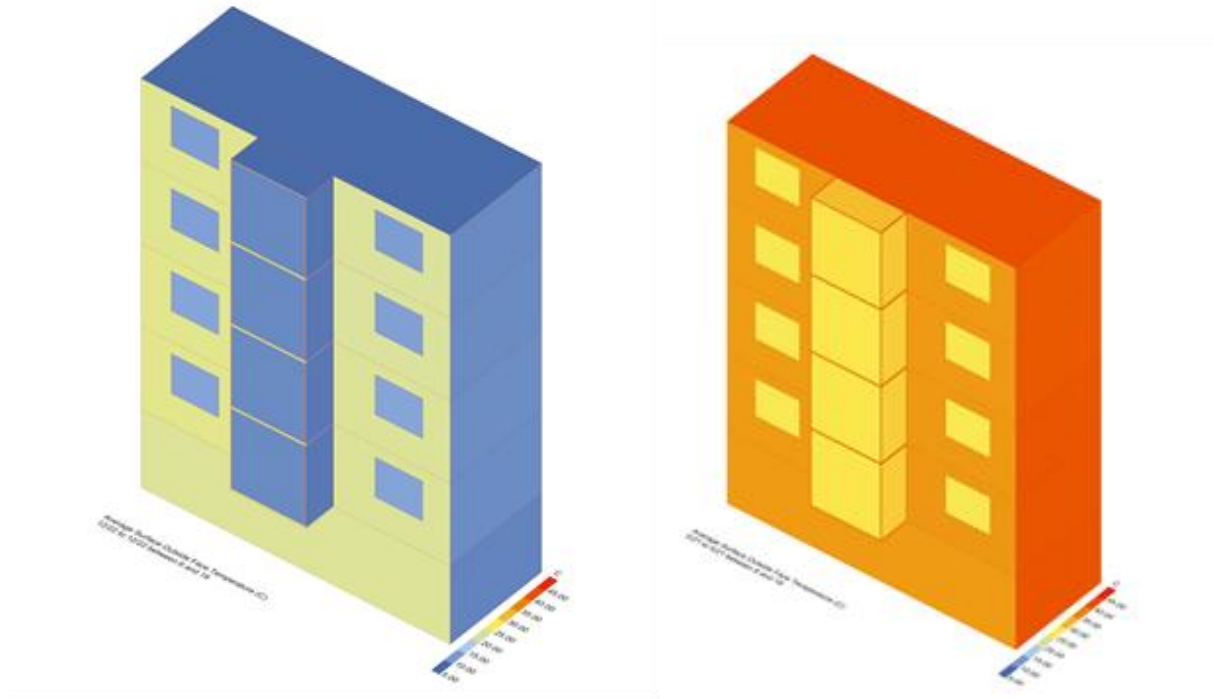


**Chart 38**

*Annual Balcony Temperature (PET) for Model No. 10*

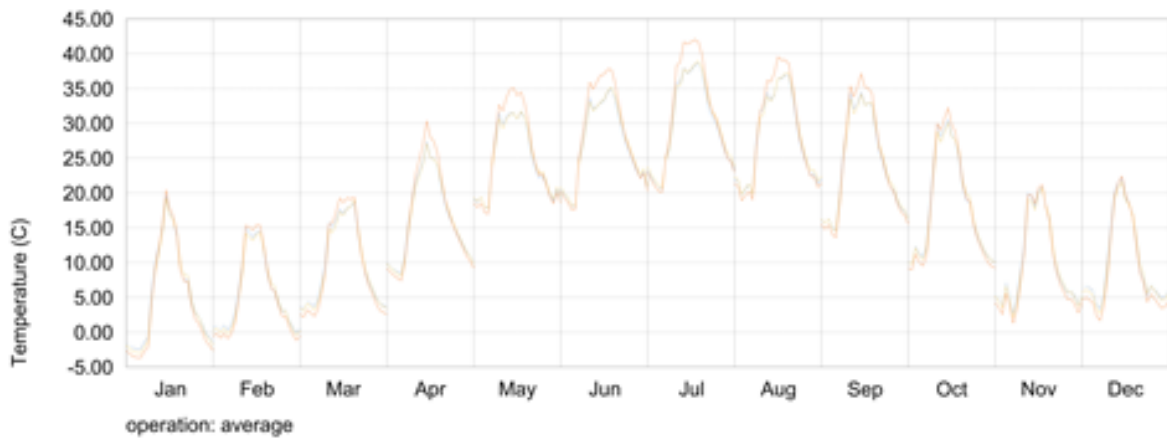


**Table 17**

*Quantitative Data from Honeybee Output for Model No. 10*

Balcony Type	Comfort Hours (Summer Solstice)	Comfort Hours (Winter Solstice)	Avg. PET (Summer Solstice)	Avg. PET (Winter Solstice)
Central, Open on Three Sides	0.05	1.50	30.93°C	19.84°C

To evaluate the thermal performance of Model No. 10, this configuration was simulated throughout the entire year,

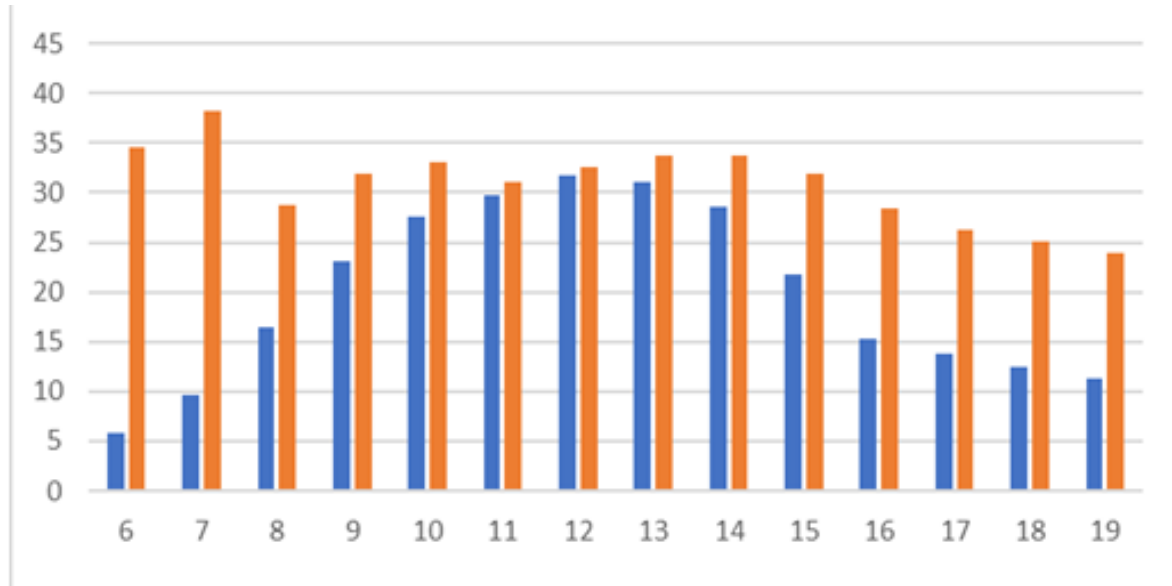
with a particular focus on the summer and winter solstices, between 6:00 and 19:00. Over the course of the year, the PET

(Physiological Equivalent Temperature) fluctuated between  $-4.2^{\circ}\text{C}$  and  $42.4^{\circ}\text{C}$ . On the summer solstice (June 21), the balcony remained within the thermal comfort range for 0.05 hours, and on the winter solstice (December 22), for 1.5 hours. The average PET on the solstice days was  $30.93^{\circ}\text{C}$  in summer and  $19.84^{\circ}\text{C}$  in winter. During the summer solstice

study period, the maximum PET was  $37.7^{\circ}\text{C}$  and the minimum  $24.2^{\circ}\text{C}$ . For the winter solstice, the maximum PET was  $32.1^{\circ}\text{C}$  and the minimum was  $5.6^{\circ}\text{C}$ . The highest PET on the summer solstice occurred at 7:00, and on the winter solstice at 12:00. The lowest PET was observed at 19:00 in summer and at 6:00 in winter.

**Chart 39**

*Balcony Temperature Within Study Hours on the Summer and Winter Solstices for Sample No. 10*



### Evaluation of Thermal Behavior in Modeled Configurations Using Honeybee Software

**Table 18**

*Summary of EnergyPlus Outputs from Honeybee Software*

Orientation	Balcony Type	Comfort Hours (Summer Solstice)	Comfort Hours (Winter Solstice)	Avg. PET (Summer Solstice)	Avg. PET (Winter Solstice)	Max/Min PET (Summer Solstice)	Max/Min PET (Winter Solstice)
East	One Side Open	0.05	1.75	28.50°C	20.06°C	34.2 / 24.6°C	30.7 / 7.3°C
	Two Sides Open	0.05	1.50	29.78°C	20.08°C	38.2 / 23.9°C	30.9 / 6.8°C
	Three Sides Open	0.05	1.25	31.09°C	19.73°C	38.4 / 24.4°C	31.6 / 6.5°C
West	One Side Open	0.05	1.75	28.39°C	20.08°C	34.7 / 23.7°C	31.3 / 7.8°C
	Two Sides Open	0.05	1.50	29.07°C	20.19°C	34.3 / 23.9°C	31.1 / 7.7°C
	Three Sides Open	0.05	1.25	30.86°C	19.71°C	34.1 / 23.8°C	31.9 / 7.3°C
Central	One Side Open	0.05	1.75	28.13°C	20.43°C	33.8 / 23.5°C	30.8 / 7.7°C
	Two Sides Open – West	0.05	2.00	29.11°C	20.03°C	33.9 / 24.1°C	31.2 / 7.2°C
	Two Sides Open – East	0.05	2.00	29.15°C	19.80°C	34.3 / 23.7°C	30.0 / 7.6°C
	Three Sides Open	0.05	1.50	30.93°C	19.86°C	37.7 / 24.2°C	32.1 / 5.6°C



Among the various configurations simulated in Honeybee, the thermal behavior analysis reveals that all models experience a very limited duration within the thermal comfort range on the summer solstice (0.05 hours), essentially indicating that thermal comfort cannot realistically be achieved on that day. However, on the winter solstice, Models No. 8 and 9 (centrally located balconies open on two sides to the west and east) achieved the longest comfort durations at 2.00 hours. Notably, following these two, all models with one side open—regardless of eastern, western, or central orientation—provided 1.75 hours of thermal comfort, ranking just below the top-performing models. Conversely, in terms of the weakest performance in achieving thermal comfort on the winter solstice, the eastern and western three-sided open models both provided only 1.25 hours of comfort, positioning them as the least effective configurations in this regard.

#### 4. Discussion and Conclusion

The simulation-based analysis of smart shading strategies in semi-open balconies revealed critical insights into the behavior of thermal comfort in hot-arid climates, specifically in the context of Mashhad. The study found that balconies with three closed sides generally demonstrated higher thermal stability and superior performance in moderating thermal comfort indicators across seasons. This observation was most evident on solstice days when thermal stress is typically most intense. For instance, Model No. 10, with three open sides and central balcony orientation, recorded the highest PET (Physiological Equivalent Temperature) values during summer hours, showing limited thermal comfort performance due to excessive solar exposure and inadequate shading.

These results align with prior research emphasizing the thermal implications of façade geometry and shading extent on semi-outdoor spaces. For example, (Rodríguez-Algeciras et al., 2018) highlighted the impact of asymmetrical street canyons in warm-humid climates, drawing attention to how enclosure and orientation directly influence mean radiant temperature. Similarly, (Zhang et al., 2018) noted that in hot-humid areas, enclosed semi-open spaces performed better in mitigating thermal extremes than their more exposed counterparts. This validates the findings in our study, particularly in the way balcony depth and wall enclosure affect thermal outcomes in hot-arid contexts.

In both summer and winter solstices, balconies with side closures—particularly those facing central orientations—

offered extended hours within thermal comfort thresholds. For example, models with double-side closures in central orientations maintained up to 2.00 hours of thermal comfort in winter. This performance confirms the significance of transitional space configuration on seasonal thermal behavior, echoing (Baniani et al., 2018), who emphasized the role of spatial continuity in achieving passive climate responsiveness in hybrid spaces.

The results also demonstrated that fully enclosed balconies were least effective during the winter solstice, offering only 1.25 hours of thermal comfort, a pattern consistent with (Ribeiro et al., 2020), who found that over-shaded balconies in colder seasons diminish access to solar gain and impede passive heating. This seasonal trade-off stresses the need for dynamic shading solutions that balance both summer and winter needs, such as movable louvers or retractable awnings, as explored by (Parsaee et al., 2021) in the context of adaptive envelopes in extreme climates.

Furthermore, this study substantiated the significance of orientation. Eastern and western balconies with partial shading consistently outperformed fully open or overly enclosed alternatives, especially during transitional seasons. This supports (Akbari & Hosseini-najad, 2019), who reported that solar radiation optimization through correct façade orientation is vital for enhancing passive heating and cooling. The thermal performance of central balconies with dual side closures was notably better during the winter solstice, providing up to 2.00 comfort hours, consistent with (Khoshbakht et al., 2020), who emphasized the importance of geometric compactness and strategic sun exposure in cold-season urban planning.

The thermal amplitude—reflected in the daily PET range—also highlighted important microclimatic behavior. For example, Model No. 10 experienced a PET range from  $-4.2^{\circ}\text{C}$  to  $42.4^{\circ}\text{C}$  across the year, showing high susceptibility to solar gains. This broad variation signals the importance of adaptive and responsive shading devices, as demonstrated by (Aleksandrowicz et al., 2023), who evaluated ENVI-met's accuracy in predicting mean radiant temperature in Mediterranean cities. Their work, like ours, underscores the need for context-sensitive calibration of simulation tools and urban design parameters.

One of the most noteworthy findings was the limited thermal comfort during the summer solstice across all models. Only 0.05 hours of comfort were recorded, indicating a critical challenge for hot-arid climates. This corroborates (Abdallah et al., 2020), who reported that in educational open spaces, traditional shading strategies often

fail under peak summer conditions. Hence, integrating thermal mass, green infrastructure, or misting systems might be necessary for maintaining acceptable comfort in such environments.

The integration of simulation tools such as Honeybee and Envi-met offered a multifaceted understanding of the thermal performance of various balcony configurations. As pointed out by (Badino et al., 2021), contrasting simulation tools produce different thermal outputs due to discrepancies in radiant temperature modeling. Our study accounted for this by cross-referencing spatial and temporal PET values, particularly during critical hours of exposure. The consistency of peak PET at 7:00 AM in summer and 12:00 PM in winter aligns with daily solar altitude patterns, corroborating findings by (Roshan et al., 2019) regarding Iran's regional comfort thresholds.

Another important aspect lies in the interaction between balcony design and environmental acoustics and humidity. (Qin et al., 2024) argued that sound and humidity interact synergistically with thermal conditions to influence perceived comfort. While our focus remained thermal, such considerations are pivotal in future designs for integrated urban wellness. In this sense, (Rocha et al., 2020) advocated for improving thermal comfort in public transportation nodes through enclosure enhancements—a notion parallel to our balcony microclimate improvements.

The comparative annual assessment revealed that, although central two-side-closed balconies had the best winter performance, their summer results were not significantly superior, indicating an ongoing challenge of balancing shading and ventilation. This reflects the dilemma articulated by (Aghniaey & Lawrence, 2018), who discussed occupant discomfort during demand response events when cooling setpoints are raised, highlighting the necessity of dynamic, user-adaptive systems.

Studies in similar climatic contexts, such as (Roshan et al., 2017), showed that defining climate-responsive thresholds is crucial in building energy optimization. In this study, we extended this approach to outdoor transitional spaces, suggesting that thermally effective balcony design is an overlooked but critical element of sustainable architecture in hot-arid regions.

Another contribution of the present study is its support for integrating vernacular design principles in contemporary architectural solutions. For instance, (Jafarian & Mahmoudian, 2024) explored thermal comfort and energy efficiency in traditional Iranian city fabrics and found that micro-shading and transitional spaces significantly

contribute to year-round comfort. These insights reaffirm the effectiveness of semi-enclosed balconies in mediating outdoor exposure in both historical and modern urban fabrics.

While climate-adaptive design is gaining traction, this study reveals the continued challenges in achieving balanced thermal comfort in semi-open urban spaces. The complex interplay of shading geometry, orientation, time of day, and season highlights the multifactorial nature of outdoor thermal comfort. Studies such as (Sudarsanam & Kannamma, 2023) and (Wu et al., 2023) underline that even user characteristics—like age or activity level—may further mediate comfort perception, suggesting that a one-size-fits-all model is impractical.

Moreover, vegetation and landscape features—though not directly modeled in this study—remain crucial modifiers of microclimates. (Zhao et al., 2018) and (Baruti et al., 2019) emphasized that tree placement and urban greenery improve thermal conditions and shading efficiency in informal and formal urban contexts alike. Future extensions of this research can integrate landscape-based modifications into balcony and façade planning.

This study also complements findings by (Pourdeihimi, 2018) and (Pakzad et al., 2018), who advocate for the climatic language of design and urban morphology. Balconies, as transitional architectural features, embody these principles by mediating between outdoor and indoor climates—an architectural space that, when designed strategically, contributes both to thermal well-being and energy performance.

Despite its strengths, this study is subject to certain limitations. The simulations were conducted based on idealized models and did not incorporate real-time data on humidity, wind flow, or human activity, all of which may significantly influence thermal perception. Additionally, the use of default material properties and ideal weather conditions in ENVI-met and Honeybee may not fully represent local microclimatic complexities. Furthermore, this research focused exclusively on thermal comfort without addressing related environmental or socio-behavioral factors, such as acoustic comfort or user adaptation patterns.

Future studies could expand the scope by integrating vegetation models, user activity simulation, and real-time environmental monitoring to enhance accuracy. Exploring alternative shading materials and kinetic façade systems, as well as including variables such as humidity, wind speed, and user diversity (e.g., age, gender, cultural expectations),

would provide a more holistic understanding of comfort. Comparative studies across different climatic zones or seasonal transitions could also help generalize findings and inform universal shading design strategies.

Architects and urban designers are encouraged to adopt flexible, seasonally adaptive balcony configurations—such as dual-side enclosures with movable canopies—to optimize thermal comfort throughout the year. Central orientations with balanced enclosure can effectively modulate solar gain and radiative exposure, especially in hot-arid cities. Simulation tools like ENVI-met and Honeybee should be integrated early in the design process to test and refine spatial strategies. Finally, shading design should be coupled with passive ventilation and landscape features to create thermally resilient, user-centered semi-open environments.

### Authors' Contributions

Authors contributed equally to this article.

### Declaration

In order to correct and improve the academic writing of our paper, we have used the language model ChatGPT.

### Transparency Statement

Data are available for research purposes upon reasonable request to the corresponding author.

### Acknowledgments

We would like to express our gratitude to all individuals helped us to do the project.

### Declaration of Interest

The authors report no conflict of interest.

### Funding

According to the authors, this article has no financial support.

### Ethics Considerations

In this research, ethical standards including obtaining informed consent, ensuring privacy and confidentiality were considered.

### References

- Abdallah, A. S. H., Hussein, S. W., & Nayel, M. (2020). The impact of outdoor shading strategies on student thermal comfort in open spaces between education buildings. *Sustainable Cities and Society*, 102124. <https://doi.org/10.1016/j.scs.2020.102124>
- Aghapour, A., & Taban, M. (2020). *Investigating the effect of vegetation cover on improving thermal comfort conditions in open spaces* Ahvaz.
- Aghniaey, S., & Lawrence, T. M. (2018). The impact of increased cooling setpoint temperature during demand response events on occupant thermal comfort in commercial buildings: A review. *Energy and Buildings*, 173, 19-27. <https://doi.org/10.1016/j.enbuild.2018.04.068>
- Akbari, H., & Hosseiniadjad, F. S. (2019). Building orientation angles for solar radiation utilization; Case study: Tehran city. *Geographical Research*, 34(3), 427-436. <https://doi.org/10.29252/geores.34.3.427>
- Aleksandrowicz, O., Saroglou, T., & Pearlmutter, D. (2023). Evaluation of summer mean radiant temperature simulation in ENVI-met in a hot Mediterranean climate. *Building and Environment*, 245, 110881. <https://doi.org/10.1016/j.buildenv.2023.110881>
- Badino, E., Ferrara, M., Shterpi, L., Fabrizio, E., Astolfi, A., & Serra, V. (2021). *Modelling mean radiant temperature in outdoor environments: contrasting the approaches of different simulation tools*
- Baniani, F., Me'marzia, K., Habibi, A., & Fattahi, K. (2018). Spatial continuity in the transition from open to enclosed spaces. *Architectural Thought*, 4(2), 63-76. <https://www.google.com/url?sa=t&source=web&rct=j&opi=89978449&url=https://civilica.com/doc/1040827/&ved=2ahUKEwjAgIC2zLKOAXV6RqQEHyVJD8QFnoECBqQAQ&usq=AOvVaw1MchOSmnefRmGcrBpNznUA>
- Baruti, M. M., Johansson, E., & Åstrand, J. (2019). Review of studies on outdoor thermal comfort in warm humid climates: challenges of informal urban fabric. *International Journal of Biometeorol*, 63, 1449-1462. <https://doi.org/10.1007/s00484-019-01757-3>
- Fattahi, M., & Sharbatdar, M. (2023). Machine-learning-based personal thermal comfort modeling for heat recovery using environmental parameters. *Sustainable Energy Technologies and Assessments*, 57, 103294. <https://doi.org/10.1016/j.seta.2023.103294>
- Jafarian, R., & Mahmoudian, A. (2024). Traditional Iranian Architecture, Thermal Comfort, and Energy Consumption Balance (Case Study: Architectural Fabric of the Historical City of Sirvan). *Ilams Studies*(32), 94-119. [https://www.ilmastudy.ir/article\\_213526.html](https://www.ilmastudy.ir/article_213526.html)
- Jun, H., & Fei, H. (2024). Research on multi-objective optimization of building energy efficiency based on energy consumption and thermal comfort. *Building Services Engineering Research & Technology*, 45(4), 391-411. <https://doi.org/10.1177/01436244241240066>
- Khoshbakht, Y., Madi, H., & Azmoudeh, M. (2020). *Investigating the geometry of urban blocks on outdoor thermal comfort during the cold season (Case study: Hamadan city)* Tehran. <https://www.google.com/url?sa=t&source=web&rct=j&opi=89978449&url=https://civilica.com/doc/1028612/&ved=2ahUKEwim5qiezrKOAXWSUKQEHEp2FnIQFnoECCUQAQ&usq=AOvVaw37Bm-K-DyR05WJAss1C2Nd>
- Moghadam Ziabari, A., & Mozaffari, F. (2018). The effect of balconies on natural ventilation, thermal comfort, and reduction of external noise in residential buildings. *Architectural Studies*, 6, 1-8. <https://www.google.com/url?sa=t&source=web&rct=j&opi=89978449&url=https://ensani.ir/fa/article/390809/>

- Pakzad, J., Torabi, M., Ghasemi, M., & Torkzad, N. (2018). *Theoretical Foundations and Process of Urban Design*. Shahidi Publications.
- Parsaei, M., Demers, C. M. H., Potvin, A., Lalonde, J. F., Inanici, M., & Hébert, M. (2021). Biophilic photobiological adaptive envelopes for sub-Arctic buildings: Exploring impacts of window sizes and shading panels' color, reflectance, and configuration. *Solar Energy*, 220, 802-827. <https://doi.org/10.1016/j.solener.2021.03.065>
- Pourdehimi, S. (2018). *Climatic Language in Sustainable Environmental Design: Application of Climatology in Architectural Planning and Design: Micro Scale*. Shahid Beheshti University Press and Publications Center.
- Qin, Z., Lu, B., Jing, W., Yin, Y., Zhang, L., & Wang, X. (2024). Creating comfortable outdoor environments: Understanding the intricate relationship between sound, humidity, and thermal comfort. *Urban Climate*, 55, 101967DO - 101910.101016/j.uclim.102024.101967.
- Ribeiro, C., Ramos, N. M. M., & Flores-Colen, I. (2020). A Review of Balcony impacts on the Indoor Environmental Quality of Dwellings. *Sustainability*, 12(16), 6453. <https://doi.org/10.3390/su12166453>
- Rocha, A., Pinto, D., Ramos, N. M., Almeida, R. M., Barreira, E., Simões, M. L., & Sanhudo, L. (2020). A case study to improve the winter thermal comfort of an existing bus station. *Journal of Building Engineering*, 29, 101123. <https://doi.org/10.1016/j.jobee.2019.101123>
- Rodríguez-Algeciras, J., Tablada, A., & Matzarakis, A. (2018). Effect of asymmetrical street canyons on pedestrian thermal comfort in warm-humid climate of Cuba. *Theoretical and Applied Climatology*, 133(3-4), 663-679. <https://doi.org/10.1007/s00704-017-2204-8>
- Roshan, G. R., Almomenin, H. S., da Silveira Hirashima, S. Q., & Attia, S. (2019). Estimate of outdoor thermal comfort zones for different climatic regions of Iran. *Urban Climate*, 27, 8-23. <https://doi.org/10.1016/j.uclim.2018.10.005>
- Roshan, G. R., Farrokhzad, M., & Attia, S. (2017). Defining thermal comfort boundaries for heating and cooling demand estimation in Iran's urban settlements. *Building and Environment*, 121, 168-189. <https://doi.org/10.1016/j.buildenv.2017.05.023>
- Sanagar Darbani, E., Rafieian, M., Hanaei, T., & Monsefi Praperi, D. (2018). Evaluation of climate change impacts on outdoor thermal comfort changes using the Physiological Equivalent Temperature (PET) index in Mashhad city. *Geographical Research Quarterly*, 33(3), 38-57. <https://doi.org/10.29252/geores.33.3.38>
- Sudarsanam, N., & Kannamma, D. (2023). Investigation of summertime thermal comfort at the residences of elderly people in the warm and humid climate of India. *Energy and Buildings*, 291, 113151. <https://doi.org/10.1016/j.enbuild.2023.113151>
- Wu, Y., Zhang, Z., Liu, H., Li, B., Chen, B., & Kosonen, R. (2023). Age differences in thermal comfort and physiological responses in thermal environments with temperature ramp. *Building and Environment*, 228, 109887. <https://doi.org/10.1016/j.buildenv.2022.109887>
- Zhang, Z., Zhang, Y., & Jin, L. (2018). Thermal comfort in interior and semi-open spaces of rural folk houses in hot-humid areas. *Building and Environment*, 128, 336-347. <https://doi.org/10.1016/j.buildenv.2017.10.028>
- Zhao, Q., Sailor, D. J., & Wentz, E. A. (2018). Impact of tree locations and arrangements on outdoor microclimates and human thermal comfort in an urban residential environment. *Urban Forestry & Urban Greening*, 32, 81-91. <https://doi.org/10.1016/j.ufug.2018.03.022>